Proceedings of the 16th International Conference on Soil Mechanics and Geotechnical Engineering

doi:10.3233/978-1-61499-656-9-3

Geo-characterisation and properties of natural soils by *in situ* tests

Geo-caractérisation et propriétés des sols naturels pas essais in-situ

Fernando Schnaid
Federal University of Rio Grande do Sul, Brazil

ABSTRACT

Site characterisation and *in situ* test interpretation have been evolving from basic empirical recommendations to a sophisticated area demanding a thorough knowledge of material behaviour and numerical modelling. With the advent of modern testing techniques and more rigorous methods of analysis, site characterisation in natural soils is gaining momentum. This Report presents a critical appraisal in the understanding and assessment of the stress-strain-time and strength characteristics of natural soil conditions and explores new interpretation methods capable of measuring soil properties shaped by effects of microstructure, stiffness non-linearity, small and large strain anisotropy, weathering and destructuration, consolidation characteristics and rate dependency. Interpretation methods in different soil formations such as clay, sand, silt and bonded geomaterials are explored using different testing techniques. Since the *in situ* behaviour of natural soils is complex, a single general recommendation is to cross-correlate measurements from different tests. When data are combined there is more scope for rational interpretation and, for this reason, emphasis has been placed on correlations with mechanical properties that are based on the combination of independent measurements.

RÉSUMÉ

La caractérisation des sols et l'interprétation des essais *in situ* a profondément évolué, passant de recommandations simples et empiriques à des méthodes plus sophistiquées nécessitant une connaissance approfondie du comportement des matériaux et des méthodes de modélisation numérique. Avec le développement de nouvelles techniques d'essais et de méthodes d'analyses de plus en plus rigoureuses, la caractérisation des sols naturels prend de plus en plus d'ampleur. Ce rapport présente une évaluation critique de notre compréhension et des méthodes de détermination des relations contraintes-deformations-temps et des caractéristiques de résistance des sols naturels en place. Il explore de nouvelles méthodes d'interprétation capable de mesurer les propriétés du sol directement liées a sa microstructure, tels que le module d'élasticité non linéaire, les petites et larges déformations en anisotropie, la déstructuration, les caractéristiques de consolidation et la dépendance a la vitesse de chargement. Les méthodes d'interprétation dans des sols différents tels que argile, sable, limon et autres geomatériaux formes par dépôt sont analysées, à partir de différentes types d'essais. Du fait de la complexité du comportement des sols en place, une première et simple recommandation est de croiser les résultats de différents essais. Lorsque les résultats sont combinés, il y a une plus grande pour une interprétation rationnelle, et pour cette raison, l'attention a été placée sur les corrélations entre propriété mécaniques basées sur des combinaisons d'essais indépendants.

1 INTRODUCTION

Because the Earth is a complex three-dimensional object with numerous structures and hydro-geomorphologies that are difficult to imagine and to characterise, it is important to develop concepts and techniques that will support the identification and description of its spatial arrangements in manipulative two-dimensional representations. Although this consists on a challenge to be approached by a hybrid of disciplines, it has prompted the development of the scientific field of Soil Mechanics and, in particular, the area of site characterisation.

The basic objective of site characterisation is to acquire topographical, hydro-geological, geotechnical and geo-environmental information that is relevant to the requirements of a project. The work of geo-engineers has expanded enormously over the past decades and therefore professionals must become aware and acknowledgeable in many areas to fully undertake the issues covered by the planning and organization of site characterisation programmes. Several publications provide surveys of many of the technical details of the field and give a good overview of the immediate purposes associated to site characterisation (e.g. Clayton et al, 1995; Rowe, 2001).

Placing the focus on geotechnical engineering, the immediate purposes associated to an investigation programme is to (a) determine the general nature and sequence of the subsurface strata, (b) locate the water table and groundwater conditions and (c) measure or assess specific properties of the ground. Any project or related activity would therefore require a fundamental understanding of its environmental constrains and, for that reason, a professional should comprehend the interplay of processes that leads to site characterisation. Figure 1 illustrates the stages associated to characterisation in a flowchart that identifies mechanical testing as an inherent part of site investigation, a part that determines the basic soil classification, supports the conceptual model adopted in design and establishes the representative strength and stiffness parameters required for engineering design calculations. Understanding laboratory and *in situ* tests and the constitutive relationships that link material behaviour is therefore considered essential to optimise engineering geotechnical design.

Important interrelationships exist between the field and laboratory which, given the numerous existing techniques available, require strategies for characterising soils to be established. A general recommendation is to examine the characteristics of the soil from a macro to a micro perspective. Surface wave methods provide a spatial 3-D or 2-D subsurface representation of large areas. Geophysical methods give a qualitative picture of the site which does not substitute the need for direct measurements attained by *in situ* tests. SPT, CPT, DMT and SBPM are designed to reveal 1-D information of the ground that, under some simplified assumptions, can be interpreted to assess average properties of soil profiles. Finally laboratory test deals with a close examination of an elemental material property. Since each testing technique responds to different physical properties and gives information of different

nature, a successful, cost-effective site characterisation programme should consist of an appropriate combination of field tests (3,2 and 1-D representations) and laboratory tests, so that the relevant information can be synthesized and understood with confidence.

The approach of this report is to give a general picture of the field of geo-characterisation with emphasis on *in situ* testing soil mechanics, to discuss the theoretical background that supports interpretation of testing data, plus add examples of the use of experimental techniques. An attempt is made to highlight new potential methods of interpretation of *in situ* tests, by emphasising what is taken to be tendencies in the field of site investigation. Rather than trying to exhaustively discuss established methods of interpretation, I would like to focus on giving engineers a close examination of recent and current developments in the following:

a) interpretation of *in situ* tests in clay, where the needs to account for stress history, soil structure, anisotropy, consolidation and viscous effects are considered;
b) analysis of the stress-strain and strength behaviour of granular soils, with emphasis on the effects of fabric, aging and cementation and their impact on correlations based on both large calibration chamber tests and centrifuge tests;
c) a critical review on the behaviour of bonded geomaterials and the development of interpretative models capable of extending the existing theoretical and empirical approaches established on the basis of the experience on "standard" clays and sands;
d) evaluation of partial drainage effects on results of *in situ* tests carried out in intermediate permeability silt soils.

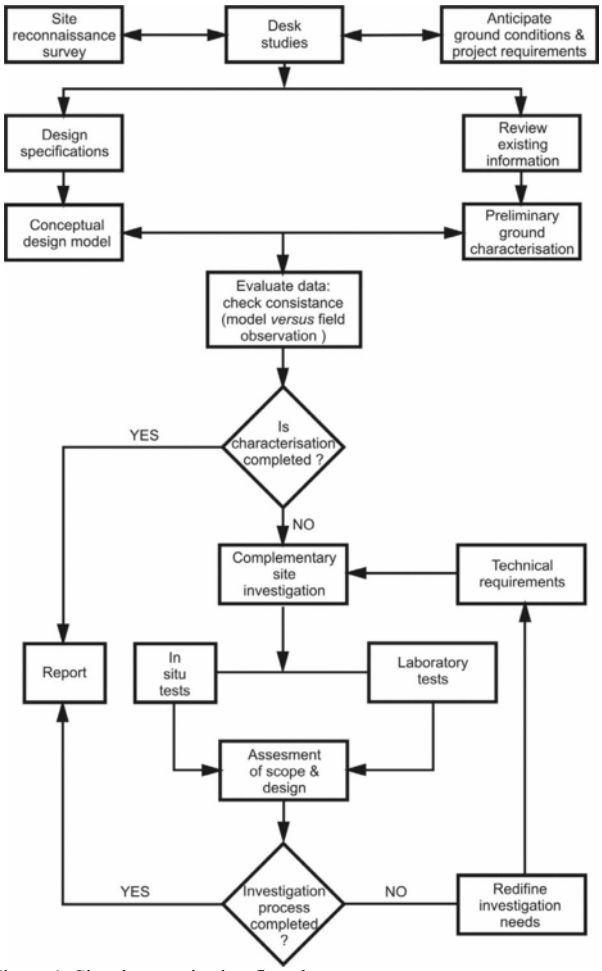

Figure 1. Site characterisation flowchart

Each of these topics is a major subject on itself. Only fundamental aspects are selected for discussion based on the authors experience and interests and the need not to deviate from fundamental Soil Mechanics.

2 BACKGROUND INFORMATION

In this Report I strive to produce a broad view of technical information and theoretical background that are necessary to prepare professionals to produce sounding engineering judgement in every stage of the geo-characterisation of natural soils. This comprises understanding of the ways the key experimental and theoretical elements are correlated in the domain of geotechnical engineering research relating to site characterisation, acknowledging potential and limitations of different tests and measurements and recognising hypotheses and assumptions associated to mechanical models developed to describe the behaviour of natural soils. Since no mathematical theory can complete describe the complex boundary conditions of a field test, the role of centrifuge and large laboratory chamber testing is emphasised in order to improve our understanding of the behaviour of prototypes under parametric studies.

We start by recalling that fundamental understanding of soil behaviour is necessarily developed on the basis of laboratory in tests. The results of triaxial tests have revealed the decisive elements to incorporate in many constitutive models of soil behaviour, in particular on the development of Critical State Soil Mechanics and the family of Cam-Clay models (e.g. Schofield &Wroth, 1968; Roscoe & Burland, 1968). The recent innovations in laboratory testing for experimentally determining the stress-strain-strength and time dependent properties of geomaterials comprises (a) growth of a new generation of devices such as hollow cylinder, resonant column and torsional shear apparatus, (b) extensive use of stress path computer based systems and (c) development of new techniques for more accurate measurements of local strains and imposed loads (e.g. Shibuya et al, 1996; Stoke et al, 1995; Tatsuoka et al, 1997; Lo Presti et al, 1999). Increasing sophistication, accuracy and capability of laboratory measurements has prompted a better understanding of the behaviour of geomaterials to assist in the solution of a variety of geotechnical problems. Recent research has provided the background necessary for the assessment of aspects of soil behaviour in more complex environments, including the effects of microstructure (fabric and bonding), small strain stiffness and stiffness non-linearity, small and large strain anisotropy, weathering and destructuration, partial saturation and viscosity. These important features of natural (and man-made) ground behaviour are now recognised and are addressed on the basis of a framework that has been established from a comprehensive characterisation of laboratory tests on reconstituted soils and a number of well known natural clays and sands (e.g. Almeida & Marques, 2003; Hight et al, 2003; Dias-Rodriguez, 2003; Lo Presti et al, 2003; Coop & Airey, 2003; Jamiolkowski & Lo Presti, 2003).

The considerable body of knowledge accumulated from laboratory tests is here re-viewed with the purpose of (a) providing a framework for describing soil behaviour that supports the interpretation of *in situ* tests and (b) producing a database against which results of *in situ* tests are calibrated. An attempt is made to extend this existing background knowledge to the field of *in situ* testing, and a necessary step in this direction is to develop a new generation of interpretation methods and constitutive models that capitalizes on existing experience. As recently pointed out by Schnaid et al (2004), the challenge in the field of *in situ* tests is threefold: to evaluate the applicability of existing theoretical and empirical approaches in order to extend the experience of 'standard' clays and sands to other geomaterials, to develop interpretative methods that incorporate new constitutive models whenever required, and to

gather experimental data that justifies the applicability of proposed interpretation methods to engineering applications. A primarily step in this direction is to identify the applicability and potential of existing techniques, a task that necessarily contains a critical appraisal on how results can be compiled to obtain a ground model and appropriate geotechnical parameters.

A variety of *in situ* tests is now available to meet the needs of geotechnical engineers (e.g. Mayne, 2001; Van Impe et al, 2001). Existing field techniques can be broadly divided into two main groups:

(a) *non-destructive or semi-destructive tests* that are carried out with minimal overall disturbance of soil structure and little modification of the initial mean effective stress during the installation process. The non-destructive group comprises seismic techniques, pressuremeter probes and plate loading tests, a set of tools that is generally suitable for rigorous interpretation of test data under a number of simplified assumptions;

(b) *invasive, destructive tests* were inherent disturbance is imparted by the penetration or installation of the probe into the ground. Invasive-destructive techniques comprise SPT, CPT and dilatometer. These penetration tools are robust, easy to use and relatively inexpensive, but the mechanism associated to the installation process is often fairly complex and therefore a rigorous interpretation is only possible in few cases.

For example, CHT and DHT are defined in geophysics as intrusive methods since they are generally performed within boreholes. However shear waves propagate in a soil mass that has not been disturbed by installation, which in geomechanics suggests a *non-destructive* type of test in attempting to distinguish from *invasive* penetration techniques in which interpretation is fairly sensitive to the shear zone created around a penetrating probe. Since the *in situ* behaviour of geomaterials is complex, current research efforts are placing emphasis on correlations with mechanical properties that are based on the combination of different sensors in a single test device, usually combining a non-destructive to an invasive technique such as the seismic cone and cone pressuremeter. A summary of the key information regarding the commonly used *in situ* tests is given in Table 1, in which measurements of each testing technique are described and common applications are identified.

The main characteristics of the field test techniques described in Table 1 are summarised in the following sections.

Table 1: Commercial in situ testing techniques (modified from Schnaid et al, 2004)

Category	Test	Designation	Measurements	Common Applications
Non-destructive or semi-destructive tests	Geophysical tests: Seismic refraction Surface waves Crosshole test Downhole test	SR SASW CHT DHT	P-waves from surface R-waves from surface P & S waves in boreholes P & S waves with depth	Ground characterisation Small strain stiffness, G_o
	Pressuremeter test Pre-bored Self-boring	PMT SBPM	G, (ψ x ε) curve G, (ψ x ε) curve	Shear modulus, G Shear strength *In situ* horizontal stress Consolidation properties
	Plate loading test	PLT	(L x δ) curve	Stiffness and strength
Invasive penetration tests	Cone penetration test Electric Piezocone	CPT CPTU	q_c, f_s q_c, f_s, u	Soil profiling Shear strength Relative density Consolidation properties
	Standard Penetration Test (energy control)	SPT	Penetration (N value)	Soil profiling Internal friction angle, ϕ'
	Flat dilatometer test	DMT	p_o, p_1	Stiffness Shear strength
	Vane shear test	VST	Torque	Undrained shear strength, s_u
Combined tests (Invasive + Non-destructive)	Cone pressuremeter	CPMT	q_c, f_s, (+u), G, (ψ x ε)	Soil profiling Shear modulus, G Shear strength Consolidation properties
	Seismic cone	SCPT	q_c, f_s, V_p, V_s, (+u)	Soil profiling Shear strength Small strain stiffness, G_o Consolidation properties
	Resistivity cone	RCPT	q_c, f_s, ρ	Soil profiling Shear strength Soil porosity
	Seismic dilatometer		p_o, p_1, V_p, V_s	Stiffness (G and G_o) Shear strength

2.1 *Seismic tests*

A geophysical survey is regarded as a powerful technique for subsurface exploration. Tests are generally non-destructive in nature and can be performed from the ground surface. Despite due recognition its risks and limitations, there has been a steady increase in the perceived value of geophysics in representing complicated subsurface conditions involving large spatial variability and stratified soils. In addition, cross and downhole methods have been extensively used in geotechnical engineering, including the adaptation of sensors in the seismic cone.

The theoretical bases upon which seismic and other geophysical measurements are found are not within the scope of this Report. For that purpose there is a number of reference textbooks that extensively covers this subject area such as Richard et al (1970), Sharma (1997) and Santamarina et al (2001). For us it is important to recall that geophysical methods rely on a significant contrast in physical properties of materials under investigation. Intrinsic properties such as density, resistivity or electrical conductivity, magnetic susceptibility and velocity of shock waves of the subsurface materials should be considered when evaluating the suitability of a given technique. Frequently used geophysical techniques are seismic refraction, high resolution surface wave reflection, vibration, down-hole and cross-hole, electrical resistivity, magnetic and gravity tests. (e.g. Stokoe & Santamarina, 2000; Stokoe et al, 2004; Becker, 2001).

The primary applications in the use of geophysical methods in geotechnical engineering are (Becker, 2001): to map stratigraphy, determine thickness of strata, depth of bedrock and define major anomalies such as channels and cavities; to locate deposits of aggregates and other construction materials; and to determine engineering properties of strata and their spatial variation. Geo-environmental projects complement the list of applications. It is always necessary to bear in mind that geophysical techniques are intended to supplement ground investigation methods. To enhance its consistency, a site investigation campaign should always encompass a combination of geophysical surveys with a mesh of boreholes and/or penetration tests.

In this report attention is given to measurement of shear wave velocities from which it is possible to obtain the small-strain stiffness of the soil at induced strain levels of less than 0.001 %:

$$G_o = \rho V_s^2 \qquad (1)$$

where G_o is the shear modulus, ρ the mass density and V_s the velocity of shear waves for a linear, elastic, isotropic medium. The CHT and DHT enable the velocity of horizontally propagating, vertically polarized (S_{hv}), vertically propagating, horizontally polarized (S_{vh}) and horizontally propagating, horizontally polarized (S_{hh}) shear waves to be measured.

2.2 *Piezocone penetration test (CPTU)*

The CPT, with the possible inclusion of pore water pressure, shear wave velocity and resistivity measurements is now recognized worldwide as an established, routine and cost-effective tool for site characterisation and stratigraphic profiling, and a means by which the mechanical properties of the subsurface strata may by assessed. CPTs were particularly popular in sands and in marine and lacustrine sediments in costal regions, but are now also commonly used in peats, silt, residual soils, a variety of hard materials (chalk, cemented sands) and reclaimed land formed by hydraulic fills, dredging and mine tailings. For a general review on the subject the reader is encouraged to refer to Lunne *et al.* (1997) – *CPT in Geotechnical Practice,* and the Proceedings of the Symposia on Penetration Testing (1981, 1988, 1995, 1998, 2004).

Figure 2 shows a diagram of a typical cone. Routine penetrometers have employed either one midface element for pore water pressure measurement (designated as u_1) or an element positioned just behind the cone tip (shoulder, u_2). The ability to measure pore pressure during penetration greatly enhances the profiling capability of the CPTU, allowing thin lenses of material to be detected. Geotechnical site characterisation can be further improved by independent seismic measurements, adding the downhole shear wave velocity (V_s) to the measured tip cone resistance (q_t), sleeve friction (f_s) and pore water pressure (u). The combination of different measurements into a single sounding provides a particular powerful means of assessing the characteristics of natural materials.

The seismic CPT is becoming a routine site investigation tool in many countries giving the facility of adding accelerometer and/or geophones to measure compression (P) and shear (S) wave velocities (e.g. Campanella et al, 1986). The additional cost and time required for a seismic measurement is modest and the input provided by the small strain shear modulus is essential for soil characterisation and prediction of ground-surface settlements under dynamic loading.

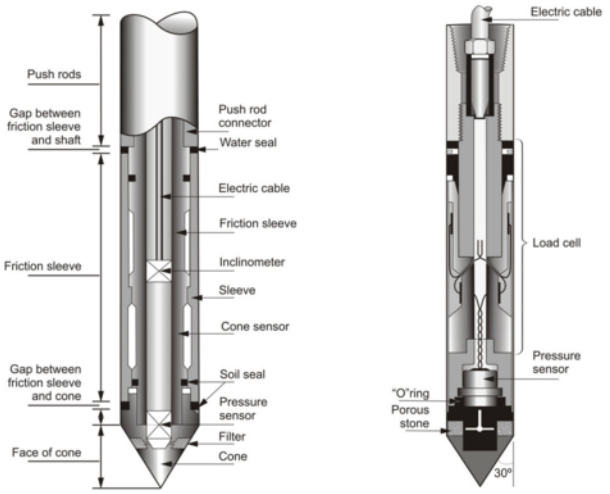

Figure 2. Design features of a piezocone

2.3 *Pressuremeter*

Pressuremeters are cylindrical devices designed to apply uniform pressure to the wall of a borehole by means of a flexible membrane. Both pressure and deformation at the cavity wall are recorded and interpretation is provided by cavity expansion theories under the assumption that the probe is expanded in a linear, isotropic, elastic, perfectly plastic soil. Under this assumption the soil surrounding the probe is subjected to pure shear only. Acknowledging that the greatest potential of the pressuremeter lies in the measurement of modulus, it is a common practice to carry out a few unloading-reloading cycles during the test. If the soil is perfectly elastic in unloading, then the unloading-reloading cycle will have a gradient of $2G_{ur}$, where G_{ur} is the unload-reload shear modulus. Numerous papers have been published on this theme and there are important textbooks such as Baguelin et al (1978), Mair & Wood (1987), Briaud (1992), Clarke (1995) and Yu (2000).

Pressuremeters are generally classified in three groups according to the method of installation into the ground. Pre-bored pressuremeter, self-boring pressuremeter and push-in pressuremeter are the three broad categories. The Menard pressuremeter is the most well known example of a pre-bored probe in which the device is lowered into a pre-formed hole. In a self-boring probe the device bores its own way into the ground with minimal disturbance (see Figure 3), whereas in a push-in device the pressuremeter is pushed into the ground attached to a

cone tip. The method of interpretation should take account of the installation process.

Theoretical interpretation methods developed for pressuremeters involve axially symmetric expansion and contraction of an infinitely long cylindrical cavity. Under this fundamental assumption the cavity-expansion/contraction curve can be analytically modelled to obtain soil properties. The symmetry of the well defined boundary conditions of a pressuremeter is the main advantage of this technique over other *in situ* tests.

In order to investigate the appropriateness of this basic assumption, several numerical studies have been carried out to investigate the effects of the finite length of a pressuremeter in clay (Yeung & Carter, 1990; Houlsby & Carter, 1993; Charles et al, 1999). These studies generally suggest that ignoring length to diameter effects will significantly overestimate the undrained shear strength. In sand, the possible effects of geometry are quantified by both numerical methods (Yu, 1993) and calibration chamber tests (Schnaid & Houlsby, 1992; Ajalloeian & Yu, 1993). Results suggest that the finite length of a pressuremeter yields a stiffer loading response which impacts the predicted values of friction angle. This effect is less pronounced on the unloading portion of the test. Cone-pressuremeter tests carried out in a laboratory chamber study are shown in Figure 4 to illustrate the influence of the length to diameter ratio on the measured pressuremeter curve.

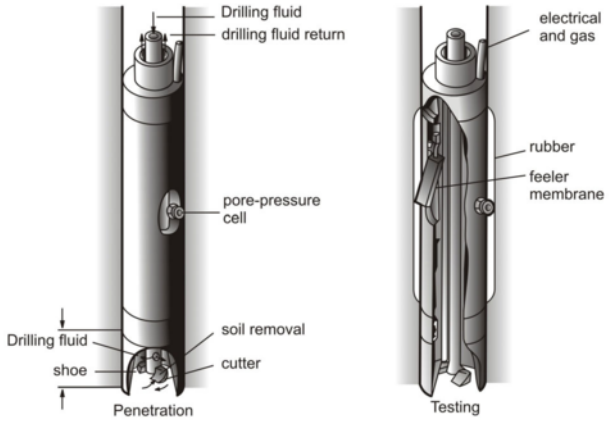

Figure 3. Self-boring pressuremeter

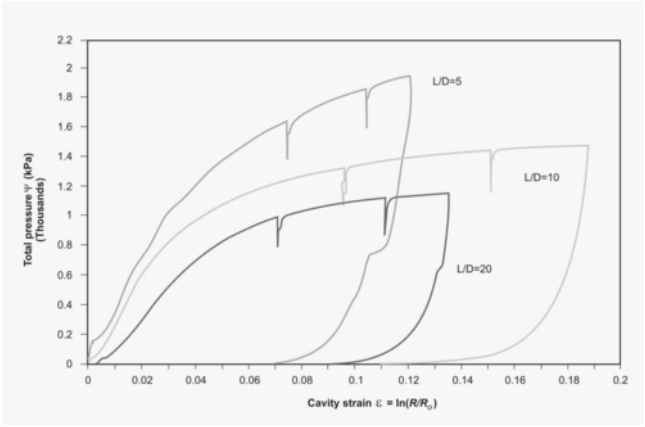

Figure 4. Laboratory results of finite pressuremeter length effects (Schnaid & Houlsby, 1992).

2.4 *Cone pressuremeter*

The CPMT is an *in situ* testing device that combines the 15 cm^2 cone with pressuremeter module mounted behind the cone tip, as illustrated in Figure 5 (after Withers et al, 1989). Since the pressuremeter test is not carried out in undisturbed ground, the effects of installation have to be accounted for and large strain analysis is required. This technique is perceived as having a great potential that has not yet been fully recognized in practice. Analysis of the test in clay is achieved by a simple geometric construction of the curve to determine the undrained shear strength, the shear modulus and the *in situ* horizontal stress (Houlsby and Withers, 1988). Analysis in sand is, however, significantly more complex and interpretation is largely based on calibration chamber tests (Schnaid & Houlsby, 1992; Nutt & Houlsby, 1992). Research in the past 10 years has provided basic interpretation procedures to allow the use of test results to determine the engineering properties of soils, including assessment to shear strength, relative density, state parameter, friction angle and *in situ* stress state.

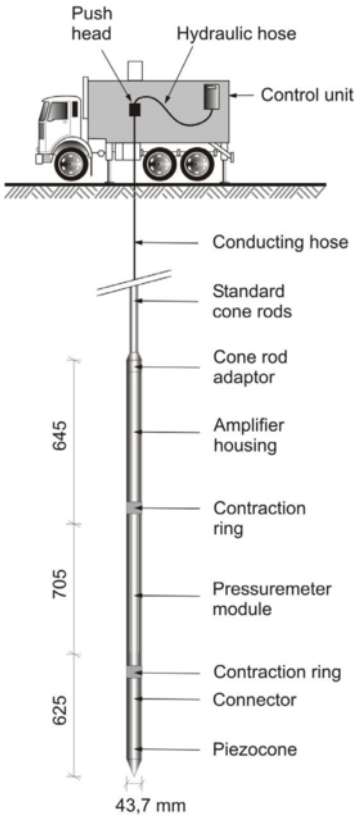

Figure 5. Cone-pressuremeter (after Withers et al, 1989)

2.5 *Dilatometer*

The flat dilatometer test (DMT) was developed in Italy (Marchetti, 1980) and has become a routine site investigation tool in more than 40 countries. A general overview of the dilatometer, guidelines for proper execution and basic interpretation methods are given by Marchetti et al (2001) in a report issued under the auspices of ISSMGE Technical Committee TC'16.

The dilatometer consists in a stainless steel blade having a flat, circular steel membrane mounted flush on one side (Figure 6). The blade is driven into the soil using pushing rigs normally adopted for the CPT. After penetration, the membrane is inflated and a sequence of pressure readings are made at prescribed displacements, corresponding to the pressure at which the membrane starts to expand ("lift-off") and the pressure required to move the centre of the membrane by 1.1mm against the soil.

Interpretation methods are essentially based on correlations obtained by calibrating DMT pressure readings against high quality parameters (e.g. Luttenegger, 1988; Lunne et al, 1989; Marchetti, 1997). These correlations are essentially empirical

based and are supported by a limited number of numerical studies (e.g. Baligh & Scott, 1975; Finno, 1993; Yu et al, 1993; Smith & Houlsby, 1995; Yu, 2004).

Figure 6. Schematic representation of a dilatometer

2.6 *Standard Penetration Test (SPT)*

The SPT is the most widely used *in situ* testing technique, primarily because of its simplicity, robustness and its ability to cope with difficult ground conditions in addition to providing disturbed soil samples. A comprehensive review of procedures and applications of the SPT is given by Decourt *et al*. (1988) and Clayton (1995). There is a range of types of SPT apparatus in use around the world (for example those employing manual and automatic trip hammers) and, consequently, variable energy losses cannot be avoided. Variability due to unknown values of energy delivered to the SPT rod system can now be properly accounted for by standardizing the measured N value to a reference value of 60% of the potential energy of the SPT hammer (N_{60}), as suggested by Skempton (1986). In many countries, however, this recommendation has not been incorporated into engineering practice.

Moreover, even an SPT N value normalized to a given reference energy is not 'standard' because of the presently contentious issue of the influence of the length of the rod string.

The energy transferred to the composition of SPT rods was recently investigated by the author (Odebrecht, 2003; Odebrecht et al, 2004a; 2004b; Schnaid et al, 2004). This study has prompted a number of recommendations outlined to interpret the test in a more rational way on the basis of wave propagation theory. Recommendations are summarized as follows:

a) the energy transferred to the rod and to the sampler due a hammer impact should be obtained through integration of equation 2, calculated by the F-V method, and known as the Enthru energy:

$$E = \int_0^\infty F(t)\,V(t)\,dt \qquad (2)$$

with an upper limit of integration equal to infinity (practical is 1/10s but may require longer time intervals of integration (1/5s) in soft soils or long composition of rods).

b) the sampler energy can be conveniently expressed as a function of nominal potential energy E^*, sampler final penetration and weight of both hammer and rods. Influence of rod length produce two opposite effects: wave energy losses increase with increasing rod length and in a long composition of rods the gain in potential energy from rod weight is significant and may partially compensate measured energy losses.

c) efficiency is accounted for by three coefficients η_1, η_2 and η_3 that should be obtained from calibration. The hammer efficiency η_1 is obtained from measurements at the top of the rod stem. Efficiency factor η_2 can be assumed as unit. The energy efficiency η_3 is negatively correlated to the length of rods.

The *maximum potential energy*, PE^*, delivered to the soil should therefore be expressed as a function of the *nominal potential energy* E^*, and an additional energy related to the sampler penetration and the weight of both hammer and rods.

$$PE^* = E^* + (M_h + \mathrm{M_r})g\,\Delta\rho \qquad (3)$$

where: M_h = hammer weight;
M_r = rod weigh;
g = gravity acceleration;
$\Delta\rho$ = Sample penetration under one blow;
E^* = nominal potential energy = 0.76m 63.5kg 9.801m/s^2 = 474 J

The *nominal potential energy* E*= 474 J (ASTM, 1986) represents a part of the hammer potential energy to be transmitted to the soil. An *additional hammer potential energy* is given by $M_h\,g\,\Delta\rho$. The other part is transmitted by the *rod potential energy* $M_r\,g\,\Delta\rho$ which cannot be disregarded for tests carried out at great depths in soft soils, i.e. conditions in which $\Delta\rho$ and M_r are significant. For convenience, equation 3 can be written in two parts where the first represents the *hammer potential energy* (*nominal* + *additional*) and the second the *rod potential energy*:

$$PE^* = (0.76 + \Delta\rho)\,M_h\,g + \Delta\rho\,M_r\,g \qquad (4)$$

Equation 4 deals with an ideal condition, where energy losses during the energy transference process are not taken into account. However, it is well known in engineering practice that these losses occur, they should not be disregarded and should be considered by the efficiency coefficients previously introduced. Equation 5 becomes:

$$PE_{\mathrm{h+r}} = \eta_3[\eta_1(0.76 + \Delta\rho)\,M_h\,g + \eta_2\Delta\rho\,M_{\mathrm{r}}\,g] \qquad (5)$$

where

$$\eta_1 = \text{hammer efficiency} = \frac{\int_0^\infty F(t)\;V(t)\;dt}{(0.76 + \Delta\rho)M_h g}$$

$$\eta_2 = \beta_2 + \alpha_2\ell \approx 1$$

$$\eta_3 = \text{energy efficiency} = 1 - 0.0042\ell$$

It follows from the foregoing that normalization to a reference value of N_{60} is no longer sufficient to fully explain the mechanism of energy transfer to the soil and it is proposed that the system energy should be calculated using equation (5). Furthermore, it interesting to recall that the maximum potential energy can be transformed into work by the non- conservative forces (W_{nc}) acting on the sampler during penetration, and since the work is proportional to the measured permanent penetration of the sampler, it is possible to calculate the dynamic force transmitted to the soil during driving:

$$PE_{\mathrm{h+r}} = W_{\mathrm{nc}} = F_{\mathrm{d}}\,\Delta\rho$$

or (6)

$$F_{\mathrm{d}} = PE_{\mathrm{h+r}} / \Delta\rho$$

The dynamic force F_d can be considered as a fundamental measurement for the prediction of soil parameters from SPT results.

3 INTERPRETATION METHODS

The frontiers of a scientific field are defined as much by the tools available for observation as by the breakthroughs in theoretical developments. Several important concepts have been introduced or adapted to Soil Mechanics in past decades bringing new perspectives for the characterisation of geomaterials. Interpretation of *in situ* tests became a highly specialised subject that evolves using formal analytical or numerical solutions in addition to previously accepted semi-empirical approaches. Guidance is here provided on how to link theory to practice by establishing four classes in which interpretation of *in situ* tests can be broadly grouped:

Class I: Analytical solutions capable of idealising the field test into an equivalent realistic form. Ability to extract a plausible solution depends on the accuracy of constitutive models in representing soil behaviour and on the correctness of the imposed boundary conditions. This is achieved in a limited number of cases. Exact close form solutions are only applicable in tests that contain sufficient geometric symmetries to reduce the problem to a simple form, such as the expansion of spherical and infinite long cylindrical cavities in a semi-infinite elastic-plastic continuum.

Class II: For cases in which close form solutions cannot be obtained, adequacy of numerical solutions largely depend upon the constitutive model adopted to represent soil behaviour. There are solutions that offer a very close approximation of the physical mechanism of a test; these solutions are regarded as rigorous and are defined as Class II, as for example the family of numerical analyses applied to describe the penetration mechanism in high plastic clays of a cone or flow penetrometer (e.g. Yu, 2004; Randolph, 2004).

Class III: Approximate analytical solutions developed on the basis of simplified assumptions imposed to reduce the constraints required for a more rigorous approach. For penetration tools, the concepts of bearing capacity (e.g. Durgunuglu & Mitchell, 1975; de Mello, 1971) and cavity expansion (e.g. Vesic, 1972; Salgado et al, 1997) form the background for this category of analysis. Since bearing capacity theories carried out using limit analysis are unable to account for soil stiffness and volume change, they can just be regarded as approximation to model penetration problems. Calibration chamber tests and centrifuge tests are recommended to validate Class III type of correlations.

Simple solutions such as Class III should be preferably achieved from a combination of measurements from independent tests. Since in the interpretation of *in situ* tests the number of controlling variables (soil parameters) well exceeds the number of measured variables, the combination of independent measurements reduces the degree of uncertainty. The author foresees increasing use of interpretation methods under this third category with a growing trend towards the combination of various sensors incorporated in a single penetration probe. This report explores extensively the ratio of the elastic stiffness to ultimate strength (G_o/q_c, G_o/N_{60}), the ratio of cone resistance and pressuremeter limit pressure (q_c/Ψ) and the association of strength and energy measurements (N_{60} and energy).

Class IV: Empirical analysis based on direct comparisons with structure performance and correlations to laboratory test results. Complexities in the interpretation of *in situ* tests in unusual geomaterials and poorly defined ground conditions still prompts the use of empirical approaches in geotechnical engineering practice (e.g. Schnaid et al, 2004).

Both the limitations associated to the interpretation of *in situ* tests in different geomaterials and the difficulty of isolating the independent factors that control the test mechanism have prompted the development and use of *laboratory physical modelling*. Two techniques are now recognised as reference: centrifuge and large calibration chamber tests. Well-planned series of laboratory physical modelling tests can be used to establish correlations for field tests that, although empirical, are set against controlled variables (such as density, stress history, horizontal and vertical stresses) and reproduce some of the environmental requirements for calibration against field data.

A calibration chamber consists of a large cylindrical homogeneous sample of known density. Chamber-walls can either support flexible rubber membranes from which uniform stresses are applied or can be rigid in the lateral direction when imposing zero lateral strain conditions (K_o) on the sample. Stress-controlled boundary conditions are more generally adopted, in order to investigate the independent effects of vertical and horizontal stress on penetration tests (e.g. Parkin & Lunne, 1982; Schnaid and Houslby, 1992). For tests carried out in sand, where a rigorous theoretical analysis is difficult, this technique represents the best way of establishing well defined calibrations of *in situ* testing devices. Note that this is in contrast with clays, for which calibration chamber tests are nearly unfeasible due to time constraints, and calibration of analytical procedures at well-documented test sites is a more sounding approach.

In sands laboratory calibration chamber tests have provided databases that support empirical interpretation procedures between tip cone resistance q_c and relative density (D_r) or friction angle (ϕ'). Typical calibration programmes involve the state of stress of the sample and reflect the combined effects of sand stiffness, dilatancy and mineralogy. There has been enough experience on penetration tests to demonstrate that there is essentially no correlation between tip cone resistance q_c and the vertical stress for tests carried out at different combinations of σ'_{vo} and σ'_{ho} (for K_o values between 0.4 and 1 considered to be the possible limits for sand). However, there is a sounding correlation between q_c and the horizontal stress which suggests the need to take into account the horizontal stress, or at least the mean stress, in field correlations (e.g. Houlsby & Hitchman, 1988; Schnaid & Houlsby, 1992).

Centrifuge tests have been gaining increasing popularity in the past 20 years as a physical modelling technique in all type of soils. The technique has been successfully applied to model classical problems such as foundation and slopes, environmental aspects of contaminant transport and seismic events. Results have been documented in conferences organised under the auspices of TC2. The fact that scale models can be prepared with prescribed soil property profiles in clay, sand or intermediate soils, and shaken in the simulated gravity environment under controlled input motion (e.g. Schofield& Steedman, 1988; Taylor, 1995) makes this approach particularly attractive as a means to produce controlled sets of *in situ* test data.

The main disadvantage of *laboratory physical modelling* is that models are of limited size and assessment of chamber size effects and boundaries conditions in the calibration of *in situ* tests is always necessary (Baldi et al, 1982; Parkin & Lunne, 1982; Been et al, 1987; Mayne & Kulhawy, 1991; Schnaid and Houslby, 1992). Experimental and numerical data demonstrate that for all sand densities the chamber size can affect the results, with the effect being more severe for dense sands due to sample dilation (even for chamber to probe diameter ratios of 40). It is vital that such effects should be properly quantified if accurate calibrations of *in situ* testing devices are to be obtained.

For large laboratory calibration chambers, a sounding alternative to substantially reduce boundary effects is the use of simulator capable of controlling horizontal stress during penetration (Foray, 1991; Ghionna & Jamiolkowski, 1991; Huang & Hsu, 2004). Using a servo-controlled mechanism connected to a series of rings, that replace the single rubber membrane, Huang & Hsu (2004) allow the lateral stress to vary

as the cone is being pushed into the sample. The increase in stress is calculated from the radial strains measured at the cavity wall (Foray, 1991) and, by doing so, the authors simulate a semi-infinite half-space at the soil-membrane interface. Figure 7 shows CPT tests in dense samples (Dr=84%) for stress state that corresponds to σ'_{vo}=56kPa and σ'_{ho}= 22 kPa, in which fairly similar q_c *versus* depth profiles have been obtained for chamber to probe diameter ratios D/B of 22 and 44 indicating the reduction in size effects.

As for the centrifuge, a direct implication is the recognition that a variation in horizontal stresses at the boundaries of the strongbox needs to be accounted for, i.e. the strain field displaced by driving a cone into the sample may eventually reach the rigid boundary of the box and will result in an increase in horizontal stress with respect to the initial σ_{ho} value. Load cells embedded in the centrifuge specimen for monitoring possible variations on σ_h during cone penetration are the only reliable way of assessing boundary effects. An example is given in Figure 8, in which the variation with time of the measured horizontal stress at four given depths (0.06m, 0.12m, 0.18m and 0.24m) for four CPT tests carried out at 30g, 20g and 10g is presented. The number inside the square indicates the distance in centimetres between the cone penetrometer and the load cell where the horizontal stress has been recorded. Cone penetration produced an increase in horizontal stresses $\Delta\sigma_h$ to a distance up to 80 cm. This distance corresponds to 66 times the diameter of the probe and is significantly higher than those recognised by a number of authors, usually restricted to the range of about 10 to 20 times the diameter of the probe (e.g. Gui et al, 1998; Bolton et al 1999). As expected, the magnitude of $\Delta\sigma_h$ reduces with increasing distance between the pressure cell and the location of the test. In addition, the strongbox is rectangular and unlike the axi-symmetric conditions imposed in a cylindrical laboratory calibration chamber, the benefits of symmetry around the cone are no longer valid. Any correction due to increasing border stresses is therefore empirical in nature and should be viewed with caution. Use of circular containers is strongly recommended when continuous in-flight strength profile of the specimens is correlated to soil properties. A first test can be conducted at the centre of the specimen and subsequently the penetrometer can be moved to the quarter points of the container.

This brief review highlights the fact that geo-characterisation and properties of natural soils can be made using different testing techniques and can rely on various methods of interpretation (Class I, II, II and IV). These approaches are extensively covered in this Report and are applied to geomaterials such as clay, sand, intermediate permeability silt and bonded soils.

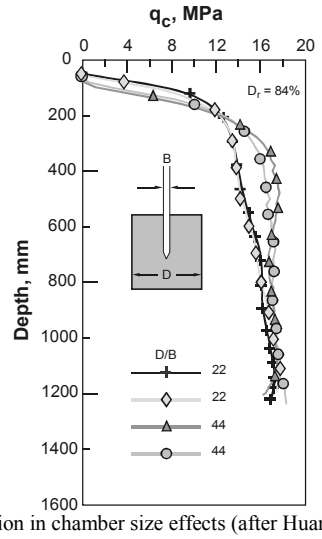

Figure 7. Reduction in chamber size effects (after Huang & Hsu, 2004).

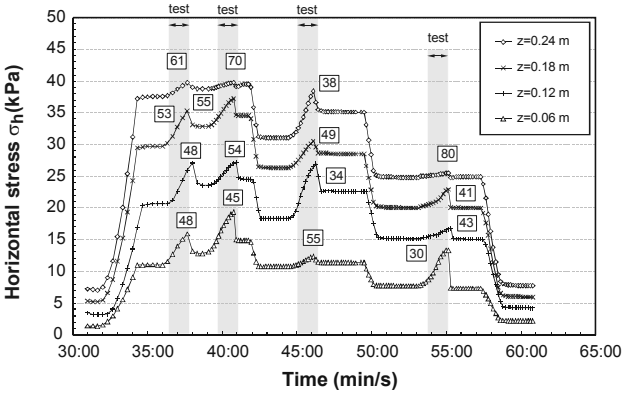

Figure 8. Centrifuge boundary effects (modified from Gaudin, Schnaid & Garnier, 2005).

4 CLAY PROPERTIES

4.1 *Background research*

Assessment to the properties of clay is on itself an extensive subject that is much beyond the scope of this report. Inevitably a short discussion cannot meet the complexity of the subject and is bound to suffer from being too selective. A comprehensive overview of the topic comprising the interpretation of both laboratory and *in situ* tests in clay has been given by Ladd et al (1997); Jamiolkowski et al (1985); Burland (1990), Leroueil & Hight (2003), Yu (2004), among others. This Report aims only at determining the factors which affect the interpretation of *in situ* tests, and for that purpose a framework for describing the behaviour of clays is outlined.

Important contributions over the last 15 years have attempted to integrate all geomaterials in a consistent and unified framework by demonstrating that soil structure is a common feature in a wide range of soils, from natural deposits to man-made earth-fills. To distinguish features of behaviour emerging from structure from those related to changes in state, a widespread approach has been to compare the response of the natural soil to that of the corresponding reconstituted material (e.g. Burland, 1990). Whilst in reconstituted soils the shear behaviour is controlled solely by a combination of deviator stress, mean effective stress and specific volume (and as a consequence the shear stiffness at any strain is expressed as a function of their current state), natural clay exhibit a structural behaviour that does not conform with the framework developed for reconstituted materials (Burland, 1990; Leroueil & Vaughan, 1990).

Typical behaviour of structured clay in isotropic compression is illustrated in Figure 9 for tests carried out in Pappadai clay compressed to stresses well beyond yield stress (Cotecchia & Chandler, 1997). Because of microstructure, natural clay samples can reach a domain of the (e-log σ'_v) space that is not permitted for the reconstituted clay leading to a higher pre-consolidation pressure. Beyond yield stress, plastic strain increments become substantially larger as a result of structure degradation.

As for stress-strain curves and stress paths from shear compression and extension tests, the characteristics to note are:

a) due to structure and overconsolidation, natural clays show a strong resistance in shear until a peak is reached at relatively small strains. Large strains developed beyond peak are associated to strain softening and strain softening effects reduce with increasing OCR.
b) stiffness increases with soil structure and reduces with increasing OCR and shear strain amplitudes. From yield locus of natural clays determined from laboratory tests, it is recognized that multiple kinematic yield surfaces have to be considered since soil does not behave as a simple elastic-plastic material. A simplified scheme proposed by Jardine

(1992) is illustrated in Figure 10 and is adopted as reference in this Report. Soils display non-linear stress strain behaviour that can be broadly characterised by the linear threshold strain, ε_{Y1} (point A in Fig. 10), the strain marking the limit to recoverable behaviour ε_{Y2} (point B) and the strain denoting the onset of large scale yielding, ε_{Y3} (point C) (e.g. Jardine, 1985; Tatsuoka *et al.,* 1997). At very small strains, within the limit state curve defined by ε_{Y1}, soils are believed to behave as elastic materials represented by the initial elastic stiffness G_o. The magnitude of G_o is measured in the laboratory using bender elements or resonant column tests (e.g. Jardine et al, 1984; Tatsuoka et al, 1995; Ishihara, 1996; Clayton & Heymann, 2001; Lo Presti et al, 2001) and in the field by seismic techniques (Sharma, 1997; Santamarina et al, 2001). Comprehensive reviews of this topic are reported both at the International Conferences of Pre-Failure Deformation Behaviour of Geomaterials" in 1995, 1997, 1999 and 2003 and by number of individual papers (e.g. Hardin, 1978; Stokoe et al, 1994; Jamiolkowski et al, 1995; Lo Presti et al, 1999; Tatsuoka et al, 1997; Rampello & Viggiani, 2001).

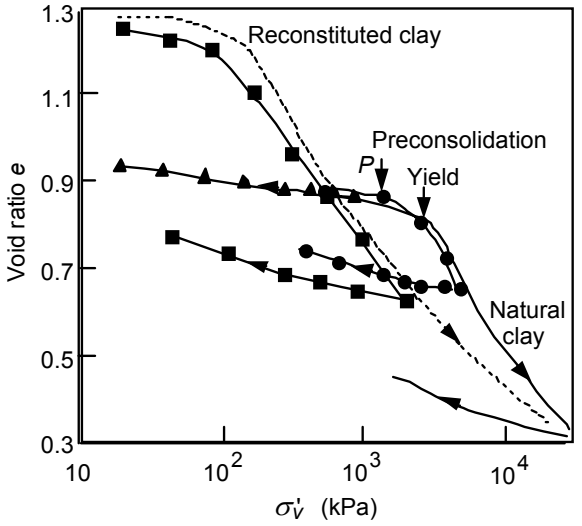

Figure 9. One-dimensional compression behaviour of the natural and reconstituted Pappadai Clay (Cotecchia & Chandler, 1997).

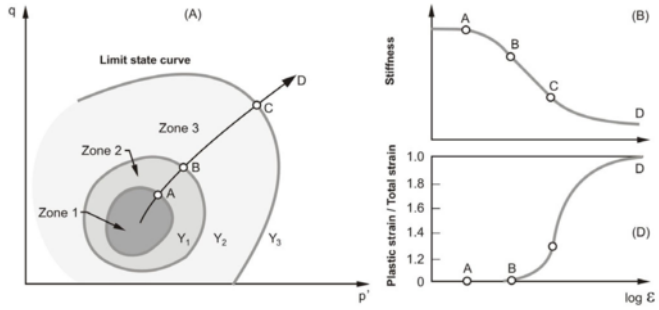

Figure 10. Scheme of multiple yield surfaces and soil response (Jardine et al, 1991).

c) for a given clay profile, the limit state curve (LSC) obtained at different depths have similar shapes and can therefore be normalised by the preconsolidation pressure (Shansep method, after Ladd et al, 1977; Graham et al, 1983). The general shape of the LSC curves of natural clays is known to depend mainly on the friction angle (Dias Rodriguez et al, 1992) and is approximately centred on the K_o(NC) line in a $(\sigma'_a-\sigma'_r)/2$ *versus* $(\sigma'_a+\sigma'_r)/2$ diagram, which is attributed to soil anisotropy (Tatsuoka & Shibuya, 1991; Belloti *et al.,* 1996; Hight *et al.,* 1997; Tatsuoka *et al*, 1997). This reflects the anisotropy of fabric developed during deposition and one-dimensional consolidation of natural soft clay deposits. With the increase in isotropic consolidation, the LSC expands and changes shape, the structure gradually breaks and becomes symmetrical with respect to hydrostatic axis. These features are shown in Figure 11, in which the LSC curve of Sarapui clay is normalised with respect to the preconsolidation pressure (Almeida & Marques, 2003).

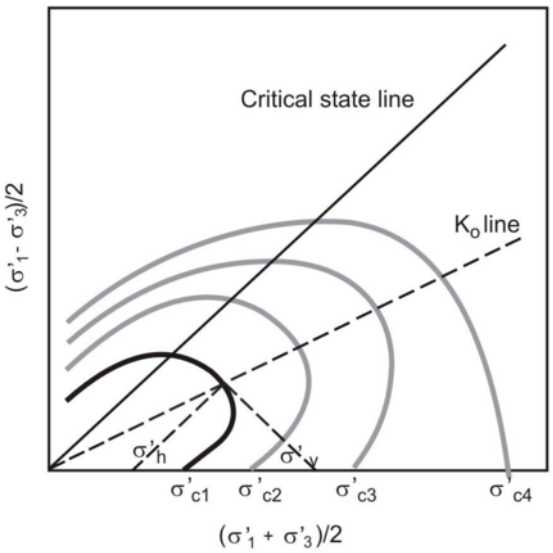

Figure 11. Limit State Line for Sarapui Clay (Almeida & Marques, 2003).

d) in addition, experimental observations in reconstituted soft clay samples show that stress anisotropy should also be taken into account and in this case the effects of anisotropy may not be erased even after a complete destructuration of the soil (e.g. Tatsuoka et al, 1997; Koskien et al, 2002).
e) at large strains the soil tends towards an ultimate condition at which there is no change in void ratio and effective stress. This ultimate state is defined as critical state from where the basic elastic-plastic concepts that govern the response of clay have been integrated in a single framework by Critical State Soil Mechanics, given rise to complete Cam-Clay models (e.g. Schofield & Wroth, 1968; Roscoe & Burland, 1968). The model parameters are the shear modulus, the slope of the critical state line in a q:p′ diagram M, the slope of the virgin consolidation λ and of the swelling line κ in the (e – lnp') diagram and the critical void ratio e_c. The M parameter is not the same in compression and in extension, the ultimate state in triaxial compression exceeds that in triaxial extension. The yield function illustrated in Figure 12a can be conveniently expressed in terms of mean effective stress p' and deviator stress q (Roscoe & Burland, 1968):

$$\frac{p'}{p'_m} - \frac{M^2}{M^2+\eta^2} = 0 \qquad (7)$$

where p'_m define the size of the yield surface.

The model conceived on the basis of tests performed on reconstituted and isotropically consolidated clays has been systematically extended to other geomaterials, more general stress states and consolidation histories in attempting to reflect some of the important features of soil behaviour previously described. Gens & Nova (1993) introduced the concepts

necessary to incorporate bonding and destructuration effects within elastic-plastic constitutive models (see Figure 12b). In addition to the yield surface of a natural structured geomaterial, an "intrinsic yield surface" is adopted to represent the size of the yield surface of an equivalent unbonded material that is assumed to have the same shape as the one of the natural soil. Concepts introduced to describe soil anisotropy are represented in Figure 12c, following the work by Whittle & Kavvadas (1994), Pestana & Whittle (1999), Wheller et al (2003), among others. Wheller et al (2003) has recently demonstrated that for simplified axi-symmetric conditions of a triaxial test on a cross-anisotropic sample, with the horizontal plane in the triaxial sample coinciding with the plane of isotropy of the sample, the yield curve can be expressed as:

$$(q-\alpha p')^2-(M^2-\alpha^2)(p'_m-p')p'=0 \qquad (8)$$

where α defines the orientation of the yield curve. The model incorporates two hardening laws: the first to describe changes of size of the yield surface and the second to describe the change in orientation of the yield surface with plastic straining so that when α=0 soil behaviour becomes isotropic.

Finally there is a recognition that strength and stiffness increase with increasing shearing rate (e.g. Shibuya et al, 1997; Stoke et al, 1995; Tatsuoka et al, 1995, 1997). Since the loading rate of most common geotechnical in situ tests (SPT, CPT, vane) is significantly higher than that of construction activities subjected to monotonic loads, typically up to 6 to 8 orders of magnitude, rate effects are of significance when deriving properties from test data.

Investigation from laboratory tests has demonstrated that natural clays will exhibit higher preconsolidation pressure, undrained shear strength and stiffness than the same soil in the same state, but unstructured. The mechanical response reflects stiffness non-linearity, small and large strains anisotropy and strain rate effects. This Report discusses the interpretation of *in situ* tests in the light of the characteristic behaviour of clay, introduces the assumptions that are made as part of the interpretation of test data and highlights the consequences of these assumptions on the predicted soil properties.

4.2 *Stiffness*

Soil stiffness depends upon interactions of structure (bonding, fabric, degree of cementation), strain level (and effects of destructuration), stress history and stress path, time dependent effects (aging and creep) and type of loading (monotonic or dynamic). Despite these complex interactions, the characteristic response of clay with respect to small strain stiffness, small strain anisotropy and stiffness non-linearity can be directly assessed from *in situ* tests.

Hardin & Black (1968) and Hardin (1978) identified various factors governing the G value and proposed a general expression:

$$G = f(\sigma'_v, e_o, OCR, S_r, C, K, T) \qquad (9)$$

where σ'_v is the effective overburden stress, e_o initial void ratio, OCR overconsolidation ratio, S_r degree of saturation, C grain characteristics, K soil structure and T temperature. Laboratory resonant column tests carried out to characterise G_o have shown that in a reconstituted clay stiffness is a function of mean stress and that the effect of OCR is partially embedded into the effect of void ratio. An empirical correlation to describe G_o can then be written as:

$$G_o = SF(e)(\sigma'_v\sigma'_h)^n p_a^{(1-2n)} \qquad (10)$$

where S and n are experimental constants and F(e) is the void ratio function. F(e) can take the form of (1/e), (1+e) or (2.17-e)^2/(1+e), leading to the following representative correlations:

$$G_o = 625\frac{1}{(0.3+0.7e^2)}(p'_o)^{0.5}OCR^k \qquad k=PI^{0.72/50}<0.5$$

Hardin (1978) (11)

$$G_o = 480(e)^{-1.43}(\sigma'_v)^{0.22}(\sigma'_h)^{0.22}(p_a)^{1-2(0.22)}$$

Jamiolkowski et al (1995) (12)

where p_o = mean effective stress, p_a = atmospheric pressure and PI= plasticity index. Coefficients in the above equations represent average recommended values and units are in kPa.

The need to express G_o as a function of the mean stress is recognized, the effects of vertical and horizontal stresses being investigated as separate variables by Jamiolkowski et al (1995). Since σ_{ho} is not usually known accurately, Shybuya et al (1997) considered more practicable to express G_o as a function of σ_{vo} with the due recognition that its validity is restricted to normally consolidated clays.

$$G_o = 24000(1+e_o)^{-2.4}(\sigma'_v)^{0.5}(kPa) \qquad (13)$$

For preliminary projects, various authors proposed to estimate G_o directly from tip cone resistance q_c or q_t (e.g Rix & Stoke, 1992; Mayne & Rix, 1993; Tanaka et al, 1994; Simonini & Cola, 2000; Powell & Butcher, 2004; Watabe et al, 2004). Mayne & Rix (1993) suggested a correlation that explicitly considers the dependency of G_o upon void ratio:

$$G_o = 406q_c^{0.695}e_o^{-1.130}(kPa) \qquad (14)$$

Tanaka et al (1994) developed the following relationship between the small stiffness measured from the seismic cone and net cone resistance:

$$G_o = 50(q_t-\sigma_{vo})(kPa) \qquad (15)$$

Care must always be taken when using equations 14 and 15, since strictly speaking a small strain value cannot be derived from an ultimate strength measurement and therefore these correlations should be seen just as an indication of stiffness that do not replace the need for direct measurements of shear wave velocities.

Information of the anisotropy of small strain stiffness (inherent and stress induced) from seismic measurements is becoming more readily available and is a generally recommended technique. The G_{vh} value from a down-hole survey where the shear wave propagates in the vertical direction with the particle motion in a horizontal direction differs from the comparable G_{hh} from a cross-hole survey. Leroueil & Hight (2003) presented a compilation of data on the anisotropy of small strain stiffness in natural and reconstituted soft and stiff clays shown in Figure 13, expressed in terms of the ratio G_{hv}/G_{hh} or G_{vh}/G_{hh} *versus* consolidation stress ratio σ'_v/σ'_h. In Bothkennar Clay, the fabric has rendered a stiffness ratio ranging from 0.8 to 1.0 in an unconfined state. Jamiolkowski et al (1994) found G_{vh}/G_{hh} ratios under isotropic stress conditions of 0.7 and about 0.65 for the natural Pisa and Panigalia clays respectively. *In situ* data for the stiff and very stiff London and Gault Clays are very similar, although under isotropic stress conditions the Gault shows a lower ratio for G_{vh}/G_{hh}.

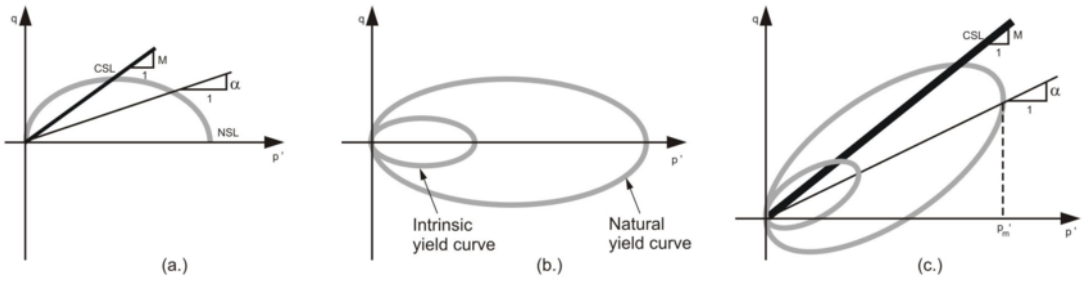

Figure 12. Yield surfaces for clay: (a) modified Cam-Clay, (b) structured material and (c) structure and anisotropy

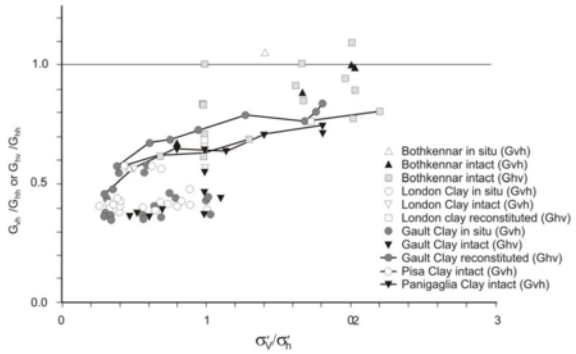

Figure 13. Small strain stiffness anisotropy in natural and reconstituted clays (Leroueil & Hight, 2003).

Since due to anisotropy G_o is not independent on the direction of propagation and polarization of shear waves, correlations with penetration resistance should preferably be expressed as a function of G_{vh}, G_{hv} or G_{hh}. Powell & Butcher (2004) recently suggested that there is no single correlation between q_t and G_{vh} for all clays as often advocated from DHT. The authors have found a strong correlation between G_{hh} and q_t, which is partially explained by the strong dependency of q_t on the horizontal stress. Figure 14 shows a set of results in a logxlog plot that, given the scatter, should also be viewed as an indication of G_o only.

Whereas the initial shear modulus G_o is considered to be a fundamental soil property, a knowledge of the non-linear and inelastic stress-strain response of geomaterials is now fully recognized as being critical to the prediction of ground movements. The ever-increasing popularity of the shear wave velocity and hence G_o measurement is encouraging, but, in its own right, is of limited value because governing strain levels in the vicinity of geotechnical structures are 'small to intermediate' and far greater than the very small strain pertaining to seismic measurements Reduction of shear stiffness with shear strain amplitude can be obtained from a combination of seismic measurements and laboratory or *in situ* tests. From the existing *in situ* tests (piezocone, pressuremeter, dilatomer, plate loading), the pressuremeter offers the most realistic possibility of assessing the non-linear response of clay.

In a pressuremeter test soil stiffness can be assessed from the complete pressure-expansion curve or from interpretation of unload-reload loops, which is particular attractive since it provides a measuring of the elastic shear stiffness in a procedure that avoids many of the problems of disturbance that are associated with laboratory testing (e.g. Wroth, 1984; Fahey, 1998; Whittle, 1999). The problem is that the test does not, however, measure an 'element stiffness' and interpretation of (non-linear) elemental stiffness characteristics relies on an appropriate numerical backanalysis method coupled with a realistic soil constitutive model (e.g. Fahey & Carter, 1993; Bolton & Whittle, 1999).

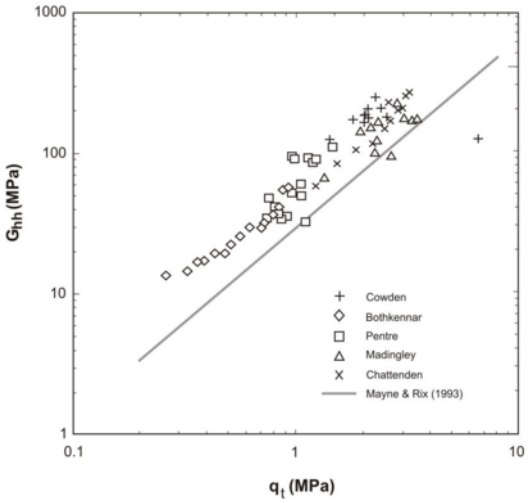

Figure 14. Comparison between G_{hh} with q_t (Powell & Butcher, 2004).

The strains undergone by elements of soil at different distances from the pressuremeter are inversely proportional to the square of the radius in an undrained test and therefore a reference shear strain has to be arbitrarily selected as representative of an unload-reload shear modulus, G_{ur}. This reference value is often taken as the strain applied at the pressuremeter surface. Houlsby (1998) justifies the choice by demonstrating that the measured G_{ur} is very much dominated by the stiffness of the soil close to the pressuremeter.

Muir Wood (1990) explores the variation of G_{ur} with shear strain amplitude in clays. In a pressuremeter it is possible to define a secant modulus $G_s^p = (\psi - \sigma_{ho})/2\varepsilon$ and a tangent modulus $G_t^p = {}^1\!/_2 \, {}^{d\psi}\!/_{d\varepsilon}$. This is similar to laboratory tests in which it is also possible to define a secant $G_s = \tau/\gamma$ and a tangent modulus $G_t = d\tau/d\gamma$, where τ is the shear stress. Following these definitions it is straightforward to demonstrate that:

$$G_t = G_s + \gamma \frac{dG_s}{d\gamma} \tag{16}$$

$$G_t^p = G_s^p + 2\varepsilon \frac{dG_s^p}{2d\varepsilon} \tag{17}$$

and

$$G_s = G_t^p = G_s^p + 2\varepsilon \frac{dG_s^p}{2d\varepsilon} \tag{18}$$

Thus in clay, according to Muir Wood (1990) the tangent modulus measured from the pressuremeter curve is equal to the secant modulus from a conventional laboratory test. This enables the results of pressuremeter tests to be properly

related to those of other tests by means of degradation models designed to express the variation of G with γ. Simple to fairly elaborated formulations have been proposed to express G *versus* γ relationships in the form of a logarithm or a hyperbola. Regardless the model adopted in the analysis, Fahey (1998) strongly recommends that combining seismic G_o measurements and SBP tests incorporating multiple unload-reload loops is currently the only accurate method of obtaining non-linear stiffness parameters from *in situ* tests.

4.3 *Undrained shear strength*

The undrained shear strength of clays, in common with all soils, depends on the mode of failure, rate of shearing, soil anisotropy and stress history. For a clay that conforms with CSSM , the ratio S_u/σ'_p ranges from 0.25 to 0.30 depending on shearing mode, where σ'_p is the preconsolidation pressure (Ladd et al, 1977; Jamiolkowski et al, 1985; Ladd, 1991). The reference test adopted to measure S_u, against which an in situ test is calibrated, should be identified and S_u should be defined as S_u(TX-CIU), S_u(TX-CKoU) or S_u(FVT).

Vane tests are used primarily to determine the undrained strength of clays. S_u values interpreted from vane tests are influenced by disturbance, rotation rate, delay between insertion and testing, as well as by the shear stress distribution around the blades. Assumptions regarding these effects are well known and systematically reported (e.g. Aas, 1965; Wroth, 1984; Chandler, 1988). Although the conventional analysis assumes that the shear strength is isotropic, the vane offers the simplest possible way of investigating the large strain anisotropy of clays. The undrained shear strength can be determined from the measured torque T by the following general expression:

$$S_{uv} = \frac{2T}{\pi D^3 \left(\frac{H}{D} \frac{1}{(n+3)} \frac{S_{uh}}{S_{uv}} \right)} \qquad (19)$$

where H/D is the aspect ratio, S_{uv}/S_{uh} is the strength ratio describing anisotropy and n is the power law describing the shear strength distribution on the top and bottom planes (Wroth, 1984). The vane torque on the vertical and horizontal planes can be separated provided a series of vane test data with different H/D is available, allowing assessment to soil anisotropy. In this case, the angular rotation rate should be adjusted to avoid the influence of the peripheral velocity on measurements of undrained shear strength (e.g. Biscontin & Pestana, 2001). This implies that vanes of different sizes and same aspect ratio should yield the same undrained shear strength, whereas different aspect ratios would give assessment to soil anisotropy.

An increasing trend for the use of piezocone in the characterisation of soft clay deposits is being observed worldwide, gradually replacing the standardized practice of performing vane tests. This tendency is justified by the recognition of the CPTU as a superior profiling tool, as well as by its capability of deriving soil parameters for geotechnical design. When carrying out cone penetration tests under undrained conditions, cone tip resistance q_c is related to S_u as follows:

$$q_c = N_c S_u + \sigma_0 \qquad (20)$$

where N_c is a theoretical cone factor and σ_o is the *in situ* total stress (either vertical or mean total stress). The theoretical solutions available for determining N_c can be grouped as (e.g. Yu and Mitchell, 1998; Yu, 2004):

a) bearing capacity theory (BCT)
b) cavity expansion theory (CET)
c) strain path methods (SPM)
d) finite element methods (FEM)

As pointed out by Yu (2004), while each theory may be used alone for cone penetration analysis, better predictions of cone penetration mechanisms may be achieved if some of the methods are used in combination (Teh and Houlsby, 1991; Abu-Farsakh et al, 2003). Table 2 summarises the most significant theoretical solutions for N_c.

Solutions generally assume isotropy of strength and stiffness and radially symmetric initial stresses. A single solution can account for effects of anisotropy that result from both structure and rotation of principal stresses around an advancing cone (Su & Liao, 2002). The authors proposed cone factors expressed as a function of the strength anisotropy ratio $A_r=(S_u)tc/(S_u)te$, with the undrained shear strength $S_u$tc and $S_u$te measured from CK_oU compression and CK_oU extension triaxial tests respectively. The effect of anisotropy is not always significant, maximum differences in cone factors of up to 20% obtained for normally to slightly overconsolidated clay with moderate to high strength anisotropy.

Whereas theoretical solutions have been contributing in the understanding of the fundamental mechanics of cone penetration, empirical correlations are still widely used in practice to estimate S_u from cone resistance. The most widely used correlation is:

$$q_t = N_{kt} S_u + \sigma_{v0} \qquad (21)$$

where q_t is the cone resistence (corrected for pore pressure), N_{kt} is an empirical cone factor and σ_{vo} is the total *in situ* vertical stress. Values of N_{kt} range from 10 to 20 and are influenced by soil plasticity, overconsolidation ratio, sample disturbance, strain rate and scale effects, as well as the reference test from which S_u has been established (Aas et al, 1986; Mesri, 1989; 2001; Lunne et al, 1997). Stress history affects strength, stiffness, strain softening and strain to failure which in turn changes N_{kt}. Comparisons between theoretical and empirical predicted N_{kt} factors are shown in Figure 15, for I_r ranging from 50 to 500 and strength anisotropy ratio of 0.5 to 0.9. In practice the choice of average I_r values is arbitrary and N_{kt} values from 12 to 15, often adopted in engineering design problems, are generally higher than theoretical predicted values for rigidity indexes between 50 and 200.

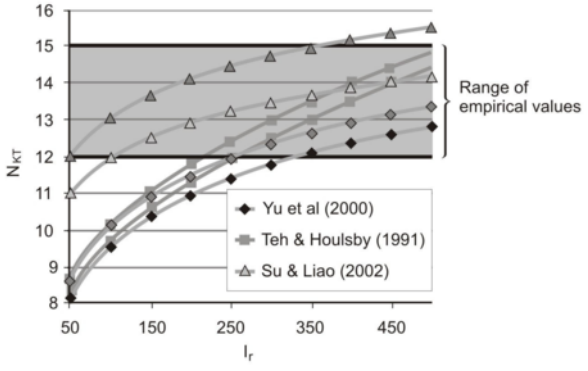

Figure 15. Theoretical predictions of N_{KT} factors for clay

Recent developments using full flow probes, including T-bar, spherical ball and plate penetrometers (e.g. Randolph, 2004), have been used with the purpose of overcoming the uncertainties in determining the undrained shear strength in soft clay, due to the usual corrections necessary with the CPTU and the complicate mechanism around the cone that

reflects on N_{kt}. In a flow bar penetrometer lower and upper bound solutions can be found, as the problem of considering an intrusive volume introduced into the soil during cone penetration is avoided. The bearing capacity factor can be conveniently expressed as the ratio of an average penetration resistance q_u to the shear strength S_u, so that $N=q_u/S_u$. A theoretical bearing capacity solution of 10.5 for the T-bar N factor was first presented by Randolph & Houlsby (1984). Recently, Randolph (2004) introduced a new solution for this penetration mechanism which is shown in Figure 16 for a plot that relates the N factor to the interface friction ratio α at the T-bar-soil interface. In this figure the theoretical solution for T-bar is compared to cone and ball penetrometers and is shown to be insensitive to Ir (upper and lower bounds are essentially the same). Long & Phoon (2004) summarized recent published data using the T-bar and demonstrated that on average the experimental values are close to the theoretical bearing capacity number of 10.5 from Randolph & Houlsby (1984) and within the range proposed by Randolph (2004).

The above discussion is concentrated on penetration problems in normally and slightly overconsolidated clay where modified Cam-Clay reproduces characteristic features of behaviour with reasonable accuracy. Heavily overconsolidated clay cannot be successfully modeled and therefore theoretical values of N_{kt} produce unrealistic predictions of undrained shear strength. Engineers should relay solely on empirical correlations which yield N_{kt} values in the range of 15 to 30 (e.g. Lunnet et al, 1997).

Without realistic theoretical solutions, and given the fact that penetration in OC geomaterials may be difficult, the SPT still offers considerable appealing for qualitative and quantitative evaluation of soil properties *in situ*. A simple approach based on limit equilibrium and wave propagation analysis has been proposed by Schnaid et al (2004) and can be useful in assessing the undrained shear strength in OC clays. First an idealization of the penetration mechanism is required. In OC materials the plug of soil which has been formed within the hollow section of the sampler is sufficiently strong not to be removed by penetration forces, and consequently bearing capacity has to be predicted on the basis of both shaft and base resistance. For a purely cohesive soil, bearing capacity equations would then take the following form:

$$F_e = (N_c\ A_b\ S_u + \gamma\ L A_b) + (S_u\ \alpha\ A_l) \qquad (22)$$

where: F_e = Static penetration resistance
N_c = bearing capacity factor
γ = bulk unit weight
L = depth of the sampler
α = adhesion factor
A_b, A_l = area of base and shaft of sampler

Combination of equations 4, 5 and 22, leads to the determination of undrained shear strength which requires a calibration from energy measurements to determine η_1, η_2 and η_3 (section 2), estimation of α (Flaate, 1968; Tomlinson, 1969) and a prediction of N_c (or $N_{k,SPT}$). $N_{k,SPT}$ should be obtained by calibration against undrained shear strength values measured from a reference test in site-specific correlations and will reflect the dynamic nature of the test. Application of equation 22 to Guabirotuba clay (Schnaid et al, 2005) is shown in Figure 17, in which considerable scattered is observed in a plot of undrained shear strength *versus* depth. Predicted values of S_u from SPT fall within the region defined by other tests in this OC clay.

Table 2: Theoretical cone factor solutions

N_c	Penetration model	Reference
7.0 to 9.94	BCT	Caquot & Kerisel (1956); de Beer (1977)
$3.90+1.33\ln I_r$	CET	Vesic (1975)
$12+\ln I_r$	CET	Baligh (1975)
$\left(1.67+\frac{I_r}{1500}\right)(1+\ln I_r)+2.4\lambda_c-0.2\lambda_s-1.8\Delta$	SPM+ FEM	Teh & Houlsby (1991)
$0.33+2\ln I_r+2.37\lambda-1.83\Delta$	FEM	Yu et al (2000)
$\frac{1+A_r}{\sqrt{1+2A_r}}\ln I_r+\frac{1-A_r}{3}+R\left(1+\frac{1+A_r}{\sqrt{1+2A_r}}+0.52A_r^{1/8}(1+A_{r)}\right)-2\Delta$	CET+ FEM	Su & Liao (2002)
$2.45+1.8\ln I_r-2.1\Delta$	CET+ FEM	Abu-Farsakh et al (2003)

Note: $I_r = G/S_u$; $\Delta = \frac{\sigma'_{vo}(1-K_o)}{2S_u}$; λ= cone roughness; A_r=strength anisotropy ratio.

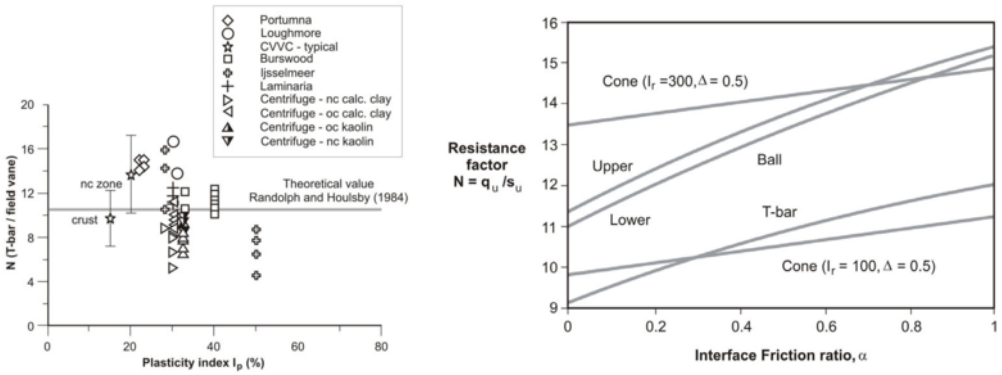

Figure 16. (a) Bearing capacity from T-bar: (a) Long & Phoon (2004) and (b) Randolph (2004)

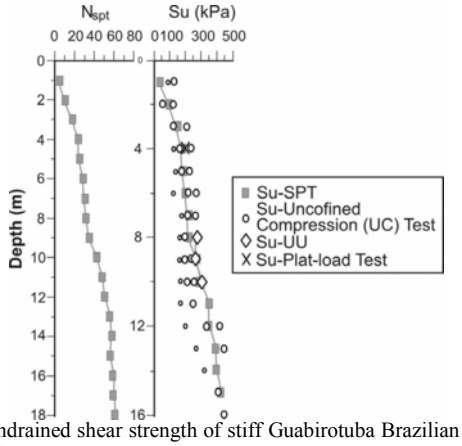

Figure 17. Undrained shear strength of stiff Guabirotuba Brazilian Clay (Schnaid et al, 2005).

The pressuremeter is a well-suited alternative to penetration, since theoretical interpretation methods that reduce the expansion process to one dimension by idealizing the geometry of a pressuremeter probe as an infinitely long, cylindrical cavity are well established. A total stress loading analysis of cylindrical expansion in cohesive material was first examined by Gibson & Anderson (1961). The authors derived a theoretical expression for the total pressuremeter pressure P at the stage of plastic loading:

$$P = \sigma_{ho} + S_u \left[1 + \ln\left(\frac{G}{S_u} \right) \right] + S_u \ln \frac{\Delta V}{V} \qquad (23)$$

where ΔV/V is the volumetric strain and σ_{ho} the total *in situ* horizontal stress. By plotting pressuremeter results in terms of cavity pressure against the logarithm of the volumetric strain, as represented in Figure 18a, the slope of the elastic portion is linear and is equal to the undrained shear strength, S_u.

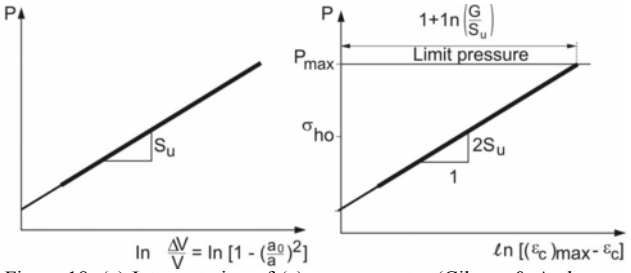

Figure 18. (a) Interpretation of (a) pressuremeter (Gibson & Anderson, 1961) and (b) cone-pressuremeter (Houlsby & Whithers, 1988).

Jefferies (1988) extended the elasto-plastic solutions to include unloading by expressing the pressuremeter unloading curve in terms of small strains as:

$$P = P_{max} - 2S_u \left[1 + \ln\left(\frac{G}{S_u} \right) \right] - 2S_u \ln\left(\frac{a_{max}}{a} - \frac{a}{a_{max}} \right) \qquad (24)$$

where P_{max} and a_{max} are respectively the cavity pressure and cavity radius at the end of the loading stage and a denotes cavity radius at any stage of pressuremeter unloading. Pressuremeter unloading results should be presented as pressuremeter pressure *versus* $-\ln(a_{max}/a\text{-}a/a_{max})$; the slope of the plastic unloading portion in this particular plot is linear and is equal to twice the undrained shear strength.

Installation problems associated to the self-boring technique are partially overcome by large strain unloading analysis which eventually led to the development of the cone pressuremeter (Withers et al, 1989). A solution to derive the undrained shear strength and shear modulus from CPMT data in clay has been developed by Houlsby and Withers (1988). Penetration is modelled theoretically as the expansion of a cylindrical cavity within the soil. The expansion of the pressuremeter test is taken as a continued expansion of the same cylindrical cavity and the contraction phase as a cylindrical contraction. As for the self-boring pressuremeter, the analysis gives rise to a simple construction of the experimental pressuremeter curve, where the slope of the unloading plastic data in a plot of P *versus* $-\ln[(\varepsilon_c)_{max}\text{-}\varepsilon_c]$ is equal to $2S_u$, as represented in Figure 18b.

An alternative approach to these well established methods is to produce an image curve of the complete pressuremeter loading and unloading data (Jefferies, 1988) using a software developed for personal computers to perform a curve-fitting analysis from which soil parameters and the *in situ* horizontal stress can be assessed. The program executes the calculations for loading and unloading equations and plots the data. The operator compares the quality of the match and modifies the input soil parameters until a curve fitting is reached. The parameters that produce an analytical curve that satisfactorily fits the experimental results are, in theory, representative of the soil behaviour. The drawback is that an equally good fit to the data may be achieved by different combinations of parameter values, so that engineering judgment is always required to avoid an unlikely set of parameters to be adopted. Curve fitting analysis has been extensively used by the author and is later explored in the interpretation of pressuremeter test results in cohesive-frictional soils, following recommendations made by Mantaras & Schnaid (2002) and Schnaid & Mantaras (2003).

In addition to isotropic materials, cross-anisotropy materials can also be model by cavity expansion (e.g. Graham & Houlsby, 1983; Wu et al, 1991). Analytical solutions that can find applicability to pressuremeter tests consider the axial direction as the axis of symmetry and the radial (r,θ) plane as the isotropic plane. Solutions are applicable to small strain

anisotropy and have relative little application to soft clay where plastic deformations are likely to govern geotechnical design. As for large strain anisotropy, the mode of shearing in a pressuremeter test is predominantly horizontal and gives an average horizontal strength that is never measured in routine laboratory tests except for a geotechnical testing programme that comprises hollow cylinder tests. Unfortunately measured values of pressuremeter undrained strength are often subjected to inaccuracies that emerge from geometry, installation disturbance, partial drainage and strain rate effects, which can overshadow the influence of anisotropy.

A steady growth in the use of DMT results in geotechnical practice has led to the development of several correlations to estimate S_u (Marchetti, 1980; Lacasse & Lunne, 1988; Powell & Uglow, 1988). The original correlation as proposed by Marchetti (1980) is:

$$S_u = 0.22\sigma'_{vo}\left(0.5K_D\right)^{1.25} \tag{25}$$

Numerical analysis of the installation of flat dilatometers reported by Huang (1989), Finno (1993), Whittle & Aubeny (1993) and Yu (2004) have provided useful insights of the dilatometer test. These studies generally support the empirical correlation from equation 25 (e.g. Marchetti, 1980; Marchetti et al, 2001). In addition, the geotechnical literature offers a wide number of examples in soft clay deposits, in which empirical correlations have been used successfully. A number of reported cases is complied in Figure 19.

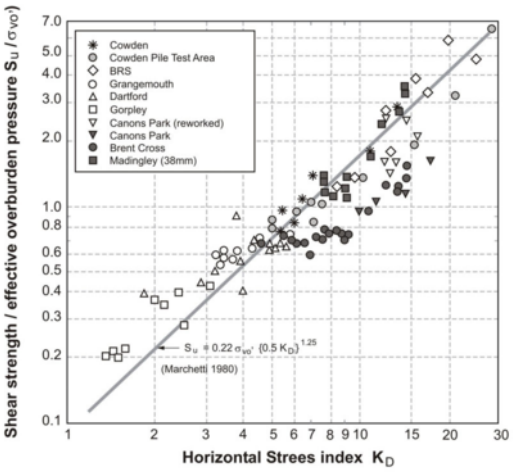

Figure 19. Undrained shear strength from dilatometer (Powell & Uglow, 1988).

4.4 *Stress history*

Stress history is expressed by the overconsolidation ratio OCR, defined as the ratio of the maximum past effective mean stress and the currently applied stress. In practice the current stress is taken as the present effective overburden stress which characterises a mechanically overconsolidated soil. The geotechnical literature offers a wide variety of methods designed to estimate OCR in clay based mainly on FVT, CPT and DMT, which are briefly summarized here.

The field vane measures the undrained shear strength and as an additional use of the device results may provide assessment of OCR from normalised undrained strength to overburden ratio (Mayne & Mitchell, 1988):

$$OCR = \alpha_{FV}\left(\frac{S_{uFV}}{\sigma'_{vo}}\right) \tag{26}$$

where parameter α should be obtained from site specific correlations but can be adopted as a first estimate as $\alpha_{FV} = 22(I_p)^{-0.48}$, where I_p is the plasticity index.

Prediction of OCR from piezocone data can be made from both theoretical and empirical correlations (Sennesset et al, 1982; Wroth, 1984; Mayne, 1991; Tavenas & Lerouiel, 1987; Konrad, 1987). Mayne (1991) suggested an approach based on cavity expansion theory and critical state theory, expressed as:

$$OCR = 2\left[\frac{1}{1.95M+1}\left(\frac{q_c - u_2}{\sigma'_{vo}}\right)\right] \tag{27}$$

In addition, empirical estimates of the preconsolidation stress can be obtained as (Chen & Mayne, 1996):

$$\sigma'_p = 0.305(q_t - \sigma_{vo})$$
or
$$\sigma'_p = 0.65(q_t - \sigma_{vo})(I_p)^{-0.23} \tag{28}$$

Other correlations in the form of $\sigma'_p = k(u_2 - u_o)$ or $\sigma'_p = k(q_t - u_2)$ can also be adopted bearing in mind that they are all site-specific correlations that should be validated locally.

A similarity between the dilatometer K_D and the OCR profiles was first pointed out by Marchetti (1980), and latter confirmed by several authors (e.g. Jamiolkowski et al, 1988; Powell & Uglow, 1988; Kamey & Iwasaki, 1995). For uncemented clays OCR can be simply predicted as:

$$OCR = (0.5K_D)^{1.56} \tag{29}$$

This correlation is simply built-in the evidence of $K_D \approx 2$ for OCR=1 and its usefulness has been extensively demonstrated experimentally (Jamiolkowski et al, 1988; Finno, 1993; Kamey & Iwasaki, 1995). Numerical studies carried out by Yu (2004), assuming that the installation of a flat dilatometer can be simulated by a flat cavity expansion process, enabled a theoretical relationship between K_D and OCR to be obtained. In Figure 20, a numerical estimative of OCR for three different clays are compared to predictions obtained directly from equation 29. With the exception of heavily overconsolidated clays (OCR>8), equation 29 can be used with reasonable confidence.

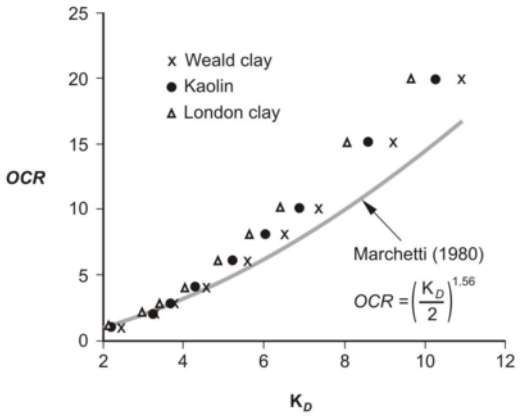

Figure 20. Theoretical correlation between K_D and OCR (Yu, 2004).

4.5 *Consolidation coefficients*

Coefficients of consolidation can be assessed *in situ* from observations of settlements under embankments or directly from *in situ* test results, preferably from piezocone dissipation tests and SBPM holding tests.

Analytical and numerical procedures have been developed to provide an estimate of the coefficient of consolidation C_h from piezocone dissipation tests in which the decay of excess pore pressure with time is monitored. Methods rely either on one-dimensional cavity expansion (Torstensson, 1977; Randolph and Wroth, 1979) or two-dimensional strain path method (Levadoux & Baligh, 1986; Baligh & Levadoux, 1986; Teh & Houlsby, 1991; Burns & Mayne, 1998). The analysis of dissipation tests are mostly predicted on the basis of uncoupled consolidation theory and requires two distinct stages. The first considers the penetration of a cone into an elastic-perfectly plastic isotropic, homogeneous material viewed as a steady flow of a soil past a static cone, leading to the prediction of total stresses and pore water pressures in the soil around the probe. The second stage of the analysis takes these pore pressures as the initial values for a Terzagui uncoupled consolidation process, and calculates the subsequent dissipation around a stationary probe. Although the precise values of the pore pressures as a function of time depend on the specific initial pore pressure distribution, Teh & Houlsby (1991) showed that this form could be generalized by the definition of a suitable dimensionless time factor for the consolidation process T*, expressed as:

$$T^* = \frac{c_h t}{R^2 \sqrt{I_r}} \qquad (30)$$

where R is a probe radius in a soil of rigidity index I_r and t is the dissipation time. Thus, for a given T* and t values, the calculated C_h values is directly proportional to the square root of the I_r value. A constant I_r is used in the solution although in fact the value of the shear modulus will depend on the shear strain amplitude, which is shown by strain path calculations to vary in a complex manner around a 60° penetrometer. Three independent sets of data from both field and laboratory testing programmes reported by Schnaid et al (1997) in which the pore pressures were measured at four different locations on the piezocone suggest that equation 30 should be applied to pore pressures measured at the shoulder immediately above the cone face. The theoretical curves provide a less good match with the experimental dissipation records measured at other locations (u_1, u_3 and u_4).

Based on the strain path method, Robertson et al (1992) produced the chart illustrated in Figure 21 that can be directly adopted to estimated C_h from the actual time that takes for 50% consolidation t_{50}. The success of the analysis in predicting C_h depends on the use of appropriate I_r values and in turn depends on the shear modulus G. For natural clay deposits, I_r ranges from less than 50 to more than 600; it is known to decrease with increasing OCR and, for the same OCR, it increases with decreasing PI. Recommendations are made to use the Houlsby and Teh theoretical solution with an I_r value calculated from triaxial tests, in which the shear stiffness G is taken at a level of 50% of the yield stress (Schnaid et al, 1997). Triaxial CIU, CK_oU and UU tests produce the following representative values: I_r of 70 for Oxford calibration chamber tests (after Schnaid et al, 1997), 44 for the Sarapui site in Brazil (Danziger et al, 1996) and 135 for Ceasa site in Brazil (Schnaid et al, 1997), also illustrated in Figure 21.

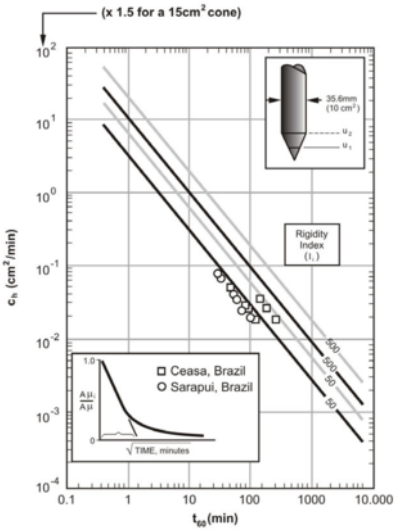

Figure 21. Prediction of C_h from piezocone tests (Robertson et al, 1992).

Strength, stiffness and horizontal stress can be assessed from SBPM tests. A further application to this device is to obtain an *indirect* estimate of horizontal coefficient of consolidation and permeability from a dissipation-type "holding test". Take the case in which the pressuremeter cavity is held constant and the measured pore pressures around the probe dissipates. The consolidation coefficient is estimated from Figure 22, in which a dimensional time factor $T_{50} = C_v\, t_{50}/a^2$ is plotted against the normalised maximum excess pore pressure, $\Delta U_{max}/S_u$ (Clarke et al, 1979). Since the solution does not take into account the viscous behaviour of the clay, the stress relaxation that may occur during strain holding tests cannot be reproduced.

Flow characteristics of clays can also be assessed from dilatometer tests (e.g. Marchetti et al, 2001). Available methodologies consists in stopping the DMT blade at a given depth for monitoring some form of decay with time from which C_h is inferred. Marchetti and Totani (1989) suggests monitoring the decay of the total contact horizontal stress whereas Schmertmann (1988) and Robertson et al (1988) recommends the decay in pore pressure in the soil facing the membrane. Although a direct analogy to pressuremeter holding tests and CPT dissipation tests can be made, the corresponding theory for DMT has not yet been developed; C_h values predicted from DMT should therefore be viewed as approximation.

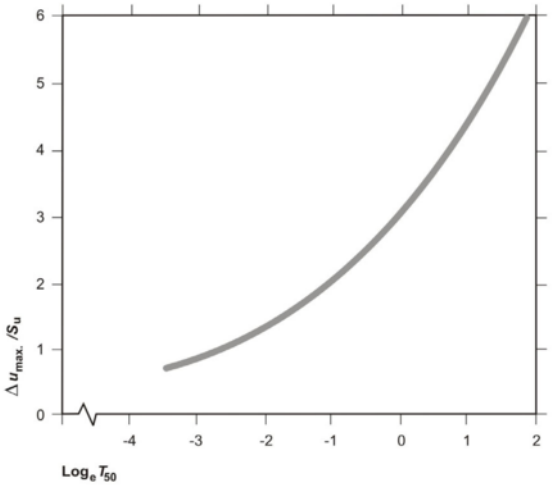

Figure 22. Solution for holding tests (Clarke et al, 1979)

Much has been written with regard to the variations on the measured values of coefficients of consolidation. Figure 23 shows a typical case study at the Champlain Sea Site (Leroueil et al, 1995), where measurements on C_h range from 10^{-8} to 10^{-5} m^2/s. Discrepancies between field and laboratory tests are due to one or more of the of the following main reasons (Simon, 1975; Hamouche et al, 1995; Leroueil et al, 1995; 2002; Leroueil & Hight, 2003):

a) hydraulic conductivity measured in small laboratory specimens may underestimate the hydraulic conductivity of the soil mass, particularly in heterogeneous stratified deposits;
b) inaccuracy of constitutive models and boundary conditions adopted in the interpretation *in situ* tests;
c) the two or three-dimensional aspect of field conditions and of permeability anisotropy neglected in the interpretation of field problems.

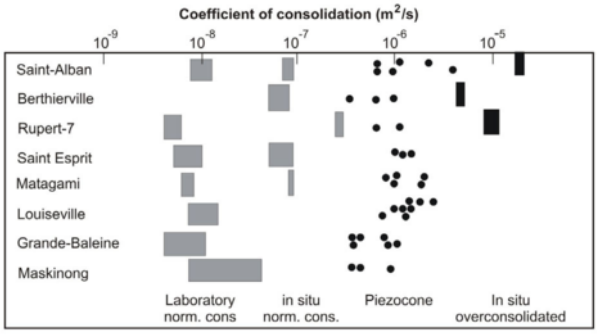

Figure 23. Range of variability of C_v for the Champlain Site (Leroueil et al, 1995).

4.6 *Viscous effects*

Strain rates may account, at least in part, for the discrepancy between field and laboratory measurements. Typical rates of laboratory testing are of 1%/hour (10^{-3} %/s) whereas field tests are associated to strain rates of 10^3 %/s. In comparison, nominal strain rates associated to geotechnical construction may range from 10^{-5} %/s to 10^{-7} %/s.

The influence of shearing rate on undrained behaviour under monotonic load is fully recognised (Tavenas & Leroueil, 1977; Vaid et al, 1979; Kulhawy & Mayne, 1990; Sheahan et al, 1996; Biscontin & Pestana, 2001; Einav & Randolph, 2005) but, despite its major impact on both strength and stiffness, attempts to incorporate this effect into the interpretation of *in situ* testing are fairly recent (e.g. Randolph, 2004). The effect of strain rate on the measured or deduced shear strength of clays can be expressed in the form of a logarithm or an inverse of a hyperbolic sine function (e.g. Randolph, 2004). Its most widespread form is:

$$S_u = S_{u,ref} + \mu \log\left(\frac{\dot{\gamma}}{\dot{\gamma}_{ref}}\right) \tag{31}$$

where

S_u = undrained shear strength at a given loading rate
$S_{u,ref}$ = undrained shear strength at a reference rate
μ= rate law coefficient (typically ranging from 0.10 to 0.15)

$\dot{\gamma}$ = strain rate

$\dot{\gamma}_{ref}$ = reference strain rate

An example of the influence of rate effects on cone penetration is illustrated in Figure 24, in which both the measured cone ratio ($q_{cnet}/q_{cnet,undrained}$) and the excess pore pressure ratio is plotted as a function of the normalised penetration ratio, V (Randolph and Hope, 2004). The normalised penetration ratio V is expressed as:

$$V = \frac{vd}{C_v} \tag{32}$$

where

v = penetration velocity
d = diameter of the penetrometer
C_v = coefficient of consolidation

Tip resistance and pore water pressure increase due to viscous effects as the penetration rate increases. Penetration data follows a reasonably linear relationship in a semi-logarithm space, defining a rate law coefficient μ= 0.13. For a dimensionless velocity lower than 10 the cone ratio also increases, this time as a function of consolidation effects. Section 7 of this Report presents a detailed discussion of the effects of partial drainage and produces recommendation for test procedures in intermediate permeability soils.

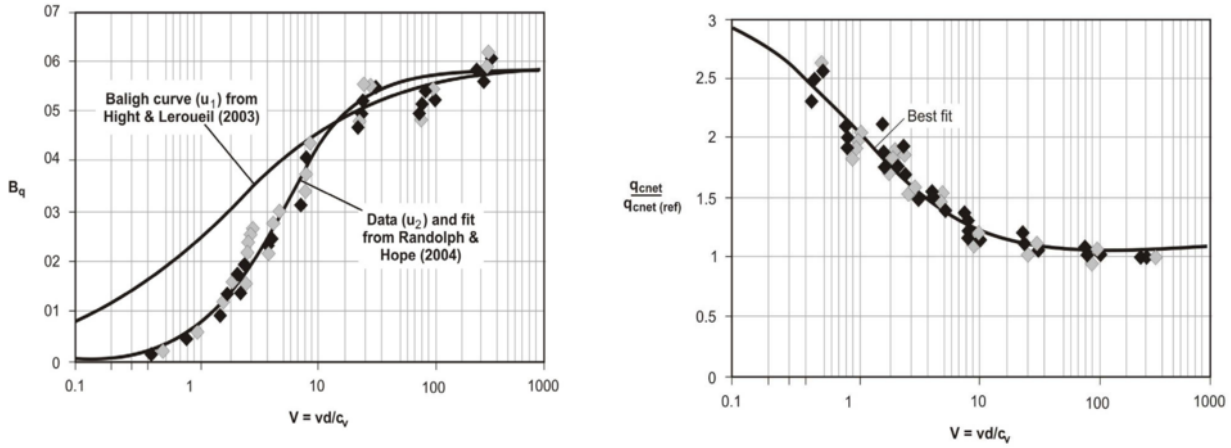

Figure 24. Strain rate effects during cone penetration (after Randolph, 2004)

4.7 *Closing remarks*

Available theoretical and empirical approaches are mainly related to high plasticity clays in which simple rate-independent, perfectly-plastic isotropic soil models are generally adopted in the interpretation of *in situ* test data. Whenever the experience of soft clays is extended to stiff overconsolidated clays, interpretation of test data should follow specific recommendations. Given the uncertainties that emerge from structure, stiffness non-linearity, anisotropy, stress history, strain rate, among other effects, site specific correlations obtained from calibration against laboratory tests are generally recommended.

Despite the due recognition of limitations in the interpretation of *in situ* tests, it is in the difficult conditions of soft clay that both laboratory and *in situ* tests offer the best and most reliable combination of test procedures and interpretation methods available for assessing constitutive parameters for engineering design problems.

5 SAND PROPERTIES

Engineering design in granular soils is about finding means of deriving constitutive parameters without recalling to the benefits of performing elemental laboratory tests. Without the possibility of retrieving undisturbed samples, academics developed interpretative methods from *in situ* tests that engineers often use without being aware of the simplifications embedded in the solutions. In this Report advantages and limitations of currently adopted interpretative techniques and analyses are highlighted. Since the *in situ* behaviour of granular soils is complex, and the characteristic dilatant response is not always accurately captured by existing soil models, a single general recommendation is to cross-correlate measurements from independent tests. When data are combined there is more scope for rational interpretation and, for this reason, emphasis has been placed on correlations with mechanical properties that are based on the combination of measurements from independent tests such as the ratio of the elastic stiffness to ultimate strength (G_o/q_c, G_o/N_{60}), the ratio of cone resistance and pressuremeter limit pressure (q_c/Ψ) and the association of strength and energy measurements (N_{60} and energy).

5.1 *Background research*

Fundamental understanding on the behaviour on granular soils has been obtained from laboratory tests in reconstituted samples. From the macromechanics point of view, a number of characteristic features are now recognized as important in granular geomaterials:

a) drained response prevails under monotonic load due to the relatively high hydraulic conductivity of sands and gravels. Under cyclic load hydraulic conductivity may not be sufficient to prevent the development of excess pore water pressure;

b) basic linear and non-linear stress-strain concepts applied for clay can be extended to other geomaterials by recognizing the dominant influence of void ratio and mean stress on soil stiffness. The variation of G_o values as a function of void ratio e for a variety of soils is shown in Figure 25, in which it is demonstrated that the slope that reflects the void ratio function F(e) does not seem to be significantly influenced by the type of soil (e.g. Lo Presti, 1989; Jamiolkowski et al, 1991);

c) for clean sands, the initial stiffness is unaffected by the rate of shearing and stress history; for carbonate and crushable sands, the effects of over-consolidation are more pronounced, as comprehensively discussed by Tatsuoka *et al.* (1997);

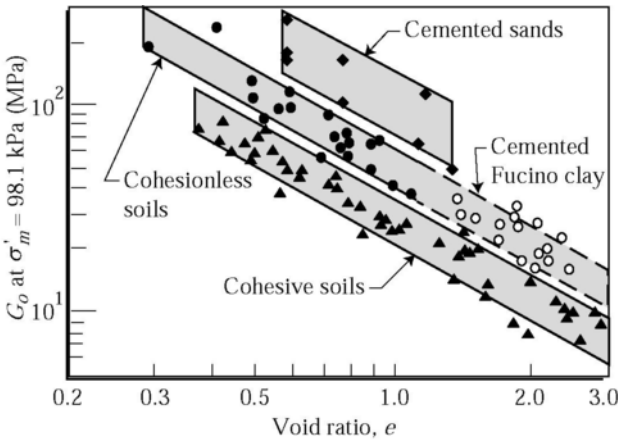

Figure 25. Normalised maximum shear modulus *versus* void ratio (Jamiolkowski et al., 1991).

d) a fundamental issue in granular geomaterials is to describe soil dilatancy, defined as the ratio of plastic volumetric strain increment to plastic deviatoric strain increment. An early, widely used and well tested stress-dilatancy equation is the one proposed by Rowe (1962) that expresses dilatancy as a function of the stress ratio and the internal interparticle friction angle:

$$\frac{\sigma'_1}{\sigma'_3} = \tan^2\left(\frac{\pi}{4} + \frac{\phi'_{cv}}{2}\right)\left(1 - \frac{d\varepsilon_v}{d\varepsilon_1}\right) \qquad (33)$$

where σ_1 and σ_3 are principal stresses, ε_v is the volumetric strain and ε_1 is the major principal strain. Rowe's work was followed by several research efforts that attempted to integrate the behaviour of granular soils over a range of densities and stress levels (e.g. Nova & Wood, 1979; Bolton, 1986; Wan & Guo, 1998; Li & Dafalias, 2000); this can be achieved by the state parameter;

e) the behaviour of granular soils prior to the achievement of the critical state is largely controlled by the state parameter. A concept introduced by Wroth & Basset (1965) and developed by Been & Jefferies (1985), the state parameter ψ is defined as the difference between current void ratio e and critical state void ratio e_c, at the same mean stress (Figure 26a). It can be conveniently expressed as:

$$\psi = e + \lambda \ln\left(\frac{p'}{p'_1}\right) - \Gamma \qquad (34)$$

where p'_1 is the reference mean effective stress taken as 1 kPa. In a manner similar to sedimented clay which is well characterised by the overconsolidation ratio, sands can be characterised by the state parameter following the recognition that it combines the effects of both relative density and stress level. Been & Jefferies (1985) evocate this dependency to establish a sounding relationship between ψ and the internal friction angle for sands. Hird & Hassona (1986) observed that sands can be characterised by the ratio of p'_{cs}/p'_o, when p'_o is the current mean effective stress and p'_{cs} is the mean effective stress on the critical line at the same void ratio. This ratio is directly related to ψ.

f) although the state parameter approach offers a simple and yet fundamental contribution to the characterisation of granular geomaterials, by implicitly combining void ratio and compressibility, important limitations associated to ψ have been recognised for some time. There is now an increasing consensus that, unlike for clays, the critical state line on sands is non-linear in the υ-ln p' space (e.g. Riemer

et al, 1994; Konrad, 1998; Jefferies & Been, 2000), exhibiting a steeper slope at high stresses due to changes in gradation and grain shape induced by grain crushing, as shown in Figure 26b. The amount of particle crushing that occurs in an element of soil under stress depends on particle size distribution, particle shape, mean effective stress, effective stress path, void ratio and particle bonding (e.g. Hardin, 1978). Triaxial tests in samples of equal relative density have distinctively shown that the dilatant component reduces with increasing mean effective stress, since at high stresses, crushing eliminates dilation (e.g. Bolton, 1986).

g) most natural soils and soft rocks are microstructured so that, at a given void ratio, they can sustain stresses higher than could the same material non-microstructured (e.g. Burland, 1990; Leroueil & Vaughan, 1990; Schmertmann, 1991; Clayton & Serratrice, 1993; Leroueil & Hight, 2003). Although this is evident for hard soils (and will be detailed in section 6) there is also evidence of microstructure in sands (Mitchell & Solymar, 1984; Schmertmann, 1991; Fernandez & Santamarina, 2001). Given the difficulty of sampling granular soils, evidences of bonding have to be obtained from field tests, allowing not only soil behaviour to be characterised but the influence of microstructure on the small strain shear modulus to be quantified (e.g. Eslaamizaad & Robertson, 1997; Schnaid, 1997; Schnaid et al, 2004).

Whereas the strength-dilation theory and critical state concepts generally apply, in sand uncertainty arises from the shear strength envelope non-linearity which increases with increasing relative density and grain crushability. Since cementation, aging and crushability are phenomena recognised as important in the behaviour of granular materials, a research challenge is to incorporate these effects into interpretation methods of *in situ* tests. We deal almost exclusively with non-cemented, cohesionless soils, because our experience has been built on calibration against a database from large laboratory calibration chamber tests on fresh sands.

5.2 *Characterisation of aging and cementation*

The preceding discussion in clay has already emphasized the importance of the rigidity index to soil characterisation, frequently used for numerical analysis in geomechanics and particularly relevant to the interpretation of *in situ* tests. In principle, a material that is stiffer in deformation may be stronger in strength, yielding the following empirical relationship that appears to be valid for various geomaterials ranging from soft soils to hard rocks (e.g. Tatsuoka & Shybuya, 1992; Shibuya et al, 2004):

$$E_{max} / q_{max} = 1000 \pm 500 \tag{35}$$

This type of correlation aims at evaluating the spatial variability of stiffness from measured strength obtained in conventional laboratory testing. Since granular materials are difficult to sample and the characteristic structure of natural sands cannot be reproduced by reconstituted samples in the laboratory, it is necessary to develop a methodology capable of identifying the existence of distinctive behaviour emerging from aging or cementation from field tests. Following recent recommendations that soil characterisation and mechanical properties should be preferably based on the combination of measurements from independent tests (Yu et al, 1996; Schnaid, 1997; Odebrecht et al, 2004; Schnaid et al, 2004), an approach has been developed on the basis of the ratio of the elastic stiffness to ultimate strength (G_o/q_c, G_o/N_{60}). This is achieved by combining cavity expansion theory and critical state concepts to the variables that control the small strain stiffness of sand (Schnaid & Yu, 2005).

Theoretical solution for cone penetration and background research of small strain stiffness that form the basis of the present analytical study are briefly summarised as follows. The stiffness of sand has been long recognized to be controlled by the confining stress and voids ratio (section 4, e.g. Hardin & Black, 1968; Hardin, 1978; Lo Presti, 1989). This has prompted the establishment of many useful correlations for predicting G_o adopting slightly different F(e) functions (e.g. Iwasaki and Tatsuoka, 1997; Lo Presti et al, 1997; Shybuya et al; 1997). Lo Presti et al (1997) suggest the following expression:

$$G_o = Ce^{-x}(p')^n (p_a)^{1-n} (kPa) \tag{36}$$

having C=710, n=0.5 and x=1.3 as average values for the material parameters.

For solutions of cone penetration in sand, the significant volume change that occurs in shear has to be captured. Give its complexity, the existing methods of interpretation of the penetration mechanism in sand can only be regarded as approximation and solutions have to be calibrated against experimental data from calibration chamber tests. Using a state parameter based, critical state soil model, Collins et al (1992) presented a solution for the expansion of a spherical cavity that can be conveniently expressed as:

$$p'_{ls} = C_1 (p'_o)^{C_2 + C_3(1+e_o)} \exp\left[C_4 (1+e_o)\right] \tag{37}$$

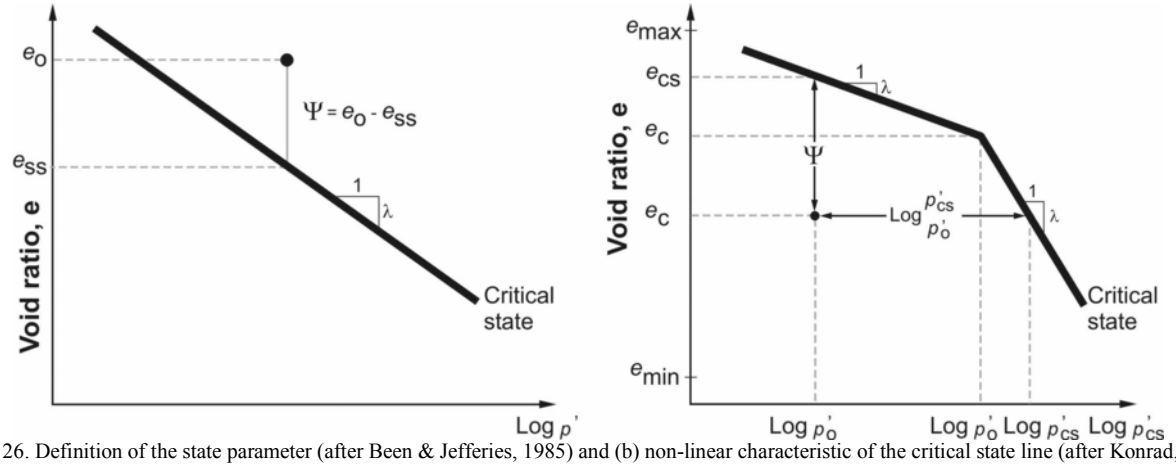

Figure 26. Definition of the state parameter (after Been & Jefferies, 1985) and (b) non-linear characteristic of the critical state line (after Konrad, 1998).

where p'_{ls} is the effective spherical cavity limit pressure. Critical state parameters and constants C_1, C_2, C_3 and C_4 have been calibrated against laboratory chamber testing data in six reference sands. The effective cone resistance q_c can be estimated from directly from p'_{ls} (Ladanyi & Johnston, 1974):

$$q_c = p'_{ls}(1+\sqrt{3}\tan\phi_{ps} \quad (38)$$

where ϕ'_{ps} is the plain strain peak friction angle of the soil, as cone penetration is assumed to occur under plane strain conditions. In equation 38 effective stresses and a rough soil-cone interface are assumed to be valid.

Theoretical values of q_c calculated from equation 38 can be related to the magnitude of G_o calculated from equation 36, provided that the initial void ratio and *in situ* stress state are known or estimated. From this correlation it is possible to express both G_o/q_c and q_{c1} from a set of given parameters: e, M, λ, Γ and p'. The approach makes use of a normalized dimensionless parameter q_{c1}, defined as:

$$q_{c1} = \left(\frac{q_c}{p_a}\right)\sqrt{\frac{p_a}{\sigma'_v}} \quad (39)$$

where p_a is the atmospheric pressure.

The theoretical correlation between G_o/q_c and q_{c1} is shown in Figure 27 in a relationship representative of unaged uncemented soils. Results were calculated in a stress interval between 50 kPa to 500 kPa which should cover the range of applications encountered in geotechnical engineering practice. The computed values are shown to be insensitive to both the initial stress state and soil compressibility which fully justifies its use for soil characterisation. For comparison with natural sands, the upper and lower boundaries empirically established by Schnaid et al (2004) are presented together with the theoretical derived database. The boundaries that represent the variation of G_o with q_c for fresh unaged uncemented sand deposits are expressed as (Schnaid et al, 2004):

$$G_o = \alpha\sqrt[3]{q_a\sigma'_v p_a} \quad (40)$$

where α is a parameter that ranges from 110 to 280 (units in.eq. 40 are in kPa) . Note that these boundaries have roughly the same slope as the one produced by the analytical solution.

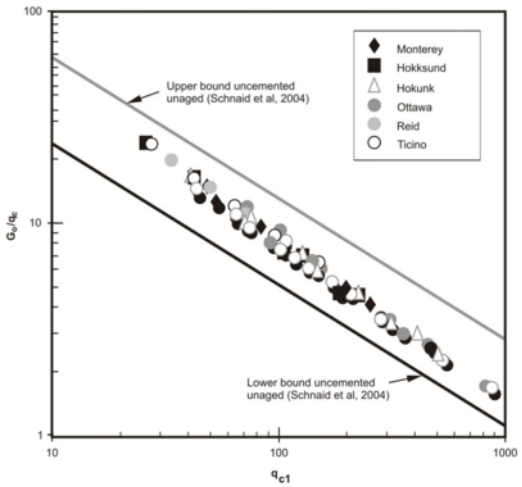

Figure 27. The ratio of the elastic stiffness to cone resistance predicted from critical state approach (Schnaid & Yu, 2004).

Four independent sets of data have been used to validate this theoretical approach (Figure 28): centrifuge tests carried out on Fontaineblue sand (Gaudin et al, 2004), compilation of a database for natural sands by Eslaamizaad & Robertson (1997), a variety of sand types from Western Australia (Schnaid et al, 2004) and data reported for the Canadian Liquefaction experimental site, Canlex (e.g. Wride et al, 2000). Gaudin et al (2004) presented a set of centrifuge tests in which both G_o and q_c have been measured. By taking account of chamber size effects, the measured data plotted in Figure 28a confirms the theoretically derived line and demonstrates that G_o/q_c ratio is relatively insensitive to stress level and relative density. The ratio of G_o/q_c observed in the centrifuge is shown to be generally higher for loose sand than that for dense specimens, primarily because the latter exhibit higher q_{c1} values.

Comparison with natural sands is provided by Figures 28b and 28c. Fresh uncemented sand characterises a region in the G_o/q_c *versus* q_{c1} space defined by equation 40. Values of q_c and G_o profiles that fall outside and above this region suggest possible effects of stress history, degree of cementation and ageing, as demonstrated by Eslaamizaad & Robertson (1997). A variety of sand types in Australia shows that the stratigraphy includes a recent deposited siliceous sand fill placed hydraulically for reclamation works and a dune sand from Spearwood which was laid down in the late Pleistocene as a limestone but was subsequently leached of virtually all its calcium carbonate content, both of which show no traces of a defined structure. In contrast, 'Safety Bay Sand', which was deposited under littoral and aeolian conditions in the mid-Holocene, contains many shells and has a calcium carbonate content in excess of 50% and 'Lower Guildford siliceous sand', which was laid down by streams during the early Pleistocene, is shaped by ageing effects. As indicated by Schnaid et al (2004), G_o/q_c ratios in the lower Guildford sand are typically about five times higher than those recorded in the hydraulic fill and results of these cemented aged sands fall above the region defined for uncemented materials.

Further evidence can be obtained from field tests using the database reported for the Canadian Liquefaction experimental site, Canlex (e.g. Wride et al, 2000). The Canlex project has produced detailed investigation of three major locations containing hydraulic placed loose sand deposits, comprising both field and laboratory tests where undisturbed samples have been retrieved from ground freezing techniques. Two locations are particularly useful for the present discussion and will be extensively analysed: the 12 years old placed, 27 to 37 m deep Mildred Lake deposit and the 2 months aged at time of test, 3 to 7 m deep J-pit deposit. Reported tip cone resistance and small strain stiffness have been plotted in Figure 28d and appear to indicate no cementation in both sites and no aging effects at the Mildred Lake 12 years old deposit.

Significant scatter observed in natural sand deposits is not a function of soil compressibility as suggested in early studies, but probably results from soil anisotropy, as well as some degree of cementation and aging. Due to anisotropy, G_o is not independent on the direction of propagation and polarization of shear waves and correlations with penetration resistance should preferably be expressed as a function of G_{vh}, G_{hv} or G_{hh}.

Scatter can also be partially attributed to the influence of the horizontal stress on both initial stiffness and tip cone resistance. (e.g. Schnaid & Houlsby, 1992). Equation 40 should ideally be referred to horizontal stress or mean *in situ* stress rather than to vertical stress. The preference for σ'_{vo} is justified by the impossibility of determining with reasonable accuracy the value of the horizontal stress in most natural deposits, because they have undergone complex stress history, cementation and aging effects that are difficult to reconstruct.

The general good agreement between the theoretical correlation, centrifuge data and field data entirely justify the use of G_o/q_c for the characterisation of natural sand deposits. The G_o/q_c ratio is useful because it provides a measure of the ratio of the elastic stiffness to ultimate strength that may be expected to increase with sand age and cementation, primarily because the

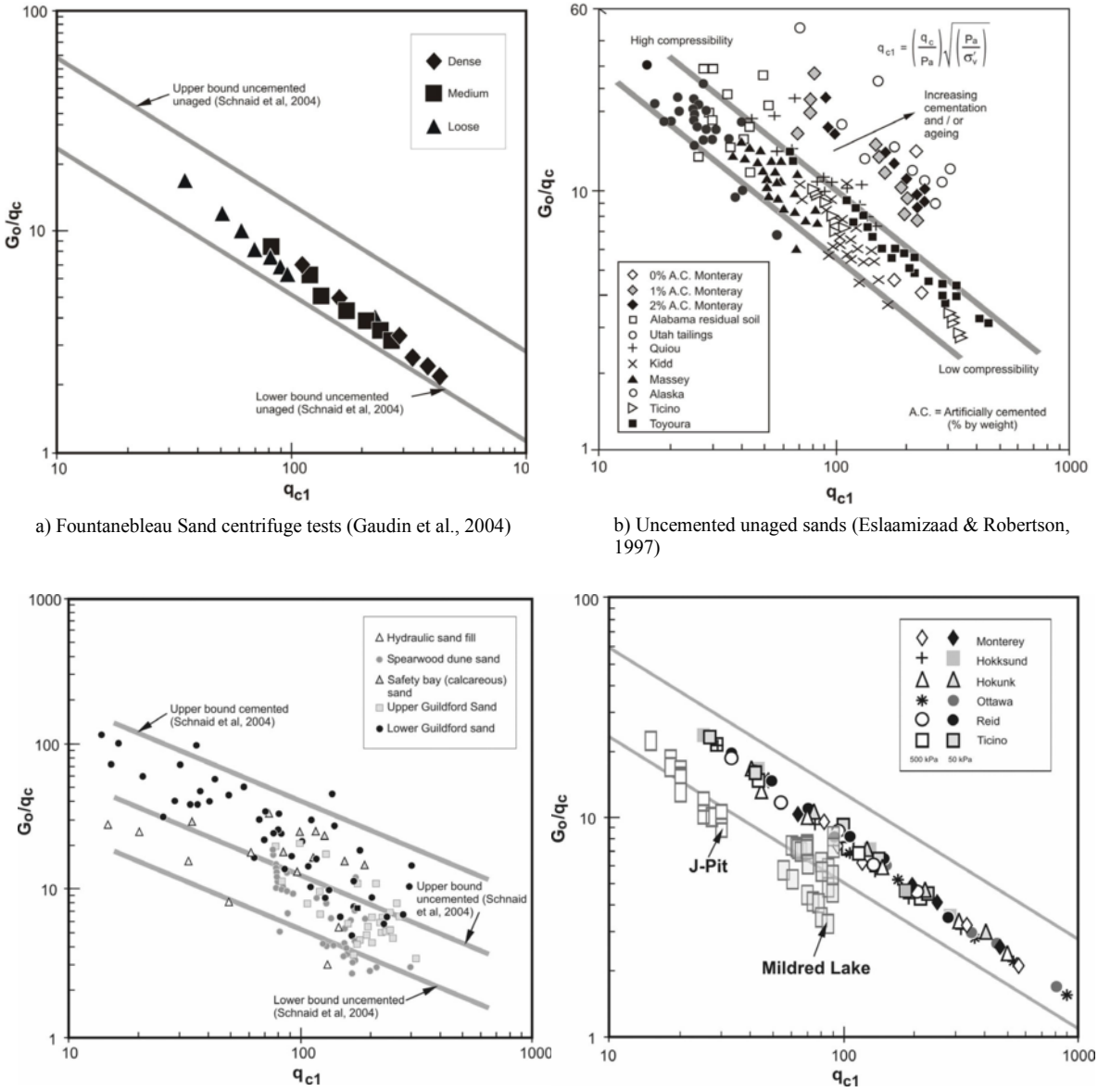

a) Fountanebleau Sand centrifuge tests (Gaudin et al., 2004)

b) Uncemented unaged sands (Eslaamizaad & Robertson, 1997)

c) Western Australia sands (Schnaid et al., 2004)

d) Calibration chamber data (Schnaid & Yu, 2005)

Figure 28. The ratio of elastic stiffness to cone resistance for centrifuge tests and natural sands

effect of these on G_o is stronger than on q_c. The ratio is not sensitive to changes in mean stress, relative density and sand compressibility.

5.3 *Stiffness*

Assessment of reliable stress-strain relationships of soils requires a correct evaluation of both the small strain stiffness and the shape of the degradation curve. In the preceding section, the variation of G_o with q_c observed for natural sands was summarised in Figure 28. Equation 40 can match the range of recorded G_o values and despite the fact that this equation has originally been proposed to distinguish cemented and uncemented soils, it is likely that practitioners may be tempted to employ it to estimate G_o. For preliminary design, in the absence of direct measurements of shear wave velocities, the proposed lower bounds are recommended for an evaluation of the small strain stiffness from q_c (Schnaid et al, 2004):

$$G_0 = 280\sqrt[3]{q_c \sigma'_v p_a} \quad : \text{lower bound, cemented} \qquad (41)$$

$$G_0 = 110\sqrt[3]{q_c \sigma'_v p_a} \quad : \text{lower bound, uncemented} \qquad (42)$$

These equations predict values of G_o that are not far from previously published relationships developed for sands (Bellotti *et al.,* 1989; Rix & Stoke, 1991; Jamiolkowski *et al.,* 1995b). However the effect of natural cementation and ageing is quantified here and is shown to produce a marked increase in both G_o/q_c ratio. Given the considerable scatter observed for different soils, these correlations are only approximate indicators of G_o and do not replace the need for *in situ* shear wave velocity measurements.

il stress-strain behaviour is non-linear and this introduces uncertainties on the selection of design parameters for routine design calculations, as outlined in Section 4. Several approaches have been developed for the description of the non-linear stress-strain behaviour of soils, adopting mathematical models expressed, for example, by logarithm or hyperbolic curves. For sands, in the absence of laboratory tests from undisturbed samples, cross-reference between small strain stiffness from seismic tests and intermediate stiffness from pressuremeter or

plate loading tests should be sufficient to represent deviatory non-linear stress-strain behaviour inside the small strain region.

The proposed method of describing the modulus degradation curve is to curve-fitting a pressuremeter test that includes unload-reload loops using a non-linear soil model. Assuming that G_o is known, the fitting process may be sufficiently accurate to determine the model parameters that represent the soil non-linear response. It is here worth to recall that a typical pressuremeter cycle is highly hysteretic and as a consequence the unloading and reloading sections do not coincide so that the actual shape of the cycle represents the non-linear response of the soil, as demonstrated in Figure 29. This figure shows typical pressuremeter unload-reload cycles and the theoretical fitting curves using a numerical analysis coupled to the hyperbolic relationship proposed by Fahey and Carter (1993):

$$\frac{G}{G_o} = \left[1 - f\left(\frac{\tau}{\tau_{\max}} \right)^g \right] \tag{43}$$

where f controls the strain to peak strength (τ_{max}) and g determines the shape of the degradation curve as a function of mobilised stress level (τ). Several similar approaches have been proposed in the literature giving specific recommendations to better characterise the non-linear response of sand from *in situ* tests (Bellotti et al, 1989; Muir Wood, 1990; Ferreira & Robertson, 1992, Fahey and Carter, 1993). Uncertainty arises when soil structure and destructuration becomes important as recently pointed out by Schnaid et al (2004) and outlined in Section 6 (Bonded geomaterials).

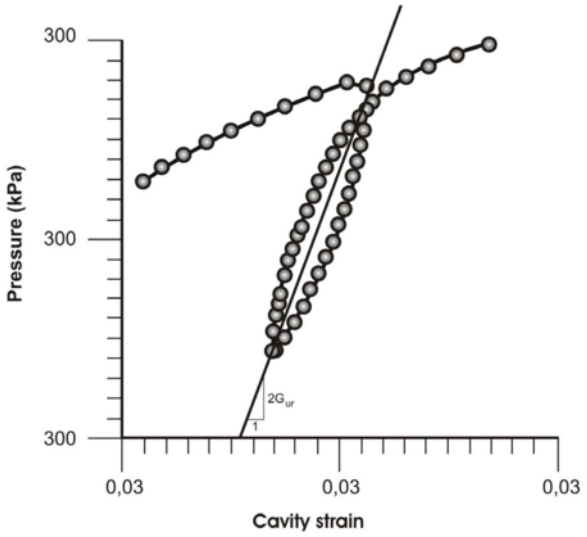

Figure 29. Typical unload-reload cycle in a pressuremeter test

5.4 *Shear strength and state parameter*

In cohesionless soils, the strength parameter of major interest is the internal friction angle ϕ' and its assessment has to be necessarily made from *in situ* tests given the difficulties in retrieving samples for laboratory tests. The significant volume change that occurs in sand during shear can be captured in the analysis of pressuremeter tests. Due to the complicated strain field produced during CPT/SPT/DMT penetration in frictional dilative soils, *in situ* penetration tests remain primarily based on empirical evidence supported against calibration in large laboratory chambers. Some established methods for interpretation of shear strength from *in situ* tests are briefly discussed and new developments are addressed.

Analysis of pressuremeter tests in sand assume fully drained conditions so that no excess pore water pressures will be developed throughout the test. A small strain cavity expansion solution developed to derive the angles of friction and dilation was first deduced by Hughes et al (1977) and is widely accept in practice. The sand is assumed to behave as an elastic-plastic Mohr-Coulomb material and the elastic deformation is disregarded in the plastic zone. An analytical solution for the cavity expansion curve in the plastic region can be expressed as:

$$\ln(P') = s \ln \varepsilon_c + A \tag{44}$$

where P' is the effective cavity pressure, ε_c is the cavity strain, $s=(1+\sin\psi)\sin\phi/(1+\sin\phi)$, A is a constant and ψ is the angle of soil dilation. A direct implication is that in a pressuremeter result plotted as P' *versus* ε_c in a logarithmic scale, the straight line slope of the plastic portion is equal to s, which in turn is a function of the friction ϕ and dilation angles ψ. From Rowe's stress-dilation (equation 33), it is possible to express ϕ and ψ as a function of s and ϕ_{cv}:

$$\sin\phi = \frac{s}{1 + (s-1)\sin\phi_{cv}} \tag{45}$$

$$\sin\psi = s + (s-1)\sin\phi_{cv} \tag{46}$$

Several other solutions have been later proposed to the analysis of both the loading (Manassero, 1989; Sousa Coutinho, 1990) and unloading (Houlsby et al, 1986) of a pressuremeter in sand. Textbooks such as Clarke (1993) and Yu (2000) are excellent references to review these methods.

As for interpretation of the CPT in sand, there are two possible approaches: (a) analysis based on bearing capacity and cavity expansion theories which, given the complexities of modelling penetration in sand, can only be regarded as approximate (Vesic, 1972; Durgunoglu & Mitchell, 1975; Salgado *et al.,* 1997) and (b) methods based on results from large laboratory calibration chamber tests (e.g. Bellotti *et al.,* 1996, Jamiolkowski *et al.,* 1985). A recent trend has been to interpret cone penetration results in terms of the state parameter by combining tip resistance with seismic measurements or pressuremeter limit pressure (Yu, Schnaid & Collins, 1996; Schnaid & Yu, 2005).

Analytical solutions have been useful as means of understanding the penetration mechanism, as well as identifying the influence of different constitutive parameters on the penetration process. Durgunoglu & Mitchell (1975) presented a well-known bearing capacity solution for deep cone penetration. A simple expression is obtained from a plane strain failure mechanism coupled to an empirical shape factor to account for the axisymmetric geometry of the cone, for cases in which the soil-cone interface friction angle is half of the soil friction angle:

$$N_q = \frac{q_c}{\sigma'_{vo}} = 0.194 \exp(7.63 \tan\phi) \tag{47}$$

where N_q is the cone factor in sand. Alternatively, Salgado et al (1997) used the analogy between cavity and cone penetration to derive a simplified solution expressed as:

$$q'_c = 2\exp(\pi \tan\phi) \frac{[(1+C)^{1+I} - (1+I)C - 1]}{C^2 I(1+I)} P'_{lc} \tag{48}$$

where P'_{lc} denotes the effective cylindrical cavity limit pressure, I is determined numerically and C is linked to the soil dilation

angle by $C = \sqrt{3}\exp[(\pi/2)\tan\psi)]$. Calibration against a large number of chamber tests suggests that measured cone resistance can be predicted to within 30%.

A wider-spread approach in engineering practice is to estimate relative density D_r from cone tip resistance adopting empirical correlations (e.g. Jamiolkowski *et al.,* 1985; 2003; Houlsby, 1998). Jamiolkowski *et al,* (2003) suggested a correlation between cone resistance, relative density and mean effective stress in the form:

$$D_r = \frac{1}{C_2}\ln\left(\frac{q_c}{C_0 p^{C_1}}\right) \tag{49}$$

According to the authors, vertical stress can substitute mean stress in equation 49 provided that the soil is normally consolidated having a K_o constant with depth. In this case parameters C_o, C_1 and C_2 can be taken as 17.68, 0.50 and 3.10 respectively.

Calibration chamber data in sand have clearly shown that, for a given density, cone resistance depends primarily on the *in situ* horizontal stress and therefore σ'_{ho} must be accounted for in a rational interpretation of field tests (Houlsby & Hitchman, 1988); Schnaid & Houlsby, 1992). The dependency of relative density (D_r) on q_c and σ'_{ho} is illustrated in Figure 30 and can be expressed in percentage as (Schnaid and Houlsby, 1992; Nutt & Houlsby, 1992):

$$D_r = \frac{1}{3}\frac{q_c - \sigma_{h0}}{\sigma_{h0}} + 10 \tag{50}$$

It is clear from Figure 30 that even well-controlled calibration chamber tests lead to a considerable scatter for different soils and soil conditions. Given the scatter observed in test data a logarithm equation was considered more appropriate (Houlsby, 1988):

$$\log_{10}\left(\frac{q_c - \sigma_{ho}}{\sigma'_{ho}}\right) = 1.51 + 1.23 D_r \tag{51}$$

Values of D_r estimated from the above equations can be combined with operational stress levels to produce an estimate of peak friction angles (e.g. Bolton, 1986):

$$\phi'_p - \phi'_{cv} = m\left[D_r\left(Q - \ln p'\right) - R\right] \tag{52}$$

where p' is the mean effective stress (in kPa), R is an empirical factor found equal 1 as a first approximation and Q is a logarithm function of grain compressive strength, known to range from about 10 for silica sand to 7 for calcareous sand (e.g. Randolph et al, 2004).

An alternative to pressuremeter and cone tests, the dilatometer is regarded as a useful mean of predicting the internal friction angle (e.g. Marchetti, 1997). The basic empirical approach relies on the measured K_D from the DMT and requires an independent rough evaluation of K_o following the principles advocated by Durgunoglu & Mitchell (1975). A recent numerical analysis presented by Yu (2004) provided an instructive divergence in the way a DMT should be interpreted in sand by demonstrating that although K_D (or a normalised K_D/K_o dilatometer horizontal index) increase with soil friction angle the influence of the rigidity index (G/p'_o) is also very significant. In the numerical analysis the DMT has been modelled as a flat cavity expansion process using linear-elastic, perfectly-plastic Mohr-Coulomb theory. A comparison between empirical and numerical predictions for a case considering K_o=1 is presented in Figure 31, in which the K_D/K_o ratio is plotted against the rigidity index. Although the numerical solution is still unable of producing realistic predictions of friction angle, it does identify the need to take the rigidity index into account. It appears that on a stiff soil the displacement that originates K_D is sufficiently small to be regarded as elastic but in a more soft soil plastic strains may occur.

Limitations to these empirical approaches are that (a) the database upon which the correlations have been established is predominantly based on tests carried out on unaged, clean fine to medium, uniform silica sands and (b) most available correlations are referred to effective overburden stress instead of mean stress and are therefore applicable only in normally consolidated deposits. Given these limitations, the author advocates the use of correlations with mechanical properties that are based on the combination of measurements from independent tests using the cone-pressuremeter, the seismic cone and the SPT with energy measurements.

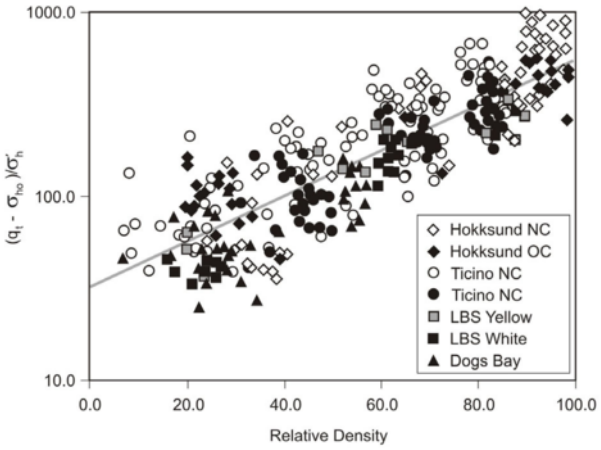

Figure 30. Relative density *versus* normalised cone resistance from calibration chamber tests (after Houlsby, 1988).

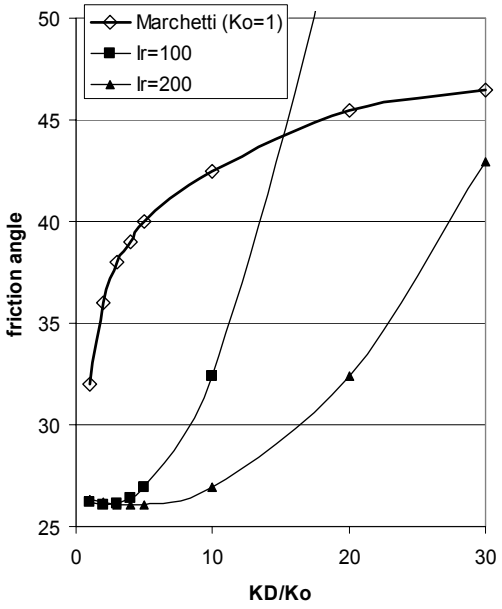

Figure 31. Prediction of friction angle from dilatometer tests for K_o=1 (numerical predictions after Yu, 2004).

a) Cone pressuremeter

Analysis of the cone pressuremeter test in clay is achieved by a simple geometric construction of the curve to determine the undrained shear strength, the shear modulus and the *in situ* horizontal stress (Houlsby and Withers, 1988). Analysis in sand is, however, significantly more complex (Schnaid & Houlsby, 1992; Nutt & Houlsby, 1992).

Experimental results of calibration chamber testing of the Fugro cone pressuremeter revealed that the ratio of cone tip resistance (q_c) and to the pressuremeter limit pressure (ψ_L) correlates well with many soil properties such as relative density and friction angle. It is worth noting that both cone resistance and pressuremeter limit pressure are dependent on the size of the calibration chamber used (Schnaid & Houlsby, 1991), but the ratio of these two quantities is relatively unaffected by chamber size, and therefore correlations established in the laboratory may be applied directly to field conditions. Approximate empirical expressions for relative density, D_r (Schnaid and Houlsby, 1992; Nutt & Houlsby, 1992), expressed as a percentage, are:

$$D_r = 9.6\frac{q_c - \sigma_{h0}}{\psi_L - \sigma_{h0}} - 30.5 \qquad (53)$$

The basis of these correlations is that both the cone resistance and the limit pressure depend on the combined effects of horizontal stress and relative density. The combination of equation (50) and (53) give σ'_{ho} as a function of q_c and Ψ_L, expressed as the root of a quadratic equation.

A theoretically sound correlation based on CPTM data has been proposed by Yu, Schnaid & Collins (1996). In the theoretical development, the authors have assumed that both the cone resistance q_c and the pressuremeter limit pressure ψ_L are strongly related to the limit pressure of spherical (P'_{ls}) and cylindrical (P'_{lc}) cavities respectively. The ratio of these two quantities can be therefore estimated by the following equation:

$$\frac{p'_{ls}}{p'_{lc}} = C_1 (p'_o)^{C_2 + C_3(1+e_o)} \exp\left[C_4(1+e_o)\right] \qquad (54)$$

where C_1, C_2, C_3, C_4 are constants calibrated against six reference sands. Solutions for cavity expansion in an elastic perfectly plastic Mohr-Coulomb soil have been used to correlate the ratio of q_c/ψ_L to the peak friction angle of the soil. In addition, the limit pressure solutions for cavity expansion in a strain hardening/softening soil using a state-parameter-based soil model are used to correlate q_c/ψ_L to the *in situ* sand state parameter. This recognizes the idea that prior to the achievement of the critical state, the behaviour of granular materials is largely controlled by the state parameter ψ and that ψ can be directly correlated with triaxial friction angles (Been & Jefferies, 1985). Figure 32 demonstrates that the ratio of q_c/ψ_L is mainly dependent on the initial state parameter of the soil and that it can be conveniently expressed as:

$$\psi = 0.4575 - 0.2966 \ln \frac{q_c}{\psi_L} \qquad (55)$$

The (plane strain) friction angle (in degrees) is (Yu & Houlsby, 1991):

$$\phi'_{ps} = \frac{14.7}{\ln I_s}\frac{q_c}{\psi_L} + 22.7 \qquad (56)$$

Although further verification of the proposed interpretation method from field tests is still needed to enhance the confidence of these correlations in engineering practice, results shown in Figure 32 from Ghionna et al (1995) and Robertson et al (2000) support its validity.

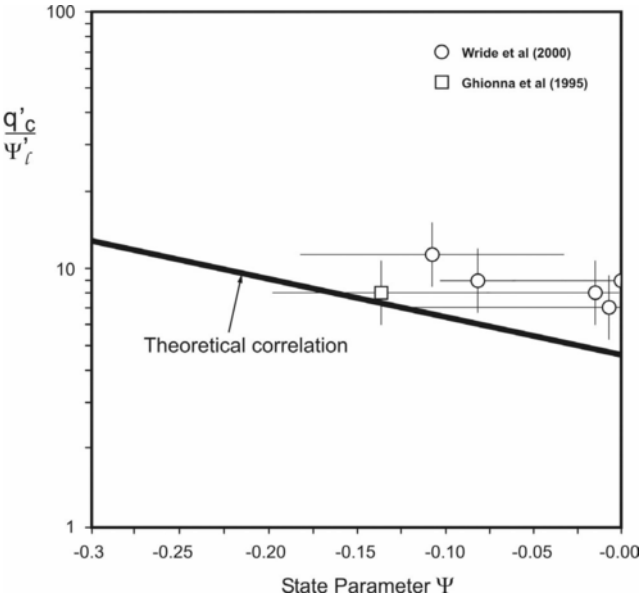

Figure 32. Theoretical ratio of cone resistance to pressuremeter limit pressure and *in situ* state parameter (after Yu et al., 1996).

b) Seismic cone

Since G_o and q_c are controlled by void ratio, mean stress, compressibility and structure and are therefore different functions of the same variables, it s possible to anticipate that as a ratio these two measurements can be useful in prediction soil properties. In the preceding discussion, a set of critical state parameters combined to initial state conditions have been used to calculated both G_o and q_c. Acknowledging that critical state parameters and initial soil state are in the root of the so called "state parameter", ψ, an obvious approach is to correlate the G_o/q_c ratio and ψ (after Schnaid & Yu, 2005).

It is important to recall that the state parameter has been successfully correlated with triaxial friction angles ϕ'_{tc} using an empirical relationship of exponential type (Been & Jefferies, 1985):

$$\phi'_{tc} - \phi'_{cv} = A\left[\exp(-\psi) - 1\right] \qquad (57)$$

where A is a curve fitting parameter ranging from 0.6 to 0.95 depending on the type of sand. A theoretical relationship between G_o/q_c with ψ can be obtained from equations 34, 54, 55 and 57. Results are plotted in Figure 33 for the six reference sands and for a stress interval between 50 and 500 kPa. For a given mean stress, the ratio of G_o/q_c decreases with decreasing ψ (i.e. G_o/q_c decreases with increasing relative density). Although the correlation is not very sensitive to variations in sand strength and stiffness, for a given ψ the G_o/q_c ratio reduces with increasing mean stress. The theoretical database generated by this approach can be represented by the following expression:

$$\psi = \alpha \ln\left(\frac{p'}{p_a}\right)^{\beta} + \chi \ln\left(\frac{G_o}{q_c}\right) \qquad (58)$$

where α=-0.520; β=-0.07 and χ=0.180 are average coefficients obtained from calibration chamber data. In practice it is recommended to obtain these coefficients from site-specific correlations. Predictions of the state parameter from the measured G_o/q_c ratio would therefore require an independent assessment to the *in situ* horizontal stress, for calculating mean stresses in equation 58, which for a normally consolidated sand can rely on Jacky's equation.

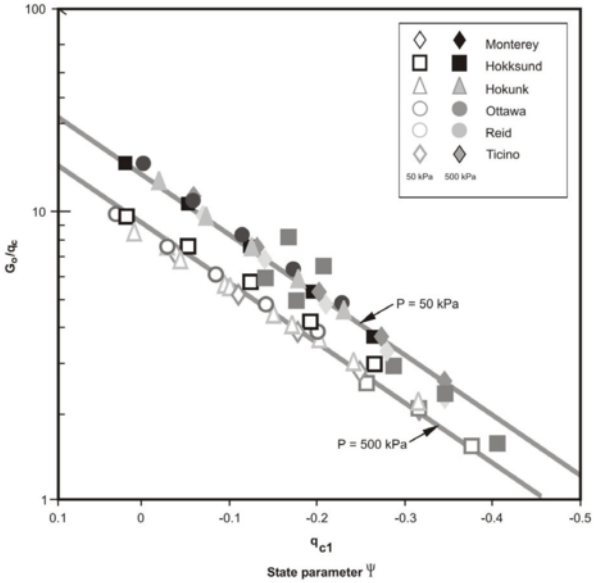

Figure 33. Theoretical ratio of elastic stiffness to cone resistance and *in situ* state parameter (Schnaid & Yu, 2005).

Validation of the proposed method from a number of case studies is necessary before this approach is used with con fidence. The database from both Fountainebleau centrifuge tests and Canlex Site can provide preliminary assessment to the usefulness of equation 58. The measured centrifuge data for relative densities corresponding to 45.1%, 68.8% and 84.2% are shown in Figure 34, in which G_o/q_c is plotted against ψ for mean stresses of ranging from 30 to 100 kPa. Experimental data clearly show that G_o/q_c decreases with decreasing ψ and increasing mean stress as indicated from equation 58. Predicted trends for p'= 30kPa and 100 kPa are also shown in the figure and appear to produce a reasonable approximation of measured data.

Penetration and seismic testing data from the Canlex site (e.g. Wride et al, 2000) are very useful to evaluate the proposed correlation since there is no other area in which the freezing technique has been adopted so extensively to retrieve undisturbed samples in sand from which the state parameter was assessed. Results are presented in Figure 35, in which data from both Mildred Lake and J-pit sites are summarised. Substantial scatter is observed in this plotted which reflects the actual scattered data reported by the authors. The two sets of measured data fall in rather distinct regions in the G_o/q_c versus ψ space, with the J pit data falling consistently above the data reported at Mildred Lake as a result of the different mean *in situ* stresses at the two locations. The J-pit data follow a line having a slope similar to that predicted from equation 58 and the state parameter can be predicted with reasonable accuracy. Data from Mildred Lake is much more scattered and does not show a clear trend of reducing G_o/q_c with reducing ψ.

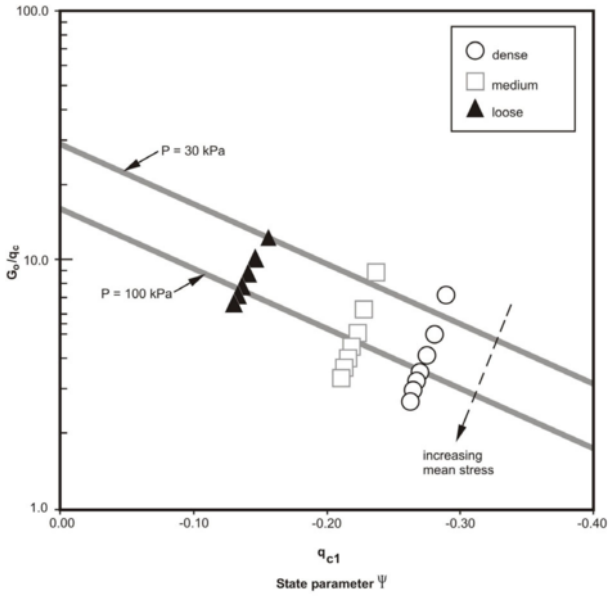

Figure 34. Predictions of the state parameter from centrifuge tests (modified from Gaudin, 2005).

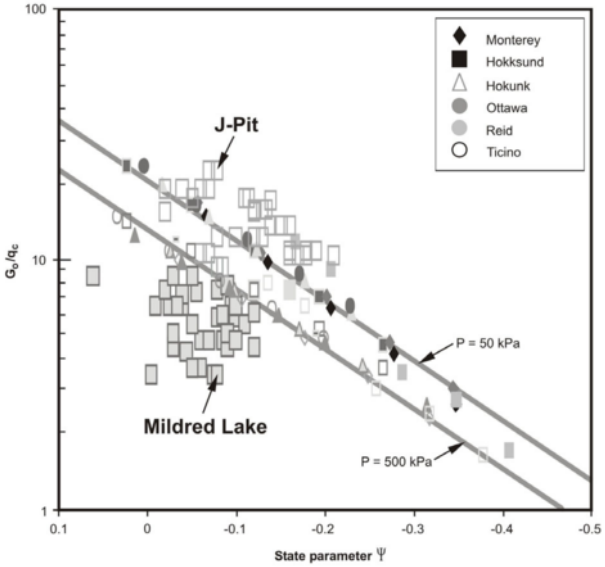

Figure 35. Prediction of the state parameter at Canlex Site (Schnaid & Yu, 2005).

c) SPT in association to energy measurements

In a series of recent publications, the author has advocated that SPT results should be interpreted as a dynamic force F_d from which soil properties can be assessed (Odebrecht et al, 2004; Schnaid et al, 2004; 2005). One example to illustrate possible applications is given in Figure 36, in which the F_d is directly related to the friction angle by assuming a rigid-plastic stress-strain relationship and Vesic's bearing capacity factors (Vesic, 1972). The correlation results in a simple set of relationships where the combined values of N_{60} and σ'_{vo} are directly related to ϕ' values. The proposed approach depicts the trends obtained from the database of the *United States Bureau of Reclamation* (Gibbs & Holtz, 1957), reproduces the correlation proposed by de Mello (1971) and incorporates into the analysis the effect of the rigidity index.

In exploring the possible applications of SPT test data, it will be important to evaluate aspects of sampler penetration that may control the actual penetration mechanism and therefore control the theoretical assumptions adopted in modelling the

test. Effects of grain size, soil crushing and sampler plugging may have to be better understood, but since they violate the continuum mechanics assumption they may have to be mathematically treated as a system of discrete particles. The Distinct Element Method (DEM) described by Cundall & Strack (1979) provides the theory for particle and discontinuous mechanics. Primary limitations to the approach are its extensive computational demands, the impossibility to consider the effect of interstitial fluid and the qualitative nature of results. The method can provide useful insights in describing penetration mechanism though, as recently demonstrated by Huang & Ma (1994) and Daniel et al (2004), among others.

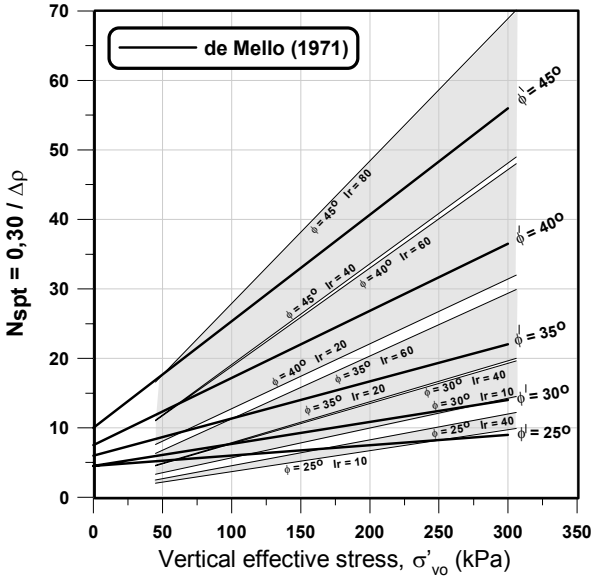

Figure 36. Prediction of internal friction angle from SPT (Schnaid et al, 2004).

Figure 37 shows an example of DEM sampler penetration simulations for different grain size to sampler diameter (Daniel et al, 2004). In this example a two-dimensional, plane strain DEM code demonstrates the penetration of a 50.8m (2") and 127mm (5") samplers in a granular soil. The superimposed black lines are proportional in thickness to the magnitude of the interparticle forces. The analysis demonstrates that the required penetration energy decreases with platen spacing, despite the fact that the platen dimensions were kept constant. This reduction in energy is thought to be related to the formation of stress arches in the soil ahead to the sampler opening, the effectiveness of which increases as the platen space decreases. In addition, the complex phenomenon of sampler plugging is predicted whenever conditions are appropriate.

DEM modelling of deep penetration in sand is required not only for studying the mechanism around the SPT sampler, but also around other penetrometers pushed into the ground such as the cone and dilatometer.

5.5 *Concluding remarks*

The potential use of *in situ* tests for engineering site characterisation of granular deposits has been widely recognised and may comprise identification of aging, cementation and crushability. In many design problems where the focus is primarily on deformations rather than strength, soil stiffness can be measured from seismic techniques and stiffness non-linearity can be conveniently assessed by measuring the stress-strain response of soils by pressuremeter or plate loading tests. Conversely, interpretation of penetration tests is not always straightforward and may require a combination of measurements from independent tests such as the ratio of the elastic stiffness to ultimate strength (G_o/q_c, G_o/N_{60}), the ratio of cone resistance and pressuremeter limit pressure (q_c/Ψ) and the association of strength and energy measurements (N_{60} and energy). Scope for future research comprises a better understanding of soil crushability and the effects of soil structure (which is reported in Section 6).

6. BONDED GEOMATERIALS

6.1 *Background research*

Burland (1990) defined the term "structure" of a natural soil as consisting of two parts: the "fabric" that represents the spatial arrangement of soil particles and inter-particle contacts, and "bonding" between particles, which can be progressively destroyed during plastic straining (given place for the term "destructuration"). Although most geomaterials are recognized as being structured after the conceptual framework proposed by Leroueil & Vaughan (1990), the natural structure of bonded soils has a dominant effect on their mechanical response since the cohesion/cementation component can dominate soil shear strength at engineering applications involving low stress levels. In fact, problems such as slope stability, excavations, shallow foundations and road pavements cannot be addressed without accounting for a cohesion/cementation component in the maintenance of long-term shear strength in overconsolidated soils, residual soil profiles, weak rocks and soil ground improvement.

Background investigation on the effects of bonded structure is based on laboratory tests carried out on natural specimens retrieved from the field (e.g. Burland, 1989 and 1990; Leroueil

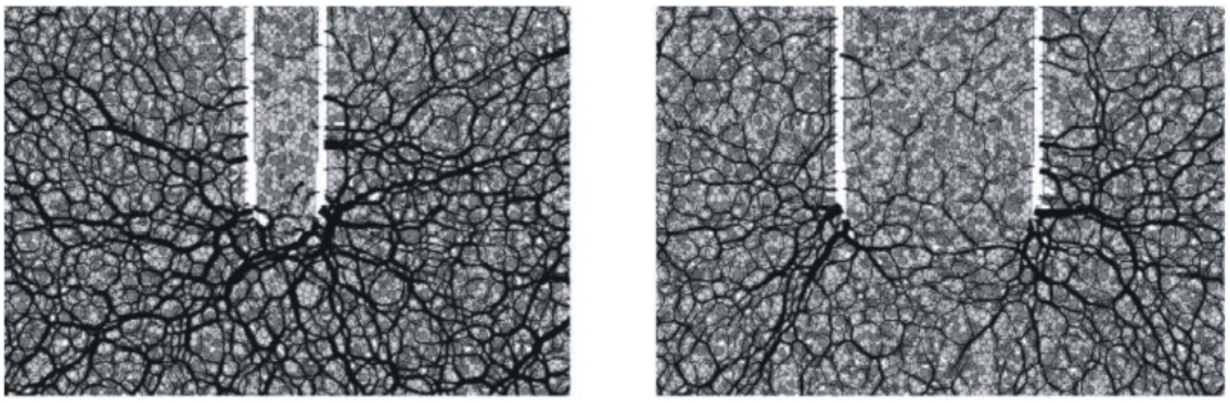

Figure 37. DEM sampler penetration simulations (Daniel et al, 2004)

& Vaughan, 1990; Airey & Fahey, 1991; Smith *et al.*, 1992; Clayton *et al.,* 1992; Airey 1993; Petley *et al.*, 1993; Cuccovillo & Coop, 1997 and 1999; Kavvadas *et al.*, 1993; Lagioia & Nova, 1995; Consoli *et al.*, 1998) as well as in artificially cemented specimens made up through the addition to the soil of a cementitious agent (e.g. Dupas & Pecker, 1979; Clough *et al.*, 1981; Coop & Atkinson, 1993; Cuccovillo & Coop, 1993; Huang & Airey, 1993 and 1998; Zhu *et al.*, 1995; Prietto, 1996; Consoli *et al.*, 2000 and 2001; Schnaid *et al.*, 2001; Rotta et al, 2003). Difficulties in testing natural soils are twofold: disturbance to the structure that can occur during the sampling process and spatial variability inherent to natural deposits emerging from both the degree of cementing and the nature of the particles (e.g. Clayton *et al.*, 1992; Stokoe & Santamarina, 2000). To overcome these shortcomings, artificially cemented specimens are frequently used despite the fact that they may not reproduce the deposition process and the distinctive structure of natural soils.

To distinguish features of behaviour emerging from bonded structure from those related to changes in state, constitutive laws conceived for the unbonded material are modified accordingly to introduce the bond component (e.g. Leroueil & Vaughan, 1990, Gens & Nova,1993; Lagioia & Nova, 1995; Kavvadas & Amorosi, 1998; Rouainia & Muir Wood, 2000). These features, described under both consolidation and shear, are outlined in this section.

Laboratory tests carried out by Rotta et al (2003) simulate, in the laboratory, the formation of a cemented sedimentary deposit in which cemented bonding occurs after burial and under geostatic stresses. Isotropic compression tests carried out on artificially cemented specimens are presented in Figure 38 and are used to illustrate concepts associated to bonding:

a) in strongly bonded materials, the zone of elastic behaviour is enlarged in respect to an unbonded soil (e.g. Tatsuoka *et al.,* 1997; Matthews *et al.,* 2000; Cuccovillo & Coop, 1997) and as a consequence the value of G_o becomes particularly important as a bench-mark for engineering applications;
b) the bonded material can be at a higher void ratio for a fixed mean stress as compared to the unbonded one, as clearly shown in Figure 38 and recognized by Vaughan (1985) and Leroueil & Vaughan (1990);
c) after primary yield, a consolidation curve follows a post-yield compression line that tends to converge towards the intrinsic compression line of the uncemented soil (Cuccovillo & Coop, 1997; Rotta et al, 2003). The zone between the two described yield lines (uncemented and 1% cemented) identifies the structure permitted space defined by Leroueil & Vaughan (1990). It is worth noticing that the onset of plastic yielding is expected to be very marked in bonded geomaterials and therefore the yield locus denoting the onset of large scale yielding, ε_{Y3} can usually be determined experimentally fairly precisely (e.g. Leroueil & Vaughan, 1990; Cuccovillo & Coop, 1997). This is unfortunately not always the case, and there are many examples reporting the difficulties in determining the yield point (e.g. Barksdale and Blight, 1997; Kavvadas *et al,* 1993; Cecconi *et al,* 1998). Take once again the example of isotropic yielding in an artificially cemented soil cured under stress illustrated in Figure 38 (Rotta et al, 2003). The specimens were initially much stiffer than the soil in its destructured state, then becoming gradually softer as the isotropic stress increases. There is no singular point that can be undisputed regarded as ε_{Y3} which may be a result of a gradual onset of the breakage of the cement bonds

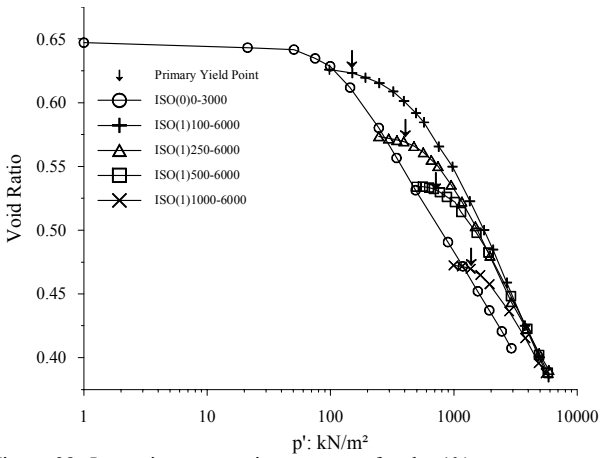

Figure 38. Isotropic compression response for the 1% cement content specimens (Rotta et al., 2003).

Stress-strain curves and failure envelopes obtained in drained and undrained triaxial shear tests exhibit the characteristic behaviour of natural bonded soils. Results from a gneiss saprolitic soil shown in Figure 39 are used to illustrate these patterns of behaviour (Futai et al, 2004):

a) bonding imparts tensile strength and real cohesion to geomaterials. The cohesive-frictional nature of these materials should then be characterized by a shear friction angle ϕ' and a cohesive intercept c';
b) specimens tested under drained shear show a transition from a brittle/dilatant behaviour to a ductile/compressive response, as confining stress increases. Initial stiffness and deviator stress at yield may decrease at high confining stresses. Most stress strain curves from undrained tests display peak deviator stresses and tests at low confining stresses display negative pore pressures.
c) factors controlling the shape of the limit state curve in bonded soils has not yet been fully identified, due to the lack of experimental data in natural samples. Whereas research suggests that residual soils and soft rocks exhibit isotropic behaviour with the yield curve centred to the hydrostatic axis (Uriel & Serrano, 1973; Sandroni & Macarinni, 1981; Leroueil & Vaughan, 1990), data from Figure 39 clearly indicate highly anisotropy of the gneiss investigated by Futai et al (2005);
d) effects of bonding on the stress-strain-volumetric response of natural and artificially cemented geomaterials revealed that dilation of the intact soil is inhibited by the presence of the cement component (e.g. Coop and Atkinson, 1993, Cuccovillo and Coop, 1999; 2000, Schnaid et al, 2001, Mantaras & Schnaid, 2002). In terms of energy it is suggested that the total work done by the stresses at the boundary of an element is partly dissipated in friction and partly in disrupting the structure of the soil. Applying the incremental energy ratio concept, Rowe (1963) demonstrates that:

$$\frac{\sigma'_1}{\sigma'_3}.\frac{1}{1-\frac{d\varepsilon_v}{d\varepsilon_1}} = \tan^2\left(\frac{\pi}{4}+\frac{\phi'_f}{2}\right)+\frac{2.c'}{\sigma'_3}.\tan\left(\frac{\pi}{4}+\frac{\phi'_f}{2}\right) \quad (59)$$

where ε_1 is the major principal strain, ε_v is the volumetric strain (often expressed as dilatancy rate $1-(d\varepsilon_v/d\varepsilon_1)=D$) and $\sigma'_1/\sigma'_3=K$ ratio of the principal stresses. For a purely frictional soil equation 59 is simply expressed as equation 33.

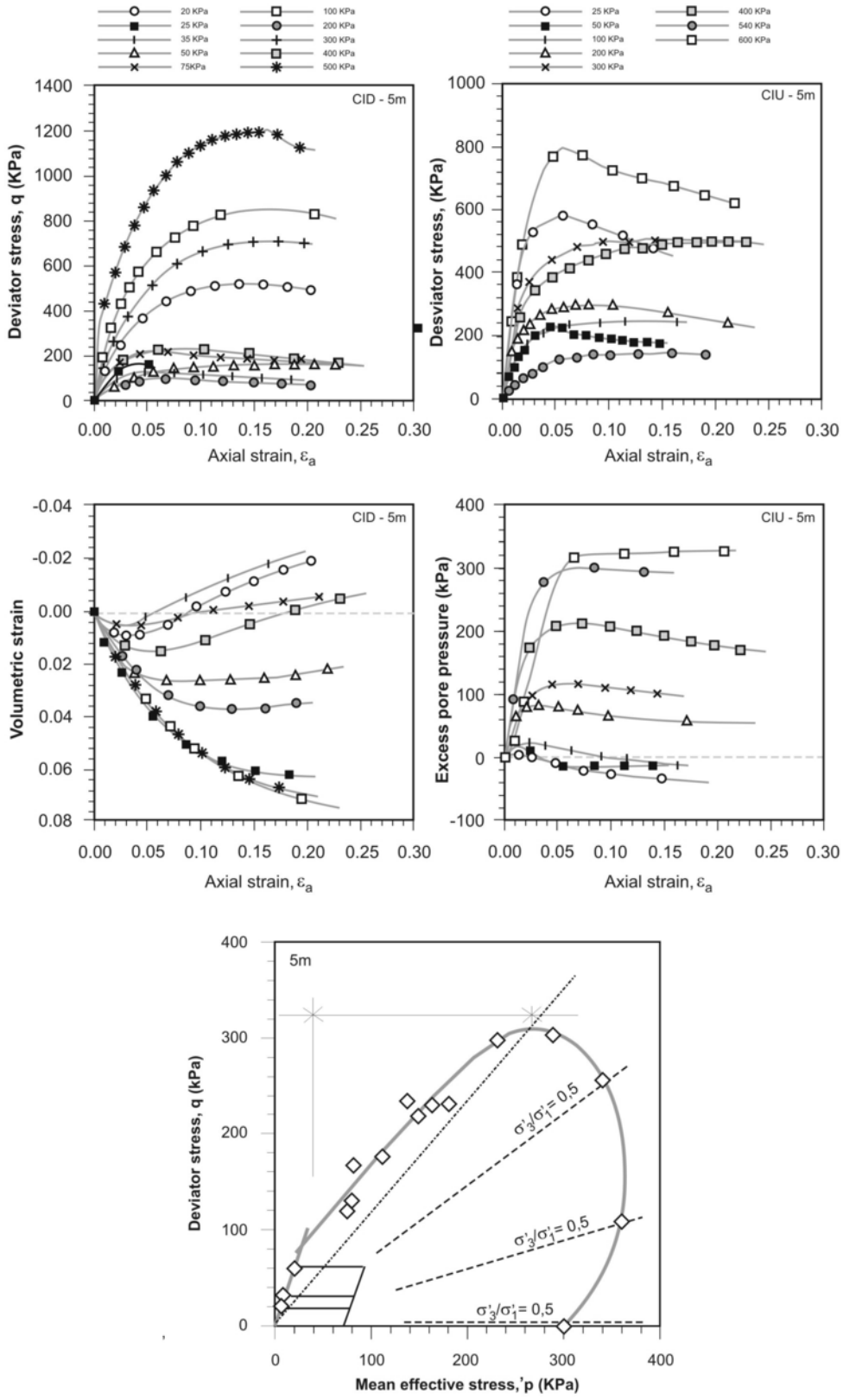

Figure 39. Triaxial response of a natural gneiss (Futai et al., 2004)

Figure 40 shows the stress-dilatancy relationships for drained triaxial tests carried out in the artificially cemented samples, in which results are plotted in terms of stress ratio R *versus* dilation component D, as well as the ratio of R/D plotted against axial strains ε_a. Prior to peak the dilatancy experienced by the cemented samples at a given stress ratio is smaller than that of the reconstituted samples. The rate of dilation increases with increasing shear strain amplitude in a continuous pattern that goes up to peak stresses. Peak states are accompanied by dilation and plastic strains which developed after the soil had yielded and the bonds started to degrade. This process starts at very small strains.

Strain measurements after peak are very unreliable due to strain localisation, but it appears that an ultimate state has been reached when the experimental data curves down towards the reconstituted line and reach a value of dilatancy D approximately equal to 1 in all tests. Mántaras (2000) extended the above discussion to the review of a large database of triaxial and plane strain tests reported by Lambe & Withman (1979), Cornforth (1961), Barden et al (1969), Oda et al (1978), Fonseca (1996) and Cecconi et al (1998). General trends lead to the same basic conclusion that it is necessary to express soil dilation as a function of both friction and cohesion in such a way that the internal energy absorbed by soil particles is a minimum.

e) the preceding discussion also demonstrates that as shear progresses, the amount of bonding will necessarily decrease with the development of irreversible plastic strains (soil degradation).

In recent years, a number of constitutive models incorporating bonding and destructuration has been published, examples given by Lagioia & Nova (1995), Kavvadas & Amorosi (2000); Rouainia & Muir Wood (2000) and Wheller et al (2003) among others. Different assumptions are made in respect to small strain and/or large strain anisotropy, stress induced anisotropy, associated and non-associated flow rules. Despite the fact that this Report does not aim at discussing constitutive modeling, it seems appropriate to recognize features of behaviour that are essential to constitutive models in the light of the assumptions illustrated previously in Figure 12, following the framework introduced by Gens & Nova (1993). A typical yield surface on the p', q space is represented in Figure 41. As the amount of bonding increases the yield surface must grow towards the right to account for the fact that higher mean stresses can be applied to the material without causing it to yield. In addition, bonding also imparts the sample with cohesion and tensile strength that is reflected in the fact that the yield surfaces are enlarged also towards the left of the stress diagram.

Implementing models with all these features of behaviour in numerical finite element solutions would produce sounding interpretation of *in situ* tests data (in particular for cavity expansion analysis), but would distract from the simplicity of decoding the pressuremeter curve to obtain the constitutive parameters of the soil. Mantaras & Schnaid (2002) and Schnaid & Mantaras (2003) introduced a simplified alternative model capable of reproducing bonding and destrucutration under a number of simplified conditions. Lets first consider results from drained triaxial tests presented in Figure 42 in order to illustrate that increasing shearing strain γ [$\gamma = {}^{2}/_{3}(\varepsilon_1 - \varepsilon_3)$] produces a continuous and substantial reduction in cohesion for tests carried out in an artificially cemented soils (Schnaid *et al*, 2001). Results are presented in terms of both normalized stresses and interparticle cohesion intercept plotted against shear strain amplitude. These observed experimental results suggest that, as a first approximation, degradation is attributed to the reduction in interparticle cohesion only, and that this reduction could be expressed simply as a hyperbole described as a function of shear strains and asymptotic to zero at large strains, so that:

$$c_f' = f[(1+\gamma)^{-n}] \qquad (60)$$

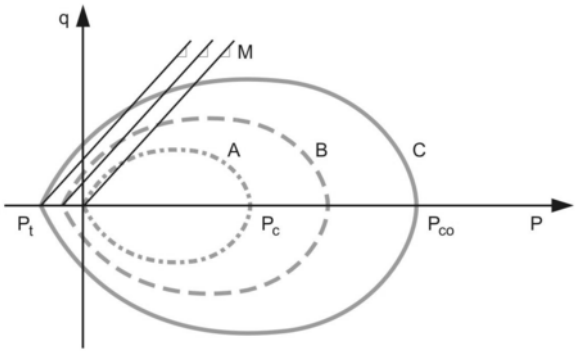

Figure 41. Yield surfaces in bonded soils (after Gens & Nova, 1993).

In the Mohr-Coulomb criterion, the variation of shear strength can then be attributed only to the reduction in the cohesion intercept during the shear process. Figure 43 illustrates this idealized concept for shear degradation on a shear stress τ *versus* normal stress σ plot, in which the reduction in cohesion is represented by a translation of the plastic failure envelopes. In a simple strength reduction idealization no degradation is considered for shear stresses lower than the peak shear strength and for γ values greater than the peak shear strain, γ_p, the observed degradation pattern is asymptotic to zero and can therefore be expressed by a simple generic equation:

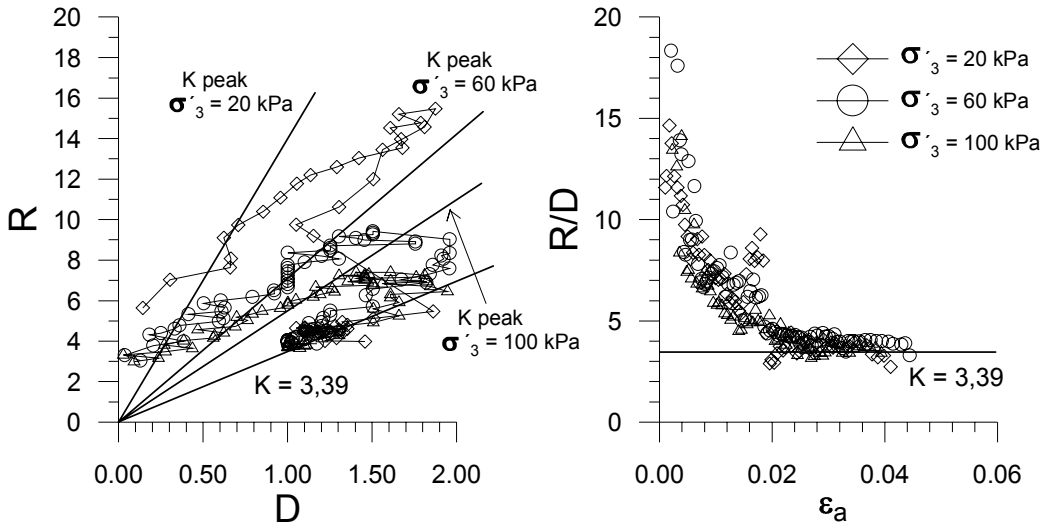

Figure 40. Stress dilatancy relationship for silty sand mixed with 1% Portland cement (K=3.39 corresponds to purely frictional material).

$$c' = \frac{c'_o}{\left(1 + \gamma - \gamma_p\right)^n} \qquad (61)$$

being:

c'_o = Mohr-Coulomb triaxial peak cohesion intercept;
n = degradation index;
γ_p = peak shear strain calculated using Hooke`s law.

In conclusion, the bonded structure of soils influences the results of *in situ* tests. Since these tests have assumed increasing importance in the characterisation of bonded geomaterials, in particular in residual soils, an attempt has been made to develop interpretative methods capable of characterising and even measuring some of the properties of these geomaterials.

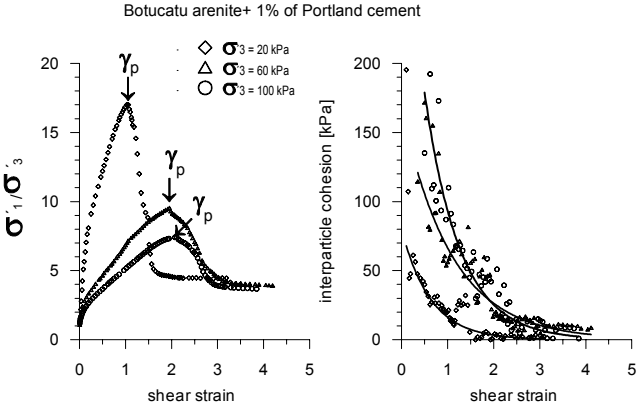

Figure 42. Variations of cohesion intercept with shear strain in artificially cemented sand (Schnaid & Mantaras, 2003).

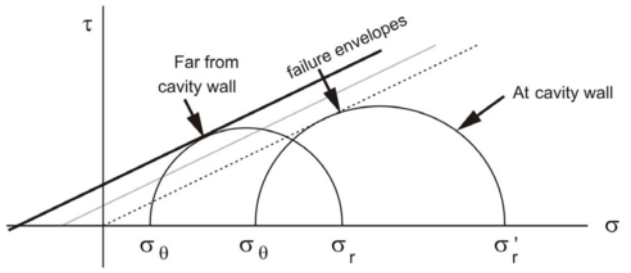

Figure 43. Shear strength degradation (Schnaid & Mantaras, 2003).

6.2 Characterisation of bonded geomaterials

Characterisation of bonded geomaterials will be mainly referred to the experience recently accumulated in the interpretation of *in situ* tests in residual soils. A ground investigation in the so called "residual soils" often reveals weathered profiles exhibiting high heterogeneity on both vertical and horizontal directions, complex structural arrangements, expectancy of pronounced meta-stability due to decomposition and lixiviation processes, presence of rock block, *boulders*, among others (e.g. Novais Ferreira, 1985; Vargas, 1985). The process of *in situ* weathering of parent rocks (which creates residual soils) gives rise to a profile containing material ranging from intact rocks to completely weathered soils. Rock degradation generally progresses from the surface and therefore there is normally a gradation of properties with no sharp boundaries within the profile.

Site investigation campaigns in residual soils are generally implemented from a mesh of boreholes associated to either SPT or CPT, to depths defined by the capacity of the penetration tool, and followed by continuous rotational coring below the soil-rock interface for a global geological characterisation of weathering patterns. To enhance consistency, recommendations are made to encompass geophysical surveys. In this highly variable environment, both laboratory and *in situ* test still assist in characterising stress-strain and strength properties on residual soils.

It follows from the foregoing on granular materials that a bonded/cemented structure produces G_o/q_c and G_o/N_{60} ratios that are systematically higher than those measured in cohesionless soils. These ratios therefore provide a useful means of assisting site characterisation. Typical results from residual profiles are presented in Figure 44, in which the G_o/q_c ratios are plotted against normalized parameter q_{c1} for CPT data (after Schnaid, 1999; Schnaid et al, 2004). The bond structure generates normalized stiffness values that are considerably higher than those for uncemented soils and as a result the datapoints for residual soils fall outside and above the band proposed for sands by Eslaamizaad & Robertson (1997) and theoretically determined by Schnaid & Yu (2004).

As for the CPT, SPT N values can also be combined with seismic measurements of G_o to assist in the assessment of the presence of a deposit's bonding structure and its variation with depth. Such a combination is provided on Figure 45, which plots G_o/N_{60} *vs* $(N_1)_{60}$ in residual soils, where $(N_1)_{60} = N_{60}(p_a/\sigma'_{vo})^{0.5}$ and is analogous to q_{c1} on Figures 44. Database comprise soils from Brazil and Portugal (Barros, 1997; Schnaid, 1997; Vianna da Fonseca, 2003; Lemos et al, 2004). The bond structure is seen to have a marked effect on the behaviour of residual soils, producing values of normalised stiffness (G_o/N_{60}) that are considerably higher than those observed in fresh cohesionless materials. A guideline formulation to compute G_o from SPT tests is given by the following equations:

$$\frac{(G_0/p_a)}{N_{60}} = \alpha N_{60}\sqrt{\frac{p_a}{\sigma'_{vo}}} \quad \text{or} \quad \frac{(G_0/p_a)}{N_{60}} = \alpha(N_1)_{60} \qquad (62)$$

where α is a dimensionless number that depends on the level of cementation and age as well as the soil compressibility and suction. The small strain stiffness to strength ratio embodied within the G_o/N_{60} term is seen on Figure 45, at a given $(N_1)_{60}$ (or relative density), to be generally appreciably higher for lateritic soils than that of the saprolites, primarily because the latter generally exhibit higher N_{60} (or strength) values.

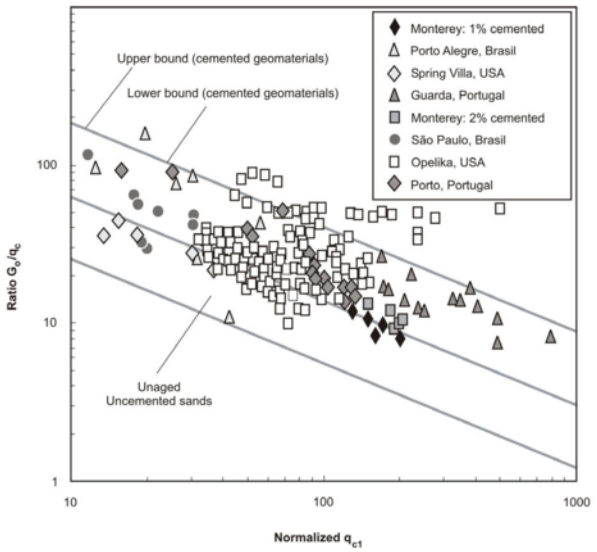

Figure 44. Relationship between G_o and q_c for residual soils (Schnaid et al., 2004).

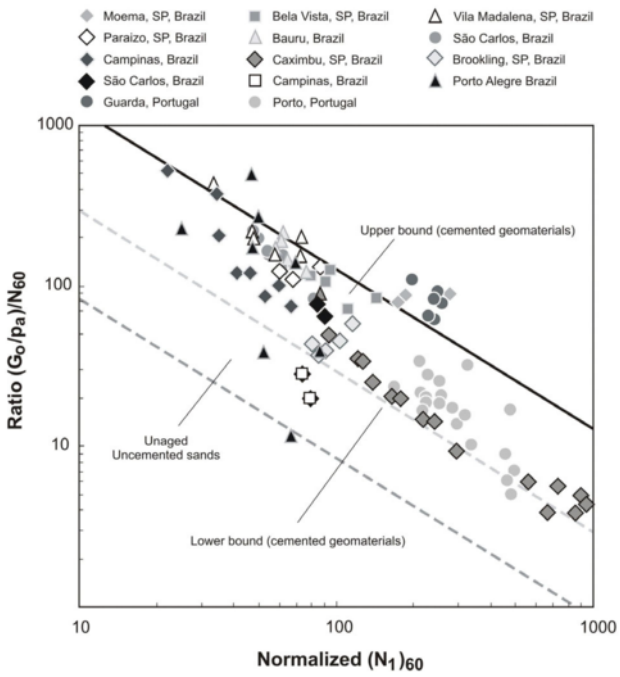

Figure 45 Correlation between G_o and N_{60} for residual soils (after Schnaid, 1997).

6.3 *Soil stiffness*

The magnitude of the small strain stiffness in bonded soils is better understood in comparison to values determined from natural sands. A reference equation adopted in the comparison is:

$$\frac{G_o}{F(e)} = S\left(p'\right)^n \tag{63}$$

with units in MPa and a void ratio function expressed as:

$$F(e) = \frac{(2.17 - e)^2}{1 + e} \tag{64}$$

Values of parameter S and n are given in Table 3 and a direct comparison is shown in Figure 46, having the data for alluvial sands from Ishihara (1982) as reference. Values of G_o diverge significantly from those established for transported soils when they exhibit the same granulometry but are uncemented. Parameter S is much higher than the value adopted for cohesionless soils, whereas n varies significantly as a result of local weathering conditions as demonstrated from the Caxingui Brazilian Subway database (Barros, 1997). Given the variations in both S and n, the need for site-specific correlations becomes evident.

Table 3: Parameters for residual soil stiffness

Soil	S	n	Reference
Alluvial sands	7.9 to 14.3	0.40	Ishihara (1982)
Porto saprolite granite	65 to 110	0.02 to 0.07	Viana da Fonseca (1996)
Guarda saprolite granite	35 to 60	0.30 to 0.35	Rodrigues & Lemos (2004)
Caxingui gneiss saprolite	60 to 100	0.30 (p´<100kPa)	Barros (1997)

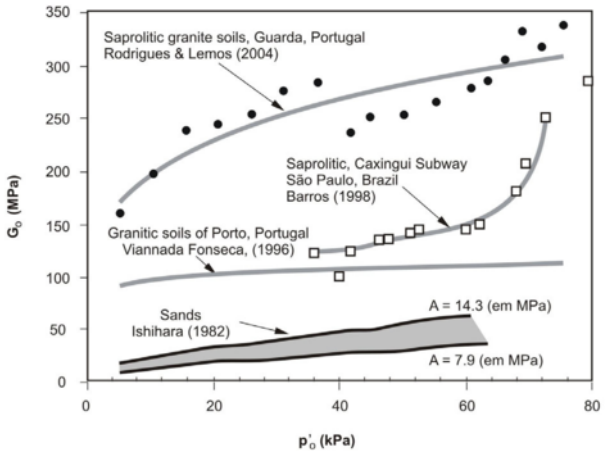

Figure 46. Relation between G_o and p'_o for residual soils (modified from Gomes Correia et al., 2004).

Considering the variation observed in natural bonded soils it is preferable to express correlations in terms of lower and upper boundaries designed to mach the range of recorded G_o values, as extensively shown throughout this Report. The variation of G_o with q_c can be expressed as (Schnaid et al, 2004):

$$\left.\begin{aligned} G_0 &= 800\sqrt[3]{q_c \sigma'_v p_a} \quad \text{upper bound : cemented} \\ G_0 &= 280\sqrt[3]{q_c \sigma'_v p_a} \quad \text{lower bound : cemented} \\ &\qquad \text{upper bound : uncemented} \\ G_0 &= 110\sqrt[3]{q_c \sigma'_v p_a} \quad \text{lower bound uncemented} \end{aligned}\right\} \tag{65}$$

The variation of G_o with N can also be expressed by upper and lower boundaries, similarly to the cone penetration data (Schnaid et al , 2004):

$$\left.\begin{aligned} G_0 &= 1200\sqrt[3]{N_{60} \sigma'_v p_a^2} \quad \text{upper bound : cemented} \\ G_0 &= 450\sqrt[3]{N_{60} \sigma'_v p_a^2} \quad \text{lower bound : cemented} \\ &\qquad \text{upper bound : uncemented} \\ G_0 &= 200\sqrt[3]{N_{60} \sigma'_v p_a^2} \quad \text{lower bound uncemented} \end{aligned}\right\} \tag{66}$$

Once again it is emphasized that given the considerable scatter observed for different soils, correlations such as given in equations (65) and (66) are only approximate indicators of G_o and do not replace the need for *in situ* shear wave velocity measurements.

The reduction in the ratio of G/G_o with shear stress and shear strain is known to be sensitive to degradation of cementation and structure, among several other factors (Tatsuoka *et al.,* 1997). The moduli degradation can be measured in the laboratory with high resolution sensors provided that high-quality undisturbed samples can be obtained. In contrast, Schnaid et al (2004) have demonstrated the level of uncertainty associated in back-figuring the degradation curve from *in situ* tests in bonded soils. Take the example given in Figure 47 intended to illustrate the interpretation of non-linear stiffness soil properties from a drained Plate Load Test, PLT (after Schnaid et al, 2004). Typical (simplified) variations of the secant Youngs modulus (E_{sec}) of a cemented sand is seen to reduce from a high initial value (E_o) of 350 MPa, which prevails until a presumed yield stress (σ'_{vy}) of 100 kPa is exceeded, to a stiffness comparable to that of an uncemented sand at axial strains in excess of 0.4%. From a numerical analysis, these two rather different materials produced the non-linear applied stress

(q_{app})-settlement (s) response of a 300mm diameter (D) plate shown in the same figure. It is apparent that, despite the significant differences in stiffness, the curves are almost linear without revealing the significant softening that may be expected on inspection of Figure 47a when the applied stresses exceeded σ'_{vy}. Independent attempts have been made to back-analyse the load-settlement curves in order to predict the input degradation curves of both cemented and uncemented materials. Departing from a given G_o, engineers were able to match the behaviour of the uncemented soils but were unable to identify the cement component of the bonded soil (as seen in the dashed area in Figure 47a).

6.4 *Shear strength*

Since the natural structure of bonded soils has a dominant effect on their mechanical response and the bonded strength is recognized as a net sign of this structure, identification of the two components of strength is crucial in geotechnical design problems. Use of triaxial tests on high quality samples to quantify the cohesive-frictional parameters of bonded soil is always advisable, but given the acknowledged difficulties of maintaining the relic structure during sampling, which masquerades bonding effects on stiffness and strength, *in situ* tests remain as a viable option in engineering practice.

Penetration tests such as SPT, CPT and DMT, extensively used in transported soils, are also commonly adopted in the investigation of structured cemented deposits, with empirical correlations for assessing soil properties being locally adapted to meet standards that reflect regional engineering practice. A limited ground investigation based on these penetration tools will not produce the necessary database for any rational assessment of soil properties, for the simple reason that two strength parameters cannot be derived (ϕ', c') from a single measurement (q_c or N_{60}). Limited investigations are, however, often the preferred option. In such cases involving cohesive frictional soils, engineers tend to (conservatively) ignore the c' component of strength and correlate the *in situ* test parameters with the internal friction angle ϕ'. Average c' values may be later assessed from previous experience and back-analyses of field performance.

Since the practice of assessing parameters from limit ground investigation and previous experience appears to be widespread, the author recommended the pressuremeter as a means of inspecting the accurateness of a given set of design parameters (Schnaid et al, 2004). All the theories for the interpretation of the pressuremeter in bonded soils make use of the *in situ* horizontal stress, soil stiffness and strength parameters: angle of internal friction, angle of dilation and cohesion intercept (which reduces with destructuration at high shear strains). The pressure expansion curve represents therefore a combination of all these parameters that cannot be assessed independently. Given this complexity, instead of attempting to derive a set of parameters from a single test in residual soils the pressuremeter should be viewed as a "trial" boundary value problem against which a theoretical pressure-expansion curve predicted using a set of independently measured parameters is compared to field pressuremeter tests. A good comparison between the measured and predicted curves gives reassurance to the process of selecting design parameters, whereas a poor comparison indicates that one or more of the constitutive parameters are unrealistic.

Adequacy of the method largely depends upon the constitutive model adopted to represent soil behaviour which, for a cohesive-frictional material, is complicated by a number of factors such as the influence of bonding on the stress-dilatancy response of soils and the effects of destructuration. Ideally the c' and ϕ' should be coupled to stiffness, dilatancy and mean stress level and for that reason the cylindrical cavity expansion analysis developed by Mantaras & Schnaid (2002) and Schnaid & Mantaras (2003) is recommended. The concept introduced by Rowe (1963) that plastic dilatancy is inhibited by the presence of soil bonding, discussed previously in this section, was investigated and used to describe the plastic components of the tangential and radial increments in an expanding cavity. A new solution is formulated within the framework of non-associated plasticity in which the Euler Method is applied to solve simultaneously two diferential equations that leads to the continuous variations of strains, stresses and volume changes produced by cavity expansion.

For the loading phase of cavity expansion the non-associated flow rule can be expressed as $\frac{\dot{\varepsilon}_\theta^p}{\dot{\varepsilon}_r^p} = -\beta$ where where ε_θ^p and ε_r^p are the plastic components of the tangential and radial strain increments. The general definition proposed by Rowe's law based on the hypothesis of minimum absolute energy increment during shear was previously expressed in equation 59. With the aim at generalising Rowe's law, not only by considering both the cohesive and frictional components but also allowing for degradation of cohesion during shear, it is possible to combine equations 59 and 61:

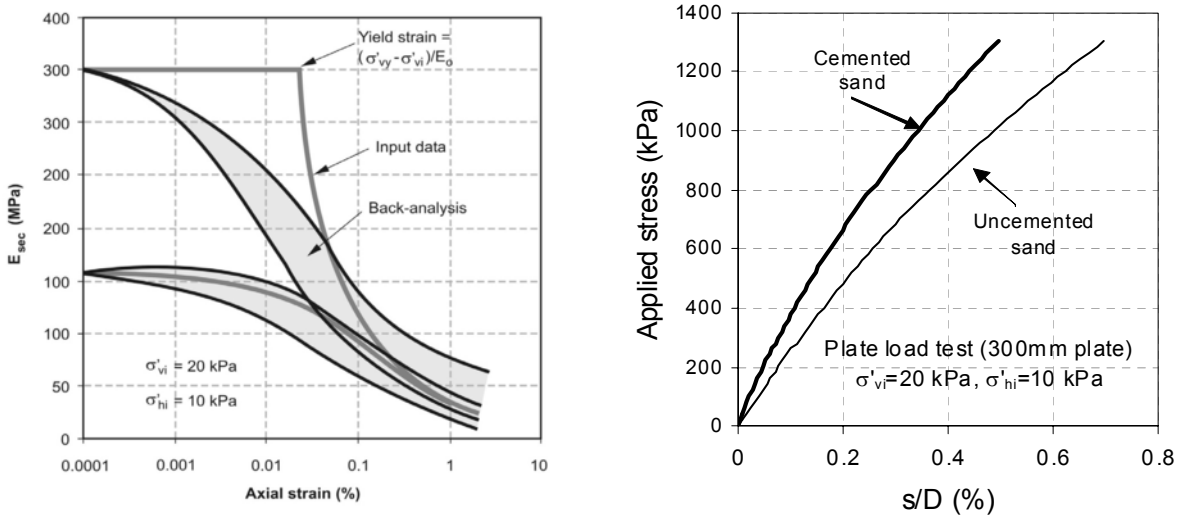

Figure 47. Analysis and back-analysis of plate loading tests for cemented and uncemented sands (modified from Schnaid et al, 2004)

$$\beta = \frac{\sigma'_r}{\left[\tan\left(\frac{\pi}{4}+\frac{\phi'_{cv}}{2}\right)\right]^2 .\sigma'_\theta + \frac{2.c'_o}{\left[1+\varepsilon_r-\varepsilon_\theta-\gamma_p\right]^n}\tan\left(\frac{\pi}{4}+\frac{\phi'_{cv}}{2}\right)} \qquad (67)$$

where:

ε_r: radial strain
ε_θ: circumferential strain
γ_p: shear strain corresponding to the onset of yielding

Adopting equation (67) to describe the flow rule can eliminate one of the main limitations regarding classical cavity expansion formulations. There is no need to select a single constant value for the cohesion intercept as representative of the complex stress variation with radii of material points within the soil at different loading stages of the test. A peak c'_o value is selected for the elastic region and in the plastic domain the analysis can keep careful track of the reduction in shear strength produced by increasing shear strain amplitudes around the cavity.

Figures 48 to 49 illustrates these features by representing the ratios of $c'/c'_{(b)}$ and $\beta/\beta_{(b)}$ plotted against cavity radius, being $c'_{(b)}$ and $\beta_{(b)}$ the cohesion intercept and dilation at the elastic-plastic interface, respectively. The variation in the cohesion ratio $c'/c'_{(b)}$ is presented in Figure 48 in which it is possible to observe the overall distribution of cohesion around the cavity for different values of the degradation index, for a dilatant material expanded to 50% its initial diameter. Material points that lie at the elastic-plastic boundary do not exhibit any structural degradation and therefore cohesion values correspond to maximum peak values, so that the ratio $c'/c'_{(b)}$ is equal to unity. After expansion the material between the cavity wall and the elastic-plastic boundary has been deformed plastically with the shear strain amplitude reducing with increasing distance from the cavity wall. The ratio $c'/c'_{(b)}$ will therefore reduce with increasing γ and n values as suggested by equation 61, this reduction being sensitive to the selected degradation index. For greater n values, the structure of the soil close to the cavity wall can be completely disrupted and $c'/c'_{(b)}$ values could approach zero. Figure 49 shows the change in $\beta/\beta_{(b)}$ with radius for the same material and boundary conditions represented previously in Figure 48. An intact material is represented at r = b which corresponds to $\beta/\beta_{(b)}$ =1. Reducing r values produces an increase in shear strains, a reduction in cohesion and therefore an increase in dilation. The ratio of β/β_b gradually increases with reducing r values, the rate of increment being a function of the degradation index n.

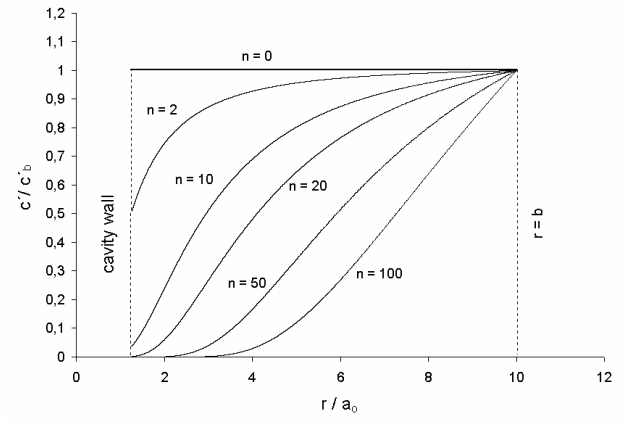

Figure 48. Variation in normalised cohesion within the plastic region (Schnaid & Mantaras, 2003).

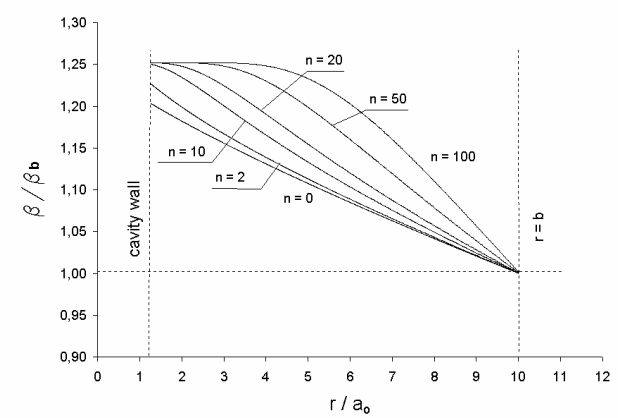

Figure 49. Normalised dilatation (β/β(b)) within the plastic region around an expanding cavity (Schnaid & Mantaras, 2003).

Schnaid & Mantaras (2003) present results from a numerical analysis to illustrate the influence of structure degradation on a material that is at critical state ($\phi' = \phi'_{cv}$). The cohesion intercept is initially taken as 50 kPa which is representative of a structured soil. Pressure expansion relationships are plotted in Figure 50 for a range of differents **n** indexes. Results from the solutions proposed by Yu & Houlsby (1991) and Mántaras & Schnaid (2003) were also plotted in these figures to give a reference benchmark for cases in which strength parameters are considered as constants. In addition, an enlarged plot of initial expansion is presented in each figure to demonstrate the patterns of deformation for small strains. From the observed results it is clear that limit pressure is strongly affected by the degradation of cohesion.

Case studies in the Hong Kong gneiss (Schnaid et al, 2000), Porto granite (Mantaras, 2002) and Sao Paulo gneiss (Schnaid & Mantaras, 2003) have illustrated the application of the described methodology. The trial fitting technique was used in all reported cases based on the recognition that strength, stiffness and *in situ* stresses interact to produce a particular pressuremeter expansion curve.

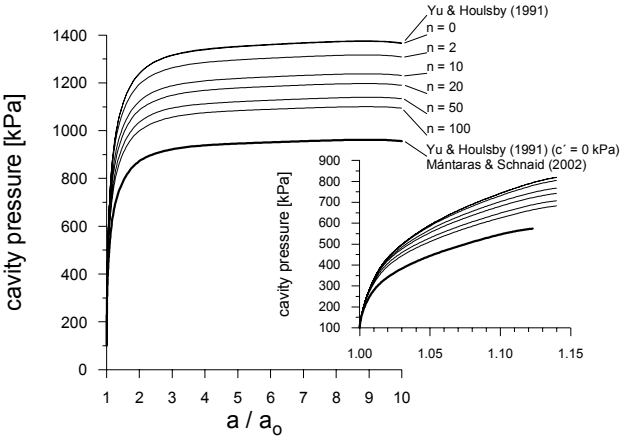

Figure 50. Typical pressure-expansion results for different n values (($\phi' = \phi'_{cv}$) (Schnaid & Mantaras, 2003).

6.5 *Final remarks*

The mechanical behaviour of bonded soils is still not fully understood and cannot be modelled even in the idealized conditions in the laboratory when testing elemental specimens. A combination of poor understanding, lack of constitutive models and complex boundary conditions give rise to interpretation methods of *in situ* tests that are empirical in nature, with the single exception of a pressuremeter test. Effects of bonding on penetration mechanisms are barely recognized

since there is no analytical and numerical framework to support empirical observations.

Cavity expansion offers a unique possibility of combining the effects of structuration and destructuration in shear mode. The flow rule has been accommodated to describe the evidence that dilation of the intact soil is inhibited by the presence of the cement component, which in energy terms suggests that the total work done by the stresses at the boundary of an element is partly dissipated in friction and partly in disrupting the structure of the soil. Examining the actual mechanism that controls dilatancy may require the use of distinct element method (DEM) to evaluate the influence of the inter-particle assemblage, bonding between particles and the progressive damage to bonding during plastic straining.

On a more general level, bonded soils should still be regarded as 'unusual geomaterials', until a more consistent framework of interpretation is developed. Recalling Schnaid et al (2004), unusual soil are characterised as those that satisfy any one or more of the following criteria:

- classical constitutive models do not offer a close approximation of its true nature;
- it is difficult to sample or to be reproduced in the laboratory (interpretation is therefore solely based on *in situ* test data);
- very little systematic experience has been gathered and reported;
- values of parameters are outside the range that would be expected for more commonly encountered soils such as sand and clay;
- the soil state is variable due to complex geological conditions.

Everyone of the above criterion can be applied to soft rocks and hard soils, indicating the need for further research in this area.

7 INTERMEDIATE PREMEABILITY SOILS

As we advance in the study of natural soils, the subject of intermediate permeability soils becomes unavoidable. Many soils exhibit a complex macro and micro structure and may have very scattered grain size distribution, and variations in mineralogy and clay content. These features have a dominant effect on soil permeability, and hence on *in situ* behaviour at given loading rates, producing geomaterials in the so called intermediate permeability range of 10^{-5} to 10^{-8} m/s. As illustrated in Figure 51, this range comprises a variety of geomaterials such as sedimentary silts, clayey silts and clayey sands (e.g. Manassero, 1994) and residual formations from granite, gneiss, basalt and migmatite (e.g. Deere & Patton, 1971; Costa Filho & Vargas, 1985; Garga & Blight, 1997; Vianna da Fonseca, 2003), not to mention man-made materials such as earth-fills and tailings.

For intermediate soils, the simplest idealized approach of a broad distinction between drained (gravels and sand) and undrained (clay) conditions for the interpretation of *in situ* tests cannot be applicable since test response can be affected by partial consolidation and consequently existing analytical, numerical or empirical correlations can lead to unrealistic assessment of geotechnical properties (e.g. Schnaid et al, 2004). Unfortunately there are no standardized recommendations to guide engineers on how to perform *in situ* tests or interpret test results in these materials. Since numerical assessment is restricted to the consolidation characteristics of clays, recommendations for intermediate soils are empirical based established from field observations. This Report provides a critical overview of recent studies in clay and silt soils and describes a method designed to recognize consolidation patterns that may take place during penetration and cavity expansion.

Previous research has identified strain rate effects on pressuremeter test results on soft clay (Anderson et al, 1987; Hanzawa & Tanakaz, 1992; Fioravante et al, 1994; Rangeard et al, 2001; 2003). The general aim was the assessment of soil permeability from pore pressure measurements around an expanding cavity, in particular from pressuremeter holding tests. Numerical studies show that soil permeability affects test results due to partial drainage and that patterns of behaviour are a function of rate of loading and coefficient of hydraulic conductivity. Rangeard et al (2003) expressed the evolution of total and effective stress around a pressuremeter as a function of the dimensionless variable:

$$\left(\frac{\Delta p}{\Delta t}\frac{1}{2G}\right)\frac{a}{k} = \frac{\delta_a a}{k} \tag{68}$$

where $\Delta p/\Delta t$ is the probe inflating rate, G is the shear modulus, a is the probe diameter, k is the coefficient of hydraulic conductivity and δa is the strain rate at the cavity wall. From this dimensionless strain variable the authors attempted to identify the consolidation regime around a cavity for a given set of critical state soil parameters, as presented in Figure 52, separating drained from partial drained from undrained expansion.

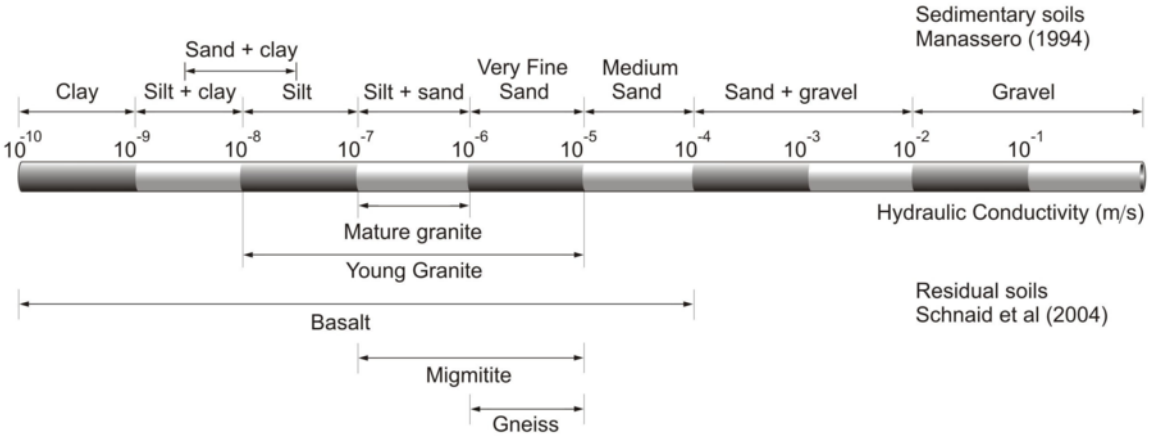

Figure 51. Typical saturated permeability in natural soils (after Schnaid et al, 2004)

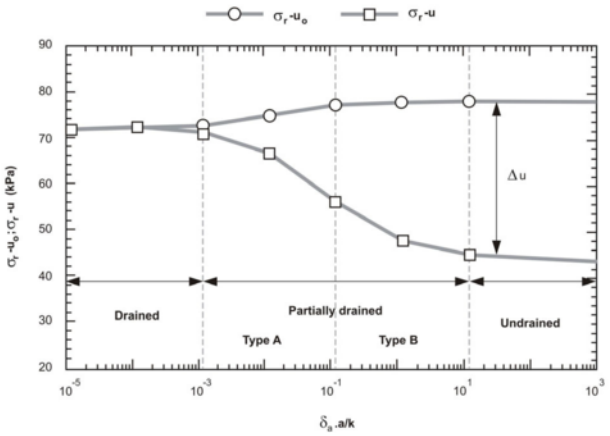

Figure 52. Evolution of the total stress σ_r - u_o and effective stress σ_r – u as a function of normalised velocity (Rangeard et al, 2003).

In contrast, early evaluation of drained effects in penetration tests was mainly empirical based and follows recommendations established from field observations (e.g. Bemben & Myers, 1974; Danziger & Lunne, 1997). McNeilan & Bugno (1985) suggested that for hydraulic conductivities greater than 10^{-4} m/s cone penetration is fully drained, whereas for hydraulic conductivities less than 10^{-8} m/s an undrained penetration will take place. Alternatively, partial drained penetration can be evaluated directly from the pore pressure parameter B_q; if B_q is less than 0.4 a direct use of N_k factors for the assessment of undrained strength is questionable (Senneset et al, 1988). Hight et al (1994) found that a relationship between B_q, $(q_t-\sigma_{vo})/\sigma'_{vo}$ and clay content could be a useful approach for interpreting results under fully undrained conditions. Their analysis appear to suggest that penetration is fully undrained for values of B_q greater than 0.5.

Recent studies place emphasis on the normalisation of penetration results that are represented by an analytical "backbone curve" of penetration resistance against rate effects expressed by a dimensionless velocity (Randolph and Hope, 2004:

$$V = \frac{vd}{C_v} \qquad (32)\ \text{idem}$$

where d is the probe diameter and C_v is the coefficient of consolidation, as previously introduced in Session 4. There is an obvious similarity between equations 32 and 68 as they both produce a dimensionless parameter to assess consolidation effects as a function of rate of loading, probe diameter and soil permeability.

Given the extensively explored experience in simulating cone penetration and pressuremeter expansion by cavity expansion theory, it is suggested that simple cylindrical cavity expansion can be adopted to couple the rate of penetration to consolidation effects in attempting to identify drainage patterns in field tests. This was achieved by Schnaid et al (2005) in a numerical study that uses a finite element program to simulate cavity expansion in the modified Cam-Clay model. The numerical program is a one-dimensional (1D) axisymmetric plane strain cavity expansion program developed by Carter (1978) that accounts for loading rate effects through the coupled analysis between applied stress and Darcy flow of pore pressures given by large strain consolidation theory. The coefficient of hydraulic conductivity k was set to range from $1x10^{-9}$ m/s to $1x10^{-3}$ m/s, whereas both permeability and rate of cavity expansion where kept constants throughout the analysis (at their initial prescribed values). For each given stress condition, different coefficient of hydraulic conductivity produced distinct patterns of dissipation allowing undrained to partial drained to drained stress paths to be identified. In the numerical solutions the dimensionless velocity is conveniently expressed as a function of the hydraulic conductivity as:

$$V = \frac{vd}{k}\frac{\gamma_w \lambda}{(1+e)\sigma'_r} \qquad (69)$$

where e and σ_r are void ratio and radial stresses adjacent to the probe at the end of testing.

Theoretical results of normalised effective stress ratio (σ_r-$u/\sigma_{r(dr)}$-u_o) against normalised velocity are presented in Figure 53 and 54, where various features of interest can be noticed. Two idealised materials have been used in the analysis, one representative of a soft soil (kaolin) and another of a stiff clay. There is a clear indication that the so called "backbone curve" is not unique, since it changes as a function critical state parameters and soil stiffness. The normalised stress curves also show a slight dependency of the values of OCR. It is worth mention that a drained reference value was adopted for normalisation essentially because this is the only field measurement that can be assessed with reasonable accuracy when *in situ* tests are performed in soils with intermediate permeability. This is simply achieved by ensuring that no excess of pore water pressure Δu is generated during loading, in contrast to undrained or partially drained conditions that are associated to variable $\Delta u/u_o$ ratios.

Despite the variations in these normalised stress curves, the transition point from drained to partial drained response starts at a normalised velocity of around $V \approx 10^{-3}$, and it appears to be largely independent of both stiffness and OCR. Similarly the transition from partial drained to undrained appears also to be independent of soil properties, the onset of a fully undrained condition occurring for a normalised velocity V of around 100. In general OCR has little effect on the "backbone curves" except for the fact that the effective stress ratio reduces with increasing OCR.

Once consolidation effects around an expanding cavity are properly evaluated, an appropriate rate law has to be selected to describe the patterns generated by the derived numerical data. An equation that departures from unity (stress ratio=1 is imparted by the normalisation for the drained effective radial stress) and reduces to a decimal value greater than zero can be conveniently expressed as a hyperbolic cosine function:

$$\frac{\sigma_r - u}{\sigma_{r,\max(dr)} - u_o} = a + (1-a)\frac{1}{\cosh(bV^c)} \qquad (70)$$

where a, b and c are fitting parameters. Note that parameter **a** represents the ratio between the undrained and the drained effective radial maximum stresses, ($\sigma_{r,max(und)}$-$u/\sigma_{r,max(dr)}$-u_o), whereas **b** and **c** control the rate of change from drained to undrained.

Solutions of the limit pressures of spherical and cylindrical cavities have been extensively used to describe the effects of installation of driven piles, to predict end bearing and shaft capacity of piles and to simulate cone penetration in soils (e.g. Vesic, 1972; Ladanyi & Johnson, 1974; Baligh, 1975; Randoph & Wroth, 1979; Yu & Houlsby, 1991; Collins et al, 1997; Carter & Kulhawy, 1992). One of the first analogies between spherical cavity expansion and end bearing failure was proposed by Gibson (1950), showing that if clay is modelled by a perfectly plastic Tresca yield criterion close form solutions exists for limit pressure that can be associated to end bearing. Ladanyi & Johnson (1974) assumed that the normal stresses acting on the cone face was equal to that required to expand a spherical cavity from zero radius. In this solution the soil is

model by a Tresca criterion to obtain the spherical cavity limit pressure. The strain path solution developed by Baligh (1975) has identified the plastic strain field around a penetration probe which has common features to those predicted by cylindrical cavity expansion. Although limitations of these methodologies are recognised and widely reported, it is at least reasonable to suggest that the overall trend observed for cavity expansion can capture some of the penetration rate effects of the piezocone.

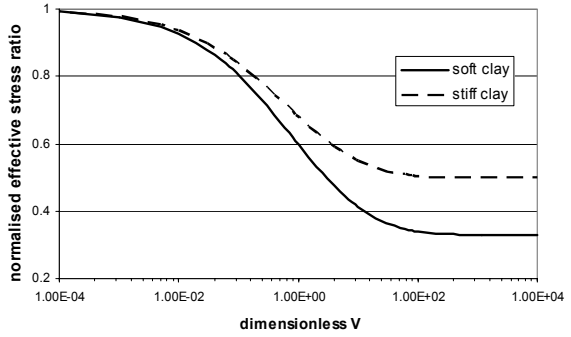

Figure 53. Normalised effective stress ratio (σ_r-u/$\sigma_{r(dr)}$-u_o) for soft and stiff clay.

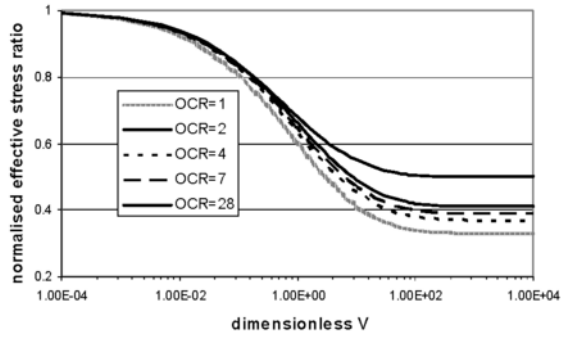

Figure 54. Effect of OCR on the "back-bone curve" of a soft clay ((Schnaid et al., 2005).

Plotted in Figure 55 is a comparison between the predicted and observed rate effects in kaolin for centrifuge tests reported by Randolph and Hope (2004) and previously shown in Figure 24. Results are plotted as normalised penetration rate (and effective stress ratio for numerical analyses) against dimensionless velocity V. The numerical results generally agree with the measure cone ratio, supporting the assumption that this ratios can be compared. The analysis accurately predicts the onset of undrained penetration; the onset of drained penetration is predicted at a much lower penetration rate though. This is probably due to (a) the choice of stiffness adopted to represent the behaviour of kaolin in the model and (b) the acknowledged limitations of representing a 3D process by a 1D analysis.

The discussion has been so far concentrated on the analysis of cone penetration. A similar study can be carried out to evaluate the excess pore water pressure generated during cone penetration, but for dilatant silty soils it is necessary to recall that negative shear induced pore pressures are generated and low (or even negative) B_q values may be observed during undrained penetration. The influence of drainage conditions on B_q measurements at variable rates of piezocone penetration tests in centrifuge clayey silt specimens has been recently discussed by Schneider et al (2005). A typical example is shown in Figure 56, in which excess pore pressure Δu_2 is plotted against time. In these dilatant materials, as the penetration rate increases, the negative shear component of pore pressure also increases. While evaluation of u_2 shear induced pore pressures for clays can be approximated using hybrid Cam-Clay cavity expansion

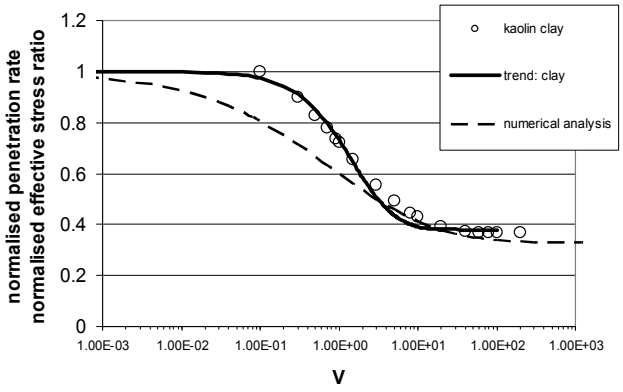

Figure 55. Comparison between measured normalised penetration rate and predicted normalized effective stress ratio for kaolin centrifuge tests (Schnaid et al., 2005).

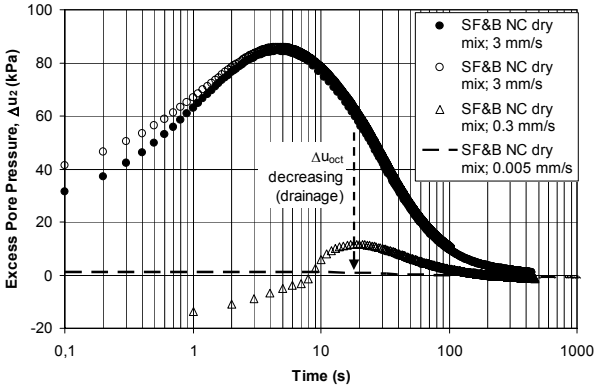

Figure 56. Typical drainage paths for centrifuge penetration tests in silty soils (Schneider Lehane & Schnaid, 2005).

(e.g. Burns & Mayne, 1998; Mayne 2001), the assessment of negative shear induced pore pressures in silty soils has not been analytically quantified.

Work by Schnaid et al (2005) and Schneider et al (2005) extended the previously reported data in clay (Randolph & Hope, 2004) in a research programme that comprises centrifuge penetration tests carried out in three different samples, corresponding to a silty soil (silica flour), silica flour mixed dry with 5% bentonite, and silica flour mixed as a slurry with 5% bentonite, tested at different rates of penetration and g-levels. Preliminary results from this experience are summarised in Figure 57, in which the variation of the normalised net cone resistance Q_c/Q_{cdr} is plotted against normalised velocity V for normally consolidated specimens. Values of q_{dr} are representative of the lowest rate of penetration tested in the centrifuge (v=0.005mm/s) and are considered to produce fully drainage conditions in all materials tested in the centrifuge.

Substantial scatter is observed due to difficulties in preparing homogeneous repeatable silty samples in the strongbox. Results for silty soils (silica flour) are representative of normalised velocities ranging from 10^{-4} to 10^{-1} and for that range no significant penetration rate effects have been observed. Recalling that no substantial excess pore pressures have been recorded during penetration, it is reasonable to suggest that measured tip resistances q_c are representative of a fully drained penetration. For silica flour with 5% betonite mixed dry, a smooth decrease in the Q_c/Q_{cdr} ratio is observed with increasing normalised velocities, a gradual transition from drained to partial drainage initiating at values of V of approximately 10^{-1}. The fastest test corresponds to a normalised V $\approx 10^{+2}$, a condition that matches a fully undrained penetration. Normalised cone resistance Q_c/Q_{cdr} reduces from unity in drained penetration to about 0.3 in an undrained test. An additional curve presented in Figure 57 corresponds to kaolin

centrifuge tests carried out by Randolph and Hope (2004) that by comparison can illustrate the changes in drainage paths observed between clay and silty soils. In clay, penetration resistance reduces with increasing V reaching a minimum ratio of about 0.38. Variance in trends between silica+bentonite and clay samples are relatively small (up to approximately 20%).

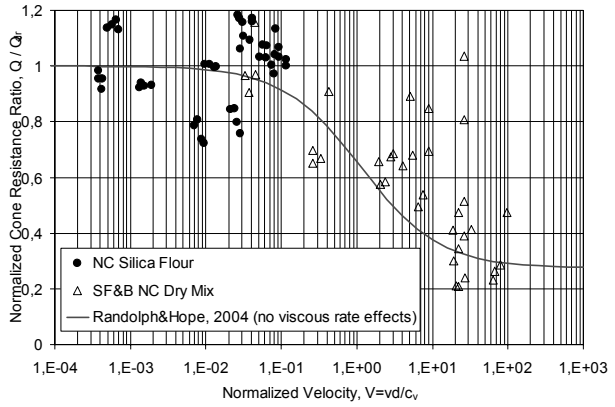

Figure 57. Normalised penetration rate for silt and clay (Schneider, Lehane & Schnaid, 2005).

Despite the range of permeabilities tested in the centrifuge, it was possible to identify the transitional response of penetration from drained to partial drained to undrained. Drainage paths for silica flour have shown a fairly similar response to clay soils. Equation 71 can be used to express the reduction on cone resistance in clay and silt geomaterials in a similar way as that represented in the analysis of cavity expansion:

$$\frac{q_c - u}{q_{c(dr)} - u_o} = a + (1-a)\frac{1}{\cosh(bV^c)} \qquad (71)$$

where a=0.30, b=3.0 and c=0.30 can be adopted as a first approximation.

Although the study covers a limited number of geomaterials and is based on model tests, some specific conclusions can be drawn. The rate of dissipation can be conveniently expressed as a function of dimensionless velocity V, but unfortunately theoretical studies suggest that different "backbone curves" are obtained for different geomaterials since the rate of dissipation has been shown to be fairly sensitive to soil stiffness and is therefore a function of rigidity index and overconsolidation ratio. It is premature to give general recommendations for field tests in intermediate permeability soils but since the rate of penetration is one of the few parameters that can be controlled in field tests, it appears reasonable to change the penetration ratio to avoid tests that yield dimensionless velocities within the range of 10^{-2} to 10^{+1}. In this range, partial drainage is expected to occur and properties assessed from field test interpretation can be overestimated, in particular the undrained shear strength.

8 CONCLUSIONS

Geotechnical site characterisation has developed over the past 50 years from a single approach involving basic empirical recommendations to a sophisticated area demanding a thorough knowledge of material behaviour and numerical modelling. Present design practice of *in situ* testing interpretation evolved from early experience gathered in reconstituted clay and sand to a more general field that covers a variety of natural geomaterials, comprising clay deposits, granular soils, intermediate permeability silts and *bonded* hard soils and soft rocks. Although different methodologies are adopted when assessing mechanical properties in different soil formations, a combination of results from independent tests to obtain some degree of redundancy is regarded as a single general recommendation. In clay *in situ* and laboratory tests should be perceived as complementary and should be combined in routine engineering design problems. Geomaterials that are difficult to sample or to be reproduced in the laboratory, and for that reason interpretation is solely based on *in situ* tests, should also rely on at least two independent measurements. Mechanical properties that are based on the combination of measurements from independent tests such as the ratio of the elastic stiffness to ultimate strength (G_o/q_c, G_o/N_{60}), the ratio of cone resistance and pressuremeter limit pressure (q_c/Ψ) and the association of strength and energy measurements (N_{60} and energy) have been extensively explored and recommended to enhance the confidence in deriving appropriate constitutive parameters for geotechnical design.

8.1 *Clay deposits*

a) a review has been made on current practice in characterising soft clay sediments, outlining the significant progress made in the development of analytical and numerical methods adopted for the interpretation of pressuremeter, cone and flow penetrometer mechanisms;
b) despite the fact that great experience has been gathered in stiff clay deposits, such as London, Boston and Gault clay, interpretation methods are still largely empirical based. Cavity expansion, bearing capacity linked to CPT and wave propagation theory for the SPT are recommended as potentially useful approaches for deriving strength properties in stiff clay;
c) special features of behaviour affect the interpretation of *in situ* tests in clay. Interpretation of test data as inverse boundary value problems allows us to use *in situ* tests to predict some of these features: non-linearity is captured by a combination of seismic and pressuremeter tests, small strain anisotropy by seismic tests with waves polarised in different directions, large strain anisotropy by vane tests;
d) field techniques involve strain rates that are several orders of magnitude greater than laboratory tests. Strain rate effects and the resulting increase in undrained shear resistance are recognised and can be evaluated from both analytical and numerical methods.

8.2 *Granular soils*

a) soil classification from *in situ* test results should preferably rely on at least two independent measurements. A measure of the ratio of the elastic stiffness to ultimate strength, expressed as G_o/q_c and G_o/N_{60}, has shown to be fairly sensitive to cementation and ageing and is therefore useful for identifying the characteristic behaviour of geomaterials;
b) in uncemented unaged sands, stiffness and stiffness non-linearity can be conveniently assessed from a combination of geophysics and measured stress-strain response of soils from pressuremeter or plate loading tests;
c) results of *in situ* test data can be potentially interpreted in terms of the state parameter, in particular from measurements taken from the cone pressuremeter and the seismic cone;
d) scope for future research comprises a better understanding of soil crushability and the effects of soil structure, which may require discrete element methods (DEM) to investigate the response of particle assemblage in penetration processes.

8.3 *Bonded geomaterials*

a) the natural structure of bonded soils has a dominant effect on their mechanical response since the bonding strength

component can dominate soil shear strength in engineering applications at low stress levels;

b) combinations of G_o/q_c and G_o/N_{60} are vital for the characterisation of the bonded structure of cemented geomaterials. The small strain stiffness to strength ratio embodied within the G_o/q_c and G_o/N_{60} terms is expected to increase with bond/cementation, primarily because the effect of these on G_o is stronger than on q_c (or N_{60});

c) the continuous pressure-displacement curve of a pressuremeter offers a unique alternative to evaluate the combined effects of structuration and destructuration. A flow rule describes the evidence that dilation of the intact soil is inhibited by the presence of the cement component, which in energy terms suggests that the total work done by the stresses at the boundary of an element is partly dissipated in friction and partly in disrupting the structure of the soil. These principles are incorporated in cavity expansion theory to produce a sounding way of assessing soil parameters.

8.4 *Intermediate permeability silt soils*

a) the simplest idealized approach of a broad distinction between drained and undrained conditions for the interpretation of *in situ* tests should not be adopted in engineering practice since test response can be affected by partial consolidation and consequently existing correlations can lead to unrealistic assessment of geotechnical properties;

b) recent studies place emphasis on the normalisation of penetration results that are represented by an analytical "backbone curve" of penetration resistance against rate effects expressed by a dimensionless velocity. Cavity expansion has been adopted to couple the rate of penetration to consolidation effects in attempting to identify drainage patterns in field tests. Centrifuge tests have provided the necessary experimental database against which theoretical concepts have been verified;

c) the rate of dissipation has been shown to be fairly sensitive to soil stiffness and is therefore a function of rigidity index and overconsolidation ratio;

d) a general recommendation for field tests in intermediate permeability soils is to avoid tests that yield dimensionless velocities within the range of 0.01 to 10. In this range, partial drainage is expected to occur and properties assessed from field test interpretation can be overestimated, in particular the undrained shear strength.

As the principles governing the behaviour of geomaterials have become better understood, interpretation methods designed to derive constitutive parameters have become more scientific. A wide variety of solutions is now available – some are recognised as rigorous whereas others are a rough approximation of soil behaviour and for this reason should be viewed just as guide to decision-making. Regardless the approach adopted in the interpretation of test data, analysis should always be supported by background theory. Overall, site characterisation is a subject to be approached by experienced engineers but geotechnical design can no longer be guided by experience only.

ACKNOWLEDGMENTS

The author is grateful to his colleges at Federal University of Rio Grande do Sul, in particular to Nilo C. Consoli and Jarbas Milititski. The authors should also acknowledge the cooperation and contribution from Michele Jamiolkowski, William Van Impe, Hai Sui Yu, Martin Fahey, Barry Lehane, Guy Houlsby, Simon Wheeler, Márcio Almeida, Roberto Coutinho, Itai Einav and James Schneider. Special thanks to some of my previous and current students Fernando Mantaras, Diego Nacci, Gabriela Medeiros, Leandro Spinelli and Pedro Prietto. Finally, the author acknowledges the funding support received from the Brazilian National Agency CNPq during his sabbatical leave in 2004 which enabled this report to be written.

REFERENCES

Aas, G. 1965. A study of the effect of vane shape and rate of strain in the measured values of in situ shear strength of clays. *Proc. 6th Int. Conf. Soil Mech. and Found. Engng*, 1:141-145.

Aas, G., Lacasse, S., Lunne, T. & Hoeg, K. 1986. Use of in situ test for foundation design on clay. *Proc. ASCE Specialty Conf. In Situ'86: Use of In Situ Tests in Geotech. Engng*, Blacksburg, pp. 1-30.

Abu-Farsakh, M.;Tumay, M. & Voyiadjis, G. 2003. Numerical parametric study of piezocone penetration test in clays. *Int. J. of Geomech., ASCE*, 3(2):170-181.

Ajalloeian, R. & Yu, H.S 1988. Chamber studies of the effects of pressuremeter geometry on test results in sand. *Geotechnique*, 48:621-636.

Almeida, M.S.S & Marques, M.E.S 2003. The behaviour of Sarapui soft clay. *Charact. and Engng. Properties of Natural Soils*, Balkema Publishers, 1: 477-504.

Anderson, W.F.; Pyrah, I.C. & Haji-Ali, F. 1987. Rate effects in pressuremeter tests in clay. *J. Geotech. Engng., ASCE*, 113(11):1344-1358.

Baguelin, F.; Jezequel, J. F. & Shields, D. H. 1978. The pressuremeter and foundation engineering. *Trans. Tech. Publications*, Clausthall, 278p.

Baldi, G.; Bellotti, R., Ghionna, V.N.; Jamiolkowski, M., & Pasqualini, E. 1982. Design parameters for sand from CPT. *Proc. 2th European Symp. on Penetration Testing*. Amsterdam, 2: 425-432.

Baligh, M.M 1975. Theory of deep site static cone penetration resistance. *MIT, Cambridge, Mass. Public*. R75-56.

Baligh, M.M 1985. Strain path method. *J. Soil Mech. Found. Engng. Div., ASCE*. 11(7):1108-1136.

Baligh, M.M & Scott, J.N 1975. Quasi static deep penetration in clays. *J. Soil Mech. Found. Engng. Div., ASCE* 101(11):1119-1133.

Baligh, M.M & Levadoux, J.N 1986. Consolidation after undrained piezocone penetration. II: Interpretation. *J. Soil Mech. Found. Engng. Div., ASCE*. 11(7), 112(7), 727-745.

Barden, L.; Ismail, H. & Tong, P. 1969. Plane strain deformation of granular material at low and high pressures. *Géotechnique* 19, No. 4, 441-452.

Barksdale, R.D. & Blight, G.E. 1997. Compressibility and settlement of a residual soil. *Mech. of Residual Soils*. Blight Ed., Blakema, 99-154.

Barros, J.M.C. 1997. Dinamic shear modulus in tropical soils, *PhD Thesis*, São Paulo University, In portuguese.

Becker, 2001 Site characterisation geotechnical and geo-environmental engineering handbook. *Kluwer Academic Publishing*. Norwell, USA, 69-105.

Been, K. & Jefferies, M.G. 1985. A state parameter for sands. *Géotechnique*, 35(2), 99-112.

Been, K.; Jefferies, M.G., Crooks, J.H.A & Hotemburg, L. 1987. The cone penetration test in sands. Part 2: General influence of state. *Geotechnique*, 37(3):285-299.

Bellotti, R.; Ghionna, V.N.; Jamiolkowski, M., Robertson, P.K. & Peterson, R.W. 1989. Interpretation of moduli from self-boring pressuremeter tests in sand, *Geotechnique*, 39(2): 269-292.

Bellotti, R.; Jamiolkowski, M., Lo Presti, D.C.F. & O'Neill, D.A. 1996. Anisotropy of small strain stiffness in Ticino sand. *Geotechnique*, 46 (1): 155-131.

Bemben, S.M. & Myers, H.J. 1974. The influence of rate on static cone resistance in Connecticut River Valley varved clay. *Proc. European Symp. on Penetration Testing*, ESOPT, Stockholm, 2:33-34.

Biscontin, G. & Pestana, J.M. 2001. Influence of peripheral velocity on vane shear strength of an artificial clay. *Geotech. Testing J.*, 24(4):423-429.

Bolton, M.D. 1986. The strength and dilatancy of sands. *Géotechnique* 36 (1), 65-78.

Bolton, M.D. & Whittle, R.W. 1999. A non-linear elastic/perfectly plastic analysis for plane strain undrained expansion tests, *Geotechnique* 49(1):133-141.

Bolton, M.D.; Gui, M.W.; Garnier, J.; Corte, J.F.; Bagge, G.; Laue, J. & Renzi, R. 1999. Centrifuge cone penetration tests in sands. *Geotechnique*, 49(4):543-552.

Briaud, J.-L. 1992. The pressuremeter. *Balkema Publisher*, Netherlands, 192p.

Burland, J.B. 1989. Small is beautiful: the stiffness of soils at small strains, *Can. Geotech. J.*, 26: 499-516.

Burland, J.B. 1990. On the compressibility and shear strength of natural clays, *Géotechnique* 40 (3), 329-378.

Burns, S.E. & Mayne, P.W. 1998. Monotonic and dilatory pore-pressure decay during piezocone tests in clay. *Can. Geotech. J*., 35(6): 1063-1073.

Campanella, R.G., Robertson, P.K. & Gillepsie, D. 1986. Seismic cone penetration test. *Proc. ASCE Spec. Conf. In Situ'86 on Use of In Situ Tests in Geotech. Engng*., Blacksburg, pp. 116-130.

Carter, J.P. 1978. CAMFE, a computer program for the analysis of cavity expansion in soil. *Cambridge Univ. Press Dest. of Engng*. Report CUEDIC – Soils TR52.

Carter, J.P. & Kulhawy, F.H. 1992. Analysis of laterally loaded shafts in rocks. *J. Geotech. Engng. DIV., ASCE*, 118(6):839-855.

Caquot, A. & Kerisel, J. 1956. Traite de mechanique des sols. *Gauthier-Villars*, Paris.

Cecconi, M.; Viggiani, G. & Rampello, S. 1988. An experimental investigation on the mechanical behaviour of pyroclastic soft rock., *Proc. 2nd Int. Symp. on Geotech. Engng. of Hard Soils-Soft Rocks*. Naples, 1:473-482.

Cecconi, M.; Viggiani, G. & Rampello, S. 1998. An experimental investigation of the mechanical behaviour of a pyroclastic soft rock. *The Geotech. of Hard Soils-Soft Rocks,* Balkema, 473-482.

Charles, M.; Yu, H.S. & Sheng, D. 1999. Finite element analysis of pressuremeter tests using critical state soil models. *Proc. 7th Int. Symp. on Num. Models in Geomech.*, Graz, 645-650.

Chen, B.S-Y. & Mayne, P.W. 1996. Statistical relationships between piezocone measurements and stress history of clays, *Can. Geotech. J.*, 33(3):488-498.

Clarke, B. G. 1993. Pressuremeter in geotechnical design. *Chapman & Hall*, London, UK.

Clarke, B.G., Carter, J.P. & Wroth, C.P. 1979. In situ determination of the consolidation characteristics of saturated clays. *Proc. 7th European Conf. on Soil Mech. and Found. Engng.*, Brighton, Vol. 2: 207-213.

Clayton, C.R.I 1995. The standard penetration test (SPT): methods and use. Report 143. *Ciria*, London.

Clayton, C.R.I. & Serratrice, J.F. 1993. General Report Session 2: The mechanical properties and behavior of hard soils and soft rocks. *Proc. 1st Int. Symp. on the Geotech. of Hard Soils – Soft Rocks*, Athens, Vol. 3: 1839-1877.

Clayton, C.R.I.; Matthews, M.C. & Simons, N.E. 1995. Site Investigation. *Blackwell Science*, 584pp.

Clayton, C.R.I. & Heymann, C. 2001. The stiffness of geomaterials at very small strains. *Géotechnique*, 51(3): 245-256.

Collins, I.F; Pender, M.J. & Wang, Y. 1997. Cavity expansion in sands under drained loading conditions. *Int. J. Num. and Anal. Methods in Geomech.* 16(1):3-23.

Consoli, N.C.; Ulbrich, L.A. & Prietto, P.D.M.. 1998. Influence of Fiber and Cement Addition on Behavior of Sandy Soil. *J. of Geotech. and Geoenvironm. Engng.*, *ASCE*, 12(124):1211-1214.

Consoli, N.C., Rotta, G.V.; & Prietto, P.D. M. 2000. The Influence of Curing under Stress on the Triaxial Response of Cemented Soils. *Géotechnique*. 50(1): 99-105.

Consoli, N.C., Prietto, P.D. M.; Carraro, J.A.H., & Heineck, K.S. 2001. Behavior of Soil-Fly Ash-Carbide Lime Compacted Mixtures. *J. of Geotech. and Geoenvironm. Engng.*, 127(9): 774-782.

Coop, M. R. & Airey, D. W. 2003. Carbonate sands. *Charact. and Engng. Properties of Natural Soils, Singapore.* Balkema Publishers*, 2: 1049-1086.*

Coop, M. & Atkinson, J. 1993. The mechanics of cemented carbonate sands. *Géotechnique* 43, No. 1, 53-67.

Cornforth, D.A. 1961. Plane strain failure characteristics of a saturated sand. *PhD Thesis*. University of London

Costa Filho, L.M. & Vargas, Jr. E. 1985. Hydraulic properties. Peculiarities of geotechnical behaviour of tropical lateritic and saprolitic soils. *Progress Report* (1982-1985). *Brazilian Society of Soil Mech*. 67-84.

Cotecchia, F. & Chandler, R.J. 1997. The influence of structure on the pre-failure behaviour of a natural clay. *Géotechnique*, 47(3): 623-544.

Cuccovillo, T. & Coop, M.R. 1997. Yielding and pre-failure deformation of structured sands. *Géotechnique*, 47(3): 491-508.

Cuccovillo, T. & Coop, M. 1999. On the mechanics of structured sands. *Géotechnique* 49, No. 4, 349-358.

Cundall, P.A. & Streck, O.D.L. 1979. A discrete numerical model for granular assembles. *Geotechnique*, 29(1):47-65.

Daniel, C.R.; Howie, J.A., Campanella, R.G. & Sy, A. 2004. Characterisation of SPT grain size effects in gravels. *2nd Int. Conf. on Site Charact.*, Milpress, Porto, 1: 299-306.

Danziger, F.A.B. & Lunne, T. 1997. Rate effects in cone penetration testing. *Geotechnique* 47(5):901-914.

Danziger, F.A.B.; Soares, M.S.S. & Sills, G.C. 1996. The significance of the strain path analysis in the interpretation of piezocone dissipation data. *Geotechnique*, 46(2):143-154.

de Beer, E.EW. 1977. Static cone penetration testing in clay and loan. *Sondeer Symp*. Utrecht.

de Mello, V.F.B. 1971. The standard penetration test. *4th Panamerican Conf. Soil Mech. Found. Engng.*, Porto Rico, 1: 1-87.

Decourt, L; Muromachi, T; Nixon, I.K.; Schmertmann, J.H.; Thorbum, C.S. & Zolkov, E. 1988. Standard Penetration test (SPT): International reference test procedure. *Proc. Int. Symp. on Penetration Testing*, ISOPT-1, USA, 1: 37-40.

Deere, D.V. & Patton, F.D. 1971. Slope stability in residual soils. *Proc. 4th Pan American Conf. Soil Mech. and Found. Engng..*, Puerto Rico, 1, 87-170.

Diaz-Rodrigues, J. A. 2003. Characterisation and Engineering Properties of Mexico City Lacustrine Soils. *Charact. and Engng. Properties of Natural Soils*, Balkema Publishers, 1: 725-756.

Diaz-Rodriguez, J.A., Leroueil, S. & Aleman, J.D. 1992. Yielding of Mexico City clay and other natural clays. *J. Geotech. Div., ASCE,* 118(7): 981-995.

Durgunoglu, H.T. & Mitchell, J.K. 1975. Static penetration resistance of soils. 1st *Proc. of the ASCE Specialty Conf. on In Situ Measurement of Soil Properties*. Raleigh, 1, 151-189.

Einav, I. & Randolph, M.F. 2005. Combining upper bound and strain path methods for evaluating penetration resistance. *Int. J. on Num. Methods in Geotech. Engng.*, forthcoming paper.

Eslaamizaad, S. and Robertson, P.K. 1997. A Framework for In-situ determination of Sand Compressibility. *49th Can. Geotech. Conf.*; St John's Newfoundland.

Fahey, M. 1998. Deformation and in situ stress measurement, *Geotech. Site Charact.,* ISC'98, Balkema, 1: 49-68.

Fahey, M. & Carter, J.P. 1993. A finite element study of the pressuremeter test in sand using a non-linear elastic plastic model, *Can. Geotech. J.*, 30: 348-362.

Fernandez, A.L. & Santamarina, J.C. 2001. Effect of cementation on the small-strain parameters of sands. *Can. Geotech. J.*, 38(1): 191-199.

Ferreira, R.S. & Robertson, P.K. 1992. Interpretation of undrained self-boring pressuremeter test results incorporating unloading. *Can. Geotech. J.*, 29:918-928.

Finno, R.J. 1993. Analytical interpretation of dilatometer penetration through saturated cohesive soils. *Geotechnique*, 43(2):241-254.

Fioravante, V. Jamiolkowski, M. & Lancellotta, R. 1994. An analysis of pressuremeter holding tests, *Geotechnique*, 44(2):227-238.

Flaate, K. 1968. Baereevne av Friksjonspeler I Leire; *om Beregning av Baereevne pa grunnlag av Geotekniske undersokelser*. Oslo, Veglabolatoriet, 38.

Fonseca, A. P. V. 1996. Mechanical characterisation of the residual granite from Porto: Design of shallow foundations, *PhD Thesis*, Porto University, Portugal (in Portuguese)

Foray, P. 1991. Scale and boundary effects on calibration chamber pile tests. *Proc.1st Int. Symp. on Calibration Chamber Testing*, Postdam, New York, 147-160.

Futai, M.M.; Almeida, M.S.S. & Lacerda, W.A. 2004. Yeild, strength and critical state of a tropical saturated soil. *Geotechnique*, forthcoming paper.

Garga, V.K. & Blight, G.E. 1997. Permeability. *Mech. of Residual Soils.* Balkema. Chapter 6, 79-94.

Gaudin, C.; Schnaid, F. & Garnier, J. 2005. Sand characterization by combined centrifuge and laboratory tests. *Int. J. of Physical Moddeling in Geotech.*. Forthcoming paper.

Gens, A. & Nova, R. 1993. Conceptual bases for a constitutive model for bonded soils and weak rocks. *Proc. 1st Int. Symp. on the Geotech. of Hard Soils – Soft Rocks*, Athens, Vol.1: 485-494.

Ghionna, V.N. & Jamiolkowski, M. 1991. A critical appraisal of calibration chamber testing of sands. *Proc.1st Int. Symp. on Calibration Chamber Testing*, Postdam, New York, 13-39.

Ghionna, V.N.; Jamiolkowski, M.; Pedroni, S. & Piccoli, S. 1995. Cone penetrometer tests in Po River sand. *The Pressuremeter and its Marine Applications*. Gerard Ballivy Editor, 471-480.

Gibbs, H. J. & Holtz, W.G. 1957. Research on determining the density of sands by spoon penetration testing. *4th Int. Conf. Soil Mech. Found. Engng*, London, 1: 35-39.

Gibson, R.E. 1950. Correspondence, *J. Inst. Civil Engineers*. 34:382-383.

Gibson, R.E. & Anderson, W.F. 1961. In situ measurement of soil properties with the pressuremeter. *Civil Engng and Public Works Review*, 56: 615-618.

Gomes Correia, Vianna da Fonseca, A. & Gambin, M. 2004 Routine and advanced analysis of mechanical in situ tests. *2nd Int. Conf. on Site Charact.*, Milpress, Porto, 1: 74-.

Graham, J. & Houlsby, G.T. 1983. Anisotropic elasticity of a natural clay. *Geotechnique*, 33(2):165-180.

Graham, J.; Crooks, J.H.A. & Bell, A.L. 1983. Time effects on the stress-strain beahviour of natural soft clays. *Geotechnique*, 33(3):327-340.

Gui, M.W.; Bolton, M.D.; Garnier, J.; Corte, J-F.; Bagge, G.; Laue, J. & Renzi, R. 1998. Guidelines for cone penetration tests in sand. *Proc. Int. Conf. Centrifuge 98*, Tokyo, Balkema, 1:155-160.

Hamouche, K., Roy, M. & Leroueil, S. 1995. A pressuremeter study of the sensitive Louiseville clay. *Proc. 4th Int. Symp. on Pressuremeter*, Sherbrooke, pp. 361-366.

Hanzawa, H. & Tanakaz, H. 1992. Numerical undrained strength of clay in normally consolidated state and in the field. *Soils & Found.*, 32(1):132-148.

Hardin, B.O. 1978. The nature of stress-strain behavior for soils. *Proc. ASCE Geot. Div. Specialty Conf. on Earthquake Engng. and Soil Dynamics,* Pasadena, Vol. 1: 3-90.

Hardin, B.O. & Black, W.L. 1968 Vibration modulus of normally consolidated clay. *J. Soil Mech. Found. Div., ASCE*, 95-SM6, 1531-1537.

Hight, D.W., Bennell, J.D., Chana, B., Davis, P.D., Jardine, R.J. & Porovic, E. 1997. Wave velocity and stiffness measurements at Sizewell. *Proc. Symp. on Pre-Failure Deformation Behaviour of Geomaterials,* London, pp. 65-88.

Hight, D.W. & Leroueil, S. 2003. Characterisation of soils for engineering purposes. *Charact. and Engng. Properties of Natural Soils*, Balkema Publishers, 1: 255-362..

Hight, D.W.; Paul, M. A., Barras, B. F.; Powell, J. M. Nash, D. F. T. Smith, P. R.; Jardine, R.J. & Edwards, D. H. 2003. The characterization of the Bothkennar Clay. *Charact. and Engng. Properties of Natural Soils*, Balkema Publishers, 1: 543-598.

Hird, C.C. & Hassona, F. 1986. Discussion on "A state parameter for sands". *Géotechnique*, 36(1): 124-127.

Houlsby, G.T. 1998. Advanced interpretation of field tests, *Geotech. Site Charact., ISC'98*, Balkema, 1, 99-112.

Houlsby, G.T & Hitchman, R. 1988. Calibration chamber tests of a cone penetrometer in sand. *Geotechnique*, 38:575-587.

Houlsby, G.T. & Withers, N.J. 1988. Analysis of the cone pressuremeter test in clays. *Geotechnique*, 38 (4): 575-587

Houlsby, G.T & Carter, J.P. 1993. The effect of pressuremeter geometry on the results of tests in clays. *Geotechnique*, 43:567-576.

Houlsby, G.T; Wroth, C.P. & Clarke, B.G. 1986. Analysis of the unloading of a pressuremeter in sand. *Proc. of the 2nd Int. Symp. on Pressuremeter and its Marine Applications*. ASTM, SPT950, 245-262.

Huang, A.B. 1989. Strain path analysis for arbitrary three dimensional penetrometers. *Int. J. Num. and Anal. Methods in Geomech.*, 13:551-564.

Huang, A.B. & Ma, M.Y. 1994. An analytical study of cone penetration tests in granular material. *Can. Geotech. J*, 31:91-103.

Huang, A.B. & Hsu, H.H. 2004. Advanced calibration chamber for cone penetration testing in cohesionless soils. *2nd Int. Conf. on Site Charact.*, Milpress, Porto, 1: 147-166.

Hughes, J.M.O; Wroth, C.P & Windler, D. 1977. Pressuremeter tests in sands. *Geotechnique*, 27(4):455-477.

Ishihara, K. 1982. Evaluation of soil properties for use in earthquake response analysis. *Proc. Int. Symp. Num. Models in Geomech.*, Zurich, 237-259.

Ishihara, K. 1996. Soil Behavior in Earthquake Geotechnics. *Edit. Clarendon Press*, Oxford.

Jamiolkowski, M., Leroueil, S. &3, D.C.F. 1991. Theme Lecture: Design parameters, from theory to practice. *Proc. Geo-Coast'91, Yokohama*. Vol.2 : 877-917.

Jamiolkowski M., Lancellotta R. & Lo Presti D.C.F. 1994. Remarks on the stiffness at small strains of six Italian clays. *Proc. First Int. Conf. on Pre-failure Deformation Charact. of Geomaterials*, Sapporo, Japan, Vol. 2, 817-836.

Jamiolkowski, M., Lancellotta, R. & Lo Presti, D.C.F. 1995a. Remarks on the stiffness at small strains of six Italian clays. Keynote Lecture 3, *Proc. Int. Symp. on Pre-Failure Deformation Charact. of Geomaterials*, Sapporo, Vol. 2: 817-836.

Jamiolkowski, M., Lo Presti, D.C.F. & Pallara, O. 1995b. Role of in-situ testing in geotechnical earthquake engineering. *Proc. 3rd Int. Conf. on Recent Advances in Geotech. Earthquake Engng. and Soil Dynamic*. State-of-the-Art 7, Vol. 3: 1523-1546.

Jamiolkowski, M. & Lo Presti, D. C. F. 2003. Geotechnical characterization of Holocene and Pleistocene Messina sand and gravel deposits. *Charact. and Engng. Properties of Natural Soils,* Singapore. Balkema Publishers, 2: 1087-11120.

Jamiolkowski, M.; Lo Presti., D.C.F. & Manassero., M. 2003. Evaluation of relative density in shear strength of sands from cone penetration tests (CPT) and flat dilatometer (DMT). *Soil Behaviour and Soft Ground Construction, ASCE* GSP119, 201-238.

Jamiolkowski, M., Ladd, C.C., Germaine, J.T. & Lancellotta, R. 1985. New developments in field and laboratory testing of soils. *Proc.11th Int. Conf. on Soil Mech. and Found. Engng.*., San Francisco, Vol. 1, pp. 57-153.

Jamiolkowski, M.; Ghionna, V.; Lancellotta, R. & Paqualini, E. 1988. New correlations of penetration tests for design practice. *Proc. Int. Symp. of Penetration Testing, ISPOT-1*, Orlando, 1:263-296.

Jardine, R.J. 1985. Investigations of pile-soil behaviour with special reference to the foundations of offshore structures. *Ph.D. Thesis*, University of London, London, U.K.

Jardine, R.J. 1992. Some observations on the kinematic nature of soil stiffness. *Soils & Found.*, 32(2): 111-124.

Jardine, R.J., Symes, M.J. & Burland, J.B. 1984. The measurement of soil stiffness in the triaxial apparatus. *Géotechnique*, 34(3): 323-340.

Jardine, R.J., St.John, H.D., Hight, D.W. & Potts, D.M. 1991. Some practical applications of a non-linear ground model. *Proc.10th European Conf. on Soil Mech. and Found. Engng.*, Florence, 1: 223-228.

Jefferies, M. G. 1988. Determination of horizontal geostatic stress in clay with self-bored pressuremeter. *Can. Geotech. J.*, 25, pp. 559-573.

Jefferies, M. G. & Been, K. 2000. Implications for critical state theory from isotropic compression of sand. *Geotechnique*, 50(4):419-429.

Kamey, T. & Iwasaki, K. 1995. Evaluation of undrained shear strength of cohesive soil using a flat dilatometer. *Soils & Found.*, 35(2):111-116.

Kavvadas, M. & Amorosi, A. 1998. A plasticity approach for the mechanical behaviour of structured soils. *Proc. 2nd Int. Symp. on the Geotech. of Hard Soils – Soft Rocks*, Napoli, Vol. 2: 603-613.

Kavvadas, M., Anagnostopoulos, A. & Kalteziontis, N. 1993. A framework for the mechanical behaviour of the cemented Corinth marl. *Proc. Int. Symp. on Geotech. Engng of Hard Soils-Soft Rocks*, Athens, 1: 577-583.

Konrad, J.M. 1987. Piezo-friction-cone penetrometer testing in soft clays. *Can. Geotech. J.*, 24:645-652.

Konrad, J.M.1997. In situ sand state from CPT: evaluation of a unified approach at two canlex sites. *Can. Geotech. J.*, 34(1):120-130.

Konrad, J.M. 1998. Sand state from cone penetrometer tests: a framework considering grain crushing stress. *Geotechnique*, 48(2):201-216.

Koskinen, M.; Karstunen, M. & Wheeler, S.J. 2002. Modelling destructuration and anisotropy of a natural soft clay. *Proc. 5th European Conf. Num. Methods. in Geotech. Engng.*, Paris, 11-20.

Kulhawy, F.H. & Mayne, P.W. 1990. Manual of estimating soil properties for foundation design. *Geotech. Engng. Group*, Cornell University, Ithaca.

Lacasse, S. & Lunne, T. 1988. Calibration of dilatometer correlations. *Proc. Int. Symp. of Penetration Testing, ISPOT-1*, Orlando, 1:539-548.

Ladanyi, B. & Johnston, G.H. 1974. Behaviour of circular footings and plate anchors embedded in permafrost. *Can. Geotech. J.*, 11:531-553.

Ladd, C.C. 1991. Stability evaluation during staged construction. *J. Geotech. Engng. Div., ASCE*, 117(4) : 540-615.

Ladd, C.C.; Foott. R.; Ishihara, K.; Schlosser, F. & Poulos, H.G. 1977. Stress-deformation and strength characteristics. State-of-the-Art Report. *9th Int. Conf. Soil Mech. Found. Engng.*, Tokyo, 2: 421-494.

Lagoia, R. & Nova, R. 1995. An experimental and theoretical study of the behaviour of a calcarenite in triaxial compression. *Géotechnique*, 45(4): 633-648.

Lambe, T.W. & Withman, R.V. 1979. Soil Mechanics, *SI version*, New York, John Wiley & Sons.

Leroueil, S. & Vaughan, P.R. 1990. The general and congruent effects of structure in natural soils and weak rocks. *Géotechnique* 40, No. 3, 467-488.

Leroueil, S. & Hight, D.W. 2003. Behaviour and properties of natural and soft rocks. *Charact. and Engng. Properties of Natural Soils*, Balkema, 1, 29-254.

Leroueil, S., Demers, D., La Rochelle, P., Martel, G. & Virely, D. 1995. Practical applications of the piezocone in Champlain sea clays. *Proc. Int. Symp. on Cone Penetration Testing, CPT-95*, Linköping, pp. 515-522.

Leroueil, S., Hamouche, K., Tavenas, F., Boudali, M., Locat, J., Virely, D., Roy, M., La Rochelle, P. & Leblond P. 2002. Geotechnical characterization and properties of a sensitive clay from Québec. *Proc. Int. Workshop on Charact. and Engng. Properties of Natural Soils, Singapore.*

Levadoux, J.-N. & Baligh, M.M. 1986. Consolidation after undrained piezocone penetration. *J. of Geotech. Engng., ASCE*, 112(7): 707-726.

Li, S.S. & Dafalias, Y.F. 2000. Dilantancy for cohesionless soils. *Geotechnique*, 52 (3): 449-460.

Long, M. & Phoon, K.K. 2004. General report: Innovative technologies and equipment. *2nd Int. Conf. on Site Charact.*, Milpress, Porto, 1: 625-634.

Lo Presti, D.C.F. 1989. Proprietà dinamiche dei terreni. *Atti delle Conferenze di Geotecnica del Politecnico di Torino.*

Lo Presti, D.C.F., Shibuya, S. & Rix, G.J. 2001. Innovation in soil testing. *Proc. Symp. on Pre-failure Charact. of Geomaterials,* Torino, Vol. 2: 1027-1076.

Lo Presti, D.C.F; Jamiolkowski, M. & Pepe, M. 2003. Geotechnical characterization of the subsoil of Pisa Tower. *Charact. and Engng Properties of Natural Soils*, Balkema Publishers, 2: 909-946.

Lo Presti, D.C.F., Pallara, O., Jamiolkowski, M. & Cavallaro, A. 1999. Anisotropy of small strain stiffness of undisturbed and reconstituted clays. *Proc. 2nd Int. Symp. on Pre-Failure Deformation Charact. of Geomaterials,* IS-Torino 99, Torino, Vol. 1: 11-18.

Lo Presti, D.C.F., Jamiolkowski, M., Pallara, O., Cavallaro, A. & Pedroni, S. 1997. Shear modulus and damping of soils. *Géotechnique*, 47(3): 603-617.

Lunne, T.; Lacasse, S. & Rad, N.S. 1989. SPT, CPT, pressuremeter testing and recent developments on in-situ testing of soils. *Proc. XII ICSMFE*, Rio de Janeiro.

Lunne, T.; Robertson, P.K. & Powell, J.J.M. 1997. Cone penetration testing in geotechnical practice, *Blackie Academic & Professional*, 312p.

Lutenegger, A.J. 1988. Current status of the Marchetti dilatometer test. *Proc. 1st Int. Symp. on Penetration Testing, ISOPT-1*, Orlando, 1:137-155

Marchetti, S. 1980. In situ tests by flat dilatometer. *J. Geot. Engng. Div. ASCE*, Vol.106 (GT3): 299-321.

Marchetti, S. 1997. The flat dilatometer: design applications. Keynote Lecture. *Proc. 3rd Int. Geotech. Engng Conf.*, Cairo, 421-448.

Marchetti, S.& Totani, G. 1889. C_h evaluations from DMTA dissipation curves. *Proc. 12th Int. Conf. Soil Mech. Found. Engng.*, Rio de Janeiro, 1:281-286

Marchetti, S.; Monaco, P; Totani, G. & Calabrese, M. 2001. The flat dilometer test (DMT) in soil investigation. *Report by the ISSMGE Committee TC 16. Proc. Int. Conf. on In Situ Measurement of Soil Properties*. Baligh, 95:132.

Mair, R.J. & Wood, D.E. 1987. Pressuremeter testing: Methods and interpretation. *Ciria Report*, Buterworths, UK, 160p.

Manassero, M. 1989. Stress-strain relationships from drained self-boring pressuremeter test in sand. *Géotechnique* 39 (2), 293-308.

Mantaras, F.M. 2000. Cavity expansion theory in cohesive-frictional materials. *PhD Thesis*. Federal University of Rio Grande do Sul. Brazil., in Portuguese.

Mantaras, F.M. & Schnaid, F. 2002. Cavity expansion in dilatant cohesive-frictional soils. *Geotechnique*, 52 (5), 337-348.

Matthews, M.C., Clayton, C.R.I. & Own, Y. 2000. The use of field geophysical techniques to determine geotechnical stiffness parameters. *Geotech. Engng*, 143(1): 31-42.

Mayne, P.W. & Rix, G.J 1993. G_{max}-q_c relationships for clays. *ASTM Geotech. Testing J.*, 16(1):54-60.

Mayne, P.W (2001) Stress-strain strength flow characteristics of enhanced in situ testing. *Int. Conf. of In Situ Measurement of Soil Properties and Case Histories*, Indonesia, 29-48.

Mayne, P.W. & Kulhawy, F.H. 1991. Calbration chamber database ad boundary effects correction for CPT data. *Proc 1st Int. Symp. on Calibration Chamber Testing*. Postdam, New York, 257-264.

Mayne, P.W. & Mitchell, J.K. 1988. Profiling of OCR in clays by field vane. *Can. Geotech. J.*, 25(1):150-157.

McNeilan, T.W. & Bugno, W.T. 1980. Cone penetration test results in offshore California soils. *Strength Testing of Marine Sediments: Laboratory and In Situ Test Measurements*, *ASTM* STP 833, 55-71

Mitchell, J.K. & Solymar, Z.V. 1984. Time-dependent strength gain in freshly deposited or densified sand. *J. of Geotech. Engng*., *ASCE*, 110(11): 1559-1576.

Muir Wood, D. 1990. Strain dependent moduli and pressuremeter tests. *Geotechnique*, 40(3):509-512.

Nova, R. & Wood, D.M. 1979. Constitutive model for sand in triaxial compression. *Int. Journ. Num. Anal. Method. Geomech.,* 3:255-498.

Nutt, N.R.F. & Houlsby, G.T. 1992. Calibration tests on the cone pessuremeter in carbonate sand. *Int. Symp. Calib. Chamber Testing*. Potsdam, New York, 265-276.

Oda, M.; Koishikawa, I. & Higuchi, T. 1978. Experimental study of anisotropic shear strength of sand by plane strain test. *Soils and found.* 18, No. 1, 25-38.

Odebrecht, E. 2003. Energy Measurements in SPT Test, *PhD Thesis*, Porto Alegre Federal University of Rio Grande do Sul, In portuguese. pp203.

Odebrecht, E.; Schnaid, F.; Rocha, M.M. & Bernardes, G.P. 2004a. Energy measurements for standard penetration tests and the effects of the length of rods. *2nd Int. Conf. on Site Charact.*, Milpress, Porto, 1: 351-358.

Odebrecht, E.; Schnaid, F.; Rocha, M.M. & Bernardes, G.P. 2004b. Energy efficiency for Standard Penetration Tests. *J. Geotech. and Geoenvironm. Engng, ASCE*, Submitted for publication.

Parkin, A.K. & Lunne, T. 1982. Boundary effects in the laboratory calibration of a cone penetrometer for sand. *Proc. 2th European Symp. on Penetration Testing*. Amsterdam, 2: 761-768.

Pestana, J.M. & Whitle, A.J. 1999. Formulation of an unified constitutive model for clays and sands. *Int. J. Num. and Anal. Methods in Geomech.*, 23:2115-2143.

Powell, J.J.M & Uglow, I.M. 1988. Interpretation of the Marchetti dilatometer test in UK clays. *Proc. on Penetration Testing in the UK*., Birmingham, 121-125.

Powell, J.J.M & Butcher, A.P. 2004. Small strain stiffness assessments from in situ tests. *2nd Int. Conf. on Site Charact.*, Milpress, Porto, 2:1717-1729.

Rampello, S. & Viggiani, G.M.B. 2001. Pre-failure deformation characteristics of geomaterials. *Proc. Symp. on Pre-failure Charact. of Geomaterials,* Torino, Vol.2: 1279-1289.

Randolph, M. F. 2004. Characterisation of soft sediments for offshore applications. *2nd Int. Conf. on Site Charact.*, Milpress, Porto, 1: 209-232.

Randolph, M. F. & Worth, C.P. 1979. An analytical solution for the consolidation around a driven pile. Proc. *Int. J. Num. and Anal. Methods in Geomech.*, 3(3):217-229.

Randolph, M. F. & Houlsby, G.T. 1984. The limiting pressure on a circular pile loaded laterally in a cohesive soil. *Geotechnique*, 34(4):613-623.

Randolph, M. F. & Hope, S. 2004. Effect of cone velocity on cone resistance and excess pore pressures. *Proc. Int. Symp. on Engng. Practice and Performance of Soft Deposits*. Osaka.

Rangeard, D.; Hicher, P.Y. & Zentar, R. 2003. Determining soil permeability from pressuremeter tests. *Int. J. Num. and Anal. Methods in Geomech..*, 27(1):1-24.

Rangeard, D.; Zentar, R.; Moulin, R. & Hicher, P.Y. 2001. Strain rate effect on pressuremeter test in soft clay. *Proc. Int. Conf. on Soil Properties and Case Histories*. Bali, 379-384.

Rix, G.J. & Stokes, K.H. 1992. Correlation of initial tangent modulus and cone resistance. *Int. Symp. Calibration Chamber Testing*, Potsdam, USA: 351-362.

Richard, F.E.Jr; Hall, J.R. & Woods, R.B. 1970. Vibrations of soils and foundations. *Englewood Cliffs*, New Jersey, Prentice Hall, 414p.

Robertson, P.K.; Campanella, R.G.; Gillespie, D.G. & By, T. 1988. Excess pore pressure and the flat dilatometer test. *Proc. Int. Symp. of Penetration Testing, ISPOT-1*, Orlando, 1:567-576..

Robertson, P.K.; Sully, J.P.; Woeller, D.J.; Lunne, T., Powell, J.J.M. & Gillespie, D.G. 1992. Estimating coefficient of consolidation from piezocone tests. *Can. Geotech. J.*, 29(4):551-557.

Robertson, P.K.; Wride, C.E.; List, B.R; Zavodni, Z. 2000. The Canadian Liquefaction Experiment: an overview. *Can. Geotech. J.*, 37(3):499-504.

Rodrigues, C.M.G. & Lemos, L.J.L. 2004. SPT, CPT and CH tests results on saprolitic soils from Guarda, Portugal. *2nd Int. Conf. on Site Charact.*, Milpress, Porto, 2:1345-1352.

Rouainia, M. & Muir Wood, D. 2000. A kinematic hardening constitutive model for natural clays with loss of structure. *Geotechnique*, 50(2):153-164.

Roscoe, K.H. & Burland, J.B. 1968. On the generalized stress-strain behaviour of 'wet' clay. *Proc. Symp. on Plasticity*, Cambridge: 535-610.

Rotta, G.V.; Consoli, N.C., Pritto, P.D.M., Coop, M.R.; & Graham, J. 2003.
Isotropic Yielding in an Artificially Cemented Soil Cured Under Stress. *Géotechnique*. 53(5): 493-501.

Rowe, P.W. 1962. The stress-dilatancy relation for static equilibrium of an assembly of particles in contact. *Proc. Royal Soc.* London, A269, 500-527.

Rowe, P.W. 1963. Stress-dilatancy, earth pressure and slopes. *J. Soil Mech. Found. Div. ASCE* 89, SM3, 37-61.

Rowe, P.W. 2001. Geotechnical and geo-environmental engineering handbook. *Kluwer Academic Publishing*. Norwell, USA.

Salgado, R.; Mitchell, J.K. & Jamiolkowski, M. 1997. Cavity expansion and penetration resistance in sand. *J. Geotech. and Geoenvironm. Engng.*, 123 (4), 344-354.

Sandroni, S.S.. & Maccarini, M. 1981 Triaxial and direct shear test in a Gneiss residual soil. *Brazilian Symp. on Tropical Soils*, COPPE, RJ, 324-339.

Santamarina, J.C.; Klein, K.A. & Fam, M.A. 2001. Soils and waves, *John Whiley & Sons Ltd*, Ontario, Canada, 488p.

Schmertmann, J.H. 1988. Guidelines for using CPT, CPTU and Marchetti DMT for geotechnical design. Report FHWA-PA-87-022+84-24, *Office of Research and Special Studies*, USA.

Schmertmann, J.H. 1991. The mechanical aging of soils. *J. of Geotech. Engng., ASCE*, 117(9): 1288-1330.

Schnaid, F. 1997. Panel Discussion: Evaluation of in situ tests in cohesive frictional materials. *14th Int. Conf. Soil Mech. Found. Engng*, Hamburg, 4: 2189-2190.

Schnaid, F. & Houlsby, G.T. 1991. An assessment of chamber size effects in the calibration of in situ tests in sand; *Geotechnique*, 41 (4), 437-445.

Schnaid, F.; Houlsby, G. T. 1992. Measurement of the proprieties of sand in a calibration chamber by cone pressuremeter test, *Geotechnique*, 42 (4), 578-601.

Schnaid, F. & Houlsby, G.T. 1994. Interpretation of shear moduli from cone-pressuremeter tests in sand; *Geotechnique*, 44 (1), 147-164.

Schnaid, F. & Mantaras, F.M. 2003 Cavity expansion in cemented materials: structure degradation effects. *Geotechnique*, 53 (9): 797-807.

Schnaid, F. & Mantaras, F.M. 2004. Interpretation of pressuremeter tests in a gneiss residual soil from Sao Paulo, Brazil. *2nd Int. Conf. on Site Charact.*, Milpress, Porto, 2: 1353-1360.

Schnaid, F. & Yu, H. S. 2005. Theoretical Interpretation of the Seismic Cone Test in Granular Soils.*Geotecnique*. Forthcoming paper.

Schnaid, F.; Prietto, P.D.M. & Consoli, N.C. 2001. Characterization of cemented sand in triaxial compression. *J. Geotech. and Geoenvironm. Engng, ASCE*, 127 (10), 857-868.

Schnaid, F.; Lehane, B.M. & Fahey. M. 2004. *In situ* test characterisation of unusual geomaterials. *2nd Int. Conf. on Site Charact.*, Milpress, Porto, 1: 49-74.

Schnaid, F,; Odebrecht, E. & Rocha, M. 2005. Applications of SPT test results. Forthcoming paper.

Schnaid, F.; Sills, G.C.; Soares, J.M. & Nyirenda, Z. 1997. Predictions of the coefficient of consolidation from piezocone tests. *Can. Geotech. J.* Vol 34, No 2, 143-159.

Schneider, J.A.; Lahane, B.M. & Schnaid, F. 2005. Evaluation of piezocone pore pressure response in normally consolidated and overconsolidated clayey. Forthcoming paper.

Schofield, A. and Wroth, P. 1968. Critical State Soil Mechanics. *Mc Graw-Hill*, London, 310pp.

Schofield, A.N. & Steedman, R.S. 1988. State of the Art Report: Recent developments of dynamic model testing in geotechnical engineering. *Proc. 9th World. Conf. on Earthquake Engng.* Tokio/Kyoto, Japan, 8:813-824.

Senneset, K.; Janbu, N. & Svano, G. 1982. Strength and deformation parameters from cone penetrometer tests. *Proc. 2nd European Symp. on Penetration Testing*. Amsterdam, 2: 863-870.

Senneset, K.; Sandven, R. Lunne, T.; By, T. & Amundesen, T. 1988. Piezocone testing in silty soil. *Penetration Testing 88*. Balkema, 955-966.

Sharma, P.V. 1997. Environmental and engineering geophysics, *Cambridge University Press*, Cambridge, UK, 475p.

Sheahan, T.C., Ladd, C.C. & Germaine, J.T. 1996. Rate dependent undrained behavior of saturated clay. *J. Geotech. Engng., ASCE*, 122(2): 99-108.

Shibuya, S.; Hwang, S.C. & Mitachi, T. 1997. Elastic shear modulus of soft clays from shear wave velocity measurement. *Geotechnique*, 47(3):593-601.

Shibuya, S; Mitashi, T.; Yamashita, S. & Tanaka, H 1996. Recent Japonese practice for investigating elastic stiffness of ground. *Advances in Site Investigation Practice*. Thomas Telford, 875-886.

Shibuya, S., Mitachi, T., Fukuda, F. & Hosomi, A. 1997. Modelling of strain-rate dependent deformation of clay at small strains. *Proc. 12th Int. Conf. on Soil Mech. and Geotech, Engng*., Hamburg, Vol. 1: 409-412.

Shibuya, S; Yamashita, S.; Watabe, Y. & Lo Presti, D.C.F. 2004. In situ seismic servey in characterising engineering properties of natural ground. . *2nd Int. Conf. on Site Charact.*, Milpress, Porto, 1: 167-185.

Simonini, P. & Cola, S. 2000. Use of piezocone to predict maximum stiffness of Venetian soils. *J. Geotech. and Geoenvironm. Engng.*, *ASCE*, 126(4):378-381.

Simons, N.E. 1975. General report 'Normally consolidated and highly over-consolidated cohesive materials. *Proc. Conf. of the British Geotech. Society on Settlements of Structures*, Cambridge, pp. 500-530.

Skempton, A. W. 1986. Standard penetration test procedures and effects in sands of overburden pressure, relative density, particle size, aging and over consolidation. *Géotechnique*, 36 (3), 425-447.

Smith, M.G. & Houlsby, G.T. 1995. Interpretation of the Marchetti dilatometer in clay. *Proc. 11th Int. Conf. Soil Mech. and Found. Engng.*, 1: 247-252.

Sousa Coutinho, A.G.F 1990. Radial expansion of cylindrical cavities in sandy soils: application to pressuremeter tests. *Can. Geotech. J.*, 27:737-748.

Stokoe, K.H.II, Hwang, S.K. & Lee, K.J.N. 1994. Effects of various parameters on the stiffness and damping of soils at small to medium strains. *Proc. 1st Int. Conf. on Pre-failure Deformation Charact. of Geomaterials*, Sapporo, Vol. 2: 785-816.

Stokoe, II K.H., Hwang, S.K., Lee, J.N.K & Andrus, R.D. 1995. Effects of various parameters on the stiffness and damping of soils at small to medium strains. *Proc. 1st Int. Conf. on Prefailure Deformation Charact. of Geomaterials*, Sapporo, Vol. 2: 785-816.

Stokoe, K.H. II & Santamarina, J.C. 2000. Seissmic-wave-based testing in geotechnical engineering. *Proc. Int. Conf. on Geotech. and Geological Engng.*, Melbourne, Vol. 1: 1490-1536.

Stokoe, K.H.II; Joh, S.H & Woods, R.D. 2004.. The contributions of in situ geophysical measurements to solving geotechnical engineering problems. *2nd Int. Conf. on Site Charact.*, Milpress, Porto, 1: 97-132.

Su, S.F. & Liao, H.J 2002. Influence of strength anisotropy on piezocone resistance in clay. *J. Geotech. And Geoenvironm. Engng., ASCE*, 128(2):166-173.

Tanaka, H., Tanaka, M. & Iguchi, H. 1994. Shear modulus of soft clay measured by various kinds of tests. *Proc. Symp. on Pre-Failure Deformation of Geomaterials*, Sapporo, Vol. 1: 235-240.

Tatsuoka, F. & Shibuya, S. 1991. Deformation characteristics of soils and rocks from field and laboratory tests. *Proc. 9th Asian Regional Conf. on Soil Mech. and Found. Engng*., Bangkok, Vol. 2: 101-170.

Tatsuoka, F., Lo Presti, D.C.F. & Kohata, Y. 1995. Deformation characteristics of soils and soft rocks under monotonic and cyclic loads and their relationships. *Proc. 3rd. Int. Conf. on Recent Advances in Geomech. Earthquake Engng. and Soil Dynamics,* St-Louis, Vol. 2: 851-879.

Tatsuoka, F.; Jardine, R.J.; Lo Presti, D.; Di Benedetto, H. & Kodaka, T. 1997. Theme Lecture: Characterising the pre-failure deformation properties of geomaterials. *14th Int. Conf. Soil Mech. Found. Engng*, Hamburg, 4: 2129-2164.

Tavenas, F. & Leroueil, S. 1977. Effects of stresses and time on yielding of clays. *Proc. 9th Int. Conf. on Soil Mech. and Found. Engng*., Tokyo, Vol.1, pp.319-326.

Tavenas, F. & Leroueil, S. 1987. State-of-the-Art on ¨Laboratory and in situ stress-strain-time behavior of soft clays¨. *Proc. Int. Symp. on Geotech. Engng. of Soft Soils*, Mexico City, Vol. 2: 1-46.

Taylor, R.N. 1995. Geotechnical centrifuge technology. *Blackie Academic and Professional*, London.

Teh, C.I. & Houlsby, G.T. 1991. An analytical study of the cone penetration test in clay. *Géotechnique*, 41(1): 17-34.

Tomlinson, M.J. 1969. Foundation design and construction. *Pitman Publishing*, 2:785.

Torstensson, B. A. 1977. The pore pressure probe. *Norsk Jord-Og Fjellteknisk Forbund*. Oslo, Foredrag 34.1-34.15. Troedheim, Norway.

Uriel, S. & Serrano, A.A. 1973. Geotechnical properties of two collapsible volcanic soils of low bulk density at the site of two dams in

Canary Islands (Spain). *Proc. 8th Int. Conf. on Soil Mech. and Found. Engng.*, Moscow, 2(2): 257-264.
Vaid, Y.P., Robertson, P.K. & Campanella, R.G. 1979. Strain rate behaviour of Saint-Jean-Vianney clay. *Can. Geotech. J.*, 16(1): 34-42.
Vaughan, P.R. 1985. Mechanical and hydraulic properties of tropical lateritic and saprolitic soil, General Report, *Int. Conf. Geomech. in Tropical Lateritic and Saprolitic Soils*, Brasilia, 3: 231-263.
Vaughan, P.R. 1997. Engineering behaviour of weak rock: Some answers and some questions. *Proc. 1st Int. Conf. on Hard Soils and Soft Rock*s, Athens, Vol. 3: 1741-1765.
Van Impe, W.F. & Van den Broeck, M. (2001) Geotechnical characterization in offshore conditions. *Conf. Di Geotecnica di Torino*. Italy, 1-15.
Vesic, A.S. 1972. Expansion of cavities in infinite soil mass. *J. of Geotch. Engng. Div., ASCE*, 98 (3): 265-290.
Vesic, A.S. 1975 Principles of pile foundation design. *Soil Mech. Series*, 38, Durham, NC.
Viana da Fonseca, A. 2003. Characterization and deriving engineering properties of a saprolitic soil from granite in Porto. *Charact. and Engng. Properties of Natural Soils*, Balkema, 2, 1341-1378.
Wheeler, S. J. ; Cudny, M.; Neher, H.P & Wiltafsky, C. 2003. Some developments in constitutive modelling of soft clays, *Int. Workshop on Geotech. Soft Soils Theory and Practice*. Karstunen & Kudny Editors.
Whittle, R.W. 1999. Using non-linear elasticity to obtain the engineering properties of clay – a new solution for the self-boring pressuremeter test. *Ground Engng.*: 30-34.
Whittle, A.J. & Aubeny, C.P. 1993. The effects of installation disturbance on interpretation of in situ tests in clays. *Predictive Soil Mech.*, Thomas Telford, London, 742-767.
Whittle, A.J. & Kavvadas, M.J. 1994. Formulation of MIT E3 constitutive model for overconsolidated clays. *J. Geotech. Engng.*, 120(1):173-198.
Withers, N.J.; Howie, J.; Hughes, J.M.O. & Robertson, P.K. 1989. Performance and analysis of cone pressuremeter tests in sand. *Geotechnique*, 39:433-454.
Wride, C.E.; Robertson, P.K.; Biggar, K.W., Campanella, R.G.; Hofmann, B.A; Hughes, J.M.O. Kupper, A. & Woeller, D.J. 2000. Interpretation of *in situ* test results from the Camlex sites. *Can. Geotech. J.*, 37(3): 505-529.
Wroth, C.P. 1984. The interpretation of in situ soil test. 24th Rankine Lecture. *Géotechnique*, 34 (4): 449-489.
Wroth, C.P. & Basset, N. 1965. A stress-strain relationship for the shearing behaviour of sand. *Geotechnique*, 15(1):32-56.
Wu, B.L.; King, M.S. & Hudson, J.A. 1991. Stress induced anisotropy in rock and its influence on wellbore stability. *Rock Mech.* As a Multidisciplinary Science, Balkema, 941-950.
Yeung, S.K & Carter, J.P. 1990. Interpretation of the pressuremeter test in clay allowing for membrane end effects and material non-homogeneity. *Proc. 3rd Int. Symp. on Pressuremeters* , Oxford, 199-208.
Yu, H.S. 1993. A new procedure for obtaining design parameters from pressuremeter tests. *Australian Civil Engng. Transactions*, Vol CE35(4):353-359.
Yu, H.S. 2000. Cavity expansion methods in geomechanics. *Kluwer Academic Publishers*, UK, 385p.
Yu, H.S. 2004. The James K. Mitchell Lecture: In situ testing: from mechanics to prediction. *2nd Int. Conf. on Site Charact.*, Milpress, Porto, 1: 3-38.
Yu, H.S. & Houlsby, G. 1991. Finite cavity expansion in dilatant soils: loading analysis. *Géotechnique* 41 (2): 173-183.
Yu, H.S. & Mitchell, J.K. 1998. Analysis of cone resistance: a brief review of methods. *J. Geotech. And Geoenvironm. Engng., ASCE*, 124(2):140-149.
Yu, H.S.; Carter, J.P. & Booker, J.R. 1993. Analysis of the dilatometer test in undrained clay. *Predictive Soil Mech.*, London, 783-795.
Yu, H.S.; Schnaid, F. & Collins 1996. Analysis of cone pressuremeter tests in sands. *J. Geotech. Engng.* 122 (8): 623-632.